

# Addressing data limitations and uncertainties in broad- scale coastal flood-risk assessments

Dissertation

zur Erlangung des Doktorgrades  
der Mathematisch-Naturwissenschaftlichen-Fakultät  
der Christian-Albrechts-Universität zu Kiel  
vorgelegt von

Claudia Wolff

Kiel, 2020



Erster Gutachter: Prof. Dr. Athanasios T. Vafeidis

Zweiter Gutachter: PD Dr. habil Jochen Hinkel

Datum der mündlichen Prüfung: 04.03.2021

gez. Prof. Dr. Frank Kempken



## SUMMARY

Coastal flooding constitutes a major risk to all low-lying coastal areas around the world. This risk is expected to increase during the 21st century with rising sea-levels and future societal development. Broad-scale coastal flood risk assessments are essential for identifying regions most at risk and evaluating the effectiveness of coastal adaptation responses in reducing future coastal impacts. Despite recent advances in coastal flood risk modelling research, there are a number of methodological and data related constraints and limitations inherent in broad-scale studies that affect the accuracy of assessment findings. Understanding and communicating these uncertainties is necessary for effectively supporting decision-makers in developing long-term robust and flexible adaptation plans. However, most uncertainties involved in broad-scale assessments are not fully quantified and their relative importance often remain unexplored. This thesis contributes to improving our understanding of data uncertainties and addresses data limitations in broad-scale coastal flood risk assessments. In particular, this thesis (1) addresses data availability, consistency and reproducibility constraints, (2) extends existing data models and increase the level of detail of assessments and (3) explores and quantifies data uncertainties in broad-scale coastal flood risk studies.

For this purpose, Chapter 1 summarizes the main data limitations and uncertainties inherent in each coastal flood risk component (coastal hazard, exposure and vulnerability) and its implications for broad-scale coastal flood risk assessments.

Chapter 2 assesses sea-level rise related coastal flood impacts for Emilia-Romagna (Italy) using the Dynamic Interactive Vulnerability Assessment (DIVA) modelling framework and investigates the sensitivity of model results to four uncertainty dimensions, namely (1) elevation, (2) population, (3) vertical land movement, (4) scale and resolution of assessment. Results show that by the end of the century coastal flood impacts are most sensitive to variations in elevation input data, followed by vertical land movement data and population data. The choice of one digital elevation model over another can lead up to 45% differences in the total extent of the coastal flood plain. Further, the inclusion of human-induced subsidence rates in the input data increases the relative sea-level rise on average by 60cm in 2100, resulting in coastal flood impacts that are up to 25% higher, highlighting that the non-consideration of human-induced subsidence in broad-scale studies underestimates coastal flood impacts.

Chapter 3 describes the development of the open-access, spatially-explicit Mediterranean Coastal Database (MCD) that contains consistent information in terms of resolution, quality, accuracy and format of around 160 parameters on characteristics of the natural and socio-economic coastal subsystems for the entire region. The MCD, as well as the code for all data processing steps, is publicly available in an online repository.

Chapter 4 illustrates the development of a new set of spatially-explicit projections of urban extent for ten countries in the Mediterranean, with a high spatial (100m) and temporal resolution (5-year time steps). These future urban projections indicate that accounting for the spatial patterns of urban development can lead to significant differences in the assessment of future coastal urban exposure. Depending on the urban development scenario chosen, the exposure of certain coastal regions can vary by up to 104 percent until 2100. The urban extent projections spanning from 2025 to 2100 and the python code to set up the urban change model are available from a public repository.

Finally, Chapter 5 summarizes the main findings and lessons learned from this thesis and highlights some key challenges related to data that require further research targeting.

## ZUSAMMENFASSUNG

Überflutungen zählen weltweit zu den größten Risiken für niedrig gelegene Küstengebiete. Ein steigender Meeresspiegel und die zukünftige gesellschaftliche Entwicklung im 21. Jahrhundert führen voraussichtlich zu einer Verschärfung dieses Risikos. Vor diesem Hintergrund sind Gefährdungsanalysen im multinationalen bis globalen Maßstab unerlässlich, um die potentiellen Auswirkungen von Überschwemmungen und die Wirksamkeit von Anpassungsmaßnahmen an Küsten bewerten zu können. Bei der Modellierung von Hochwasserrisiken an Küsten in dieser Maßstabsdimension konnten in der jüngsten Vergangenheit immense Fortschritte gemacht werden. Allerdings gibt es bei diesen Studien eine Reihe von methodischen und datenbezogenen Unsicherheiten, welche die Genauigkeit der Hochwasserrisikoanalysen beeinflussen können. Um Entscheidungsträger:innen wirksam bei der Entwicklung langfristiger, robuster und flexibler Anpassungsstrategien unterstützen zu können, ist sowohl das Verständnis, als auch die Kommunikation dieser Unsicherheitsfaktoren erforderlich. Die meisten dieser Unsicherheiten sind derzeit jedoch nicht vollständig quantifiziert. Darüber hinaus ist ihre relative Bedeutung in Gefährdungsanalysen häufig nicht bekannt. Die vorliegende Dissertation leistet einen Beitrag dazu, unser Verständnis von Datenunsicherheiten in multinationalen bis globalen Gefährdungsanalysen zu verbessern und die Datenverfügbarkeit für derartige Analysen zu optimieren. Die Arbeit befasst sich im Speziellen mit (1) Datenverfügbarkeit-, Konsistenz- und Reproduzierbarkeitsbeschränkungen. Sie (2) erweitert vorhandene Küstendatenmodelle und erhöht dadurch den Detailgrad von Gefährdungsanalysen. Zudem werden (3) Datenunsicherheiten in Risikobewertungen untersucht und quantifiziert.

In Kapitel 1 werden die wichtigsten Datenlimitierungen und -unsicherheiten in multinationalen bis globalen Gefährdungsanalysen zusammengefasst, die jeder der einzelnen Küstenhochwasserrisikokomponenten (Küstenhochwassergefahr, Exposition und Verwundbarkeit) inhärent sind. Ferner werden die Auswirkungen dieser Unsicherheiten auf die Bewertung des Hochwasserrisikos an Küsten resümiert.

In Kapitel 2 wird mithilfe des ‚Dynamic Interactive Vulnerability Assessment (DIVA)‘ Modellierungs-Frameworks eine Gefährdungsanalyse hinsichtlich der Überflutung für die Region Emilia-Romagna (Italien) durchgeführt. Dabei wird die Sensitivität der Modellergebnisse gegenüber vier Unsicherheitsdimensionen untersucht: (1) Geländehöhe, (2) Bevölkerung, (3) vertikale Landbewegung, (4) Maßstab und Auflösung der Untersuchung. Die Ergebnisse zeigen, dass die Gefährdungsanalysen besonders sensitiv gegenüber Schwankungen der Höheneingabedaten sind, gefolgt von Daten zur vertikalen Landbewegung und Bevölkerung. Die Unterschiede in der modellierten Überflutungsfläche bei der Nutzung verschiedener Höheneingabedaten können bis zu 45% betragen. Werden durch den Menschen verursachte Landabsenkungsraten in die Eingabedaten einbezogen, führt dies zu einer

Erhöhung des durchschnittlichen relativen Meeresspiegelanstiegs um 60 cm im Jahr 2100. Dies bewirkt, dass die Bewertung potenzieller Auswirkungen von Überschwemmungen an Küsten bis zu 25 % höher ausfallen. Dies weist darauf hin, dass Studien, die menschlich verursachte Absenkungsraten nicht berücksichtigen, die Auswirkungen von Küstenüberflutungen unterschätzen.

In Kapitel 3 wird die Entwicklung einer räumlich expliziten Open-Access-Datenbank für die Mittelmeerküste (MCD) beschrieben. Die Datenbank ist konsistent in Bezug auf Auflösung, Qualität, Genauigkeit und Format und enthält Informationen zu rund 160 Parametern zu Merkmalen des natürlichen und sozioökonomischen Küstensystems. Die MCD sowie der Code für alle Datenverarbeitungsschritte sind in einem Online-Repository öffentlich verfügbar.

Kapitel 4 erläutert die Entwicklung neuer, räumlich expliziter und sowohl räumlich (100m) als auch zeitlich (5-Jahres-Zeitschritte) hochaufgelöster Projektionen der städtischen Ausdehnung für zehn Länder im Mittelmeerraum. Diese Projektionen wurden anschließend genutzt um zu untersuchen, wie die Stadtentwicklung das zukünftige Hochwasserrisiko an der Küste beeinflusst. Die Ergebnisse zeigen deutlich, dass es erhebliche Unterschiede in der Bewertung der Gefährdung von Städten durch Überflutung gibt. Der potentielle Anstieg der Gefährdung bestimmter Küstenregionen kann im Zeitraum bis zum Jahr 2100, je nach gewählten Stadtentwicklungsszenario, um bis zu 104 Prozent variieren. Der für die Erstellung des Stadtentwicklungsmodells genutzte Python-Code, sowie die räumlich expliziten Projektionen sind öffentlich in einem Repository erhältlich.

Abschließend werden in Kapitel 5 die wichtigsten Ergebnisse und Lehren aus dieser Arbeit zusammengefasst. Zudem werden eine Reihe relevanter Herausforderungen im Zusammenhang mit den für diese Arbeit genutzten Daten aufgezeigt, die weitere Forschung erfordern.



# CONTENTS

SUMMARY.....	i
ZUSAMMENFASSUNG.....	iii
<b>1 INTRODUCTION.....</b>	<b>1</b>
1.1 COASTS AT RISK.....	2
1.2 BROAD-SCALE COASTAL FLOOD RISK ASSESSMENTS .....	3
1.3 DATA LIMITATIONS AND UNCERTAINTIES IN BROAD-SCALE COASTAL FLOOD RISK ASSESSMENTS.....	4
1.3.1 Coastal flood hazards.....	4
1.3.2 Coastal flood exposure.....	8
1.3.3 Coastal flood vulnerability .....	16
1.4. RESEARCH OBJECTIVES AND OUTLINE .....	19
<b>2 EFFECTS OF SCALE AND INPUT DATA ON ASSESSING THE FUTURE IMPACTS OF COASTAL FLOODING: AN APPLICATION OF DIVA FOR THE EMILIA-ROMAGNA COAST.....</b>	<b>21</b>
2.1 INTRODUCTION.....	22
2.2 STUDY AREA, METHODS AND DATA .....	24
2.2.1 Overview .....	24
2.2.2 Study Area.....	25
2.2.3 Methods .....	26
2.2.4 Data.....	28
2.3. RESULTS .....	34

2.3.1 Segmentation.....	34
2.3.2 Sensitivity to Segmentation .....	34
2.3.3 Sensitivity to Elevation Data .....	37
2.3.4 Sensitivity to Vertical Land Movement Data.....	39
2.3.5 Sensitivity to Population Data .....	39
2.4. DISCUSSION .....	40
2.4.1 Effects of Different Coastlines and Segmentations to Coastal Flood Impact Assessment .....	40
2.4.2 Model Sensitivity to Input Data .....	41
2.5 CONCLUSION .....	44
ACKNOWLEDGEMENT .....	45
<b>3 A MEDITERRANEAN COASTAL DATABASE FOR ASSESSING THE IMPACTS OF SEA-LEVEL RISE AND ASSOCIATED HAZARDS .....</b>	<b>47</b>
3.1 BACKGROUND & SUMMARY.....	48
3.2 METHODS.....	49
3.2.1 Coastal data model.....	49
3.2.2 Extreme sea levels and waves .....	53
3.2.3 Computational data processing .....	53
3.2.4 Code availability .....	58
3.3 DATA RECORDS .....	58
3.4 TECHNICAL VALIDATION .....	58
3.4.1 Geomorphological classification.....	59
3.4.2 Extreme sea level datasets .....	60
3.4.3 Data attribution.....	63
3.5 USAGE NOTES.....	63

<b>4 FUTURE URBAN DEVELOPMENT EXACERBATES COASTAL EXPOSURE IN THE MEDITERRANEAN</b> .....	65
4.1 INTRODUCTION.....	66
4.2 RESULTS .....	69
4.2.1 Spatially explicit projections of urban extent .....	69
4.2.2 Future coastal urban exposure in 2100.....	72
4.3 DISCUSSION.....	73
4.4 CONCLUSION.....	76
4.5 METHODS.....	77
4.5.1 Urban change model.....	77
4.5.2 Future coastal flood exposure.....	79
4.5.3 MLP performance .....	79
4.6 DATA AVAILABILITY .....	81
<b>5 SYNTHESIS</b> .....	83
5.1 SUMMARY OF THE MAIN RESEARCH FINDINGS .....	84
5.1.1 Data availability, consistency and reproducibility .....	84
5.1.2 Coastal data model and assessment scale.....	85
5.1.3 Data uncertainties .....	85
5.2 RECOMMENDATIONS FOR FUTURE RESEARCH .....	87
REFERENCES .....	93
APPENDIX A.....	109
APPENDIX B.....	113
ACKNOWLEDGEMENTS .....	119
ERKLÄRUNG.....	123



# 1

## INTRODUCTION

## 1.1 COASTS AT RISK

Climate-change induced sea-level rise (SLR) and associated hazards, in combination with continued socio-economic development, will lead to an increase in coastal flood risk in low-lying coastal regions in the future (Vousdoukas et al., 2020b, Vousdoukas et al., 2018b, Hinkel et al., 2014). Even a small increase in mean sea level can disproportionately increase the occurrence of extreme sea levels (ESLs) and thus coastal flood risk (Taherkhani et al., 2020). Coastal flood risk is shaped by multiple drivers that are dynamic and therefore, variable across time and space (Nicholls et al., 2018).

### Box 1 | Coastal flood risk

The Intergovernmental Panel on Climate Change (IPCC) defines risk as the interaction of climate-related hazards with exposure and vulnerability of human and natural systems. The components of risk are defined as:

**Hazards** refer to the potential occurrence of a natural or human-induced physical event (e.g. ESLs) or trend (e.g. SLR) that may cause impacts on the natural or human systems.

**Exposure** encompasses the presence of all elements, such as people, livelihoods, infrastructure or cultural assets, in hazard-prone areas.

**Vulnerability** refers to the degree to which a natural or social system can withstand or cope with negative effects caused by a hazard (IPCC, 2019).

Changes, for instance, in the climate system or socio-economic conditions along with adaptation and mitigation actions may influence hazards, exposure, and vulnerability (Oppenheimer et al., 2014), leading to changes in the temporal and spatial variability of risk. Several studies indicate that the main driver of future coastal flood risk is the combination of increased coastal flood hazards and exposure due to SLR (Tiggeloven et al., 2020) and the increasing concentration of people and economic services in coastal regions (Neumann et al., 2015, McGranahan et al., 2007). Coastward migration combined with rapid economic development has led to higher coastal population growth and urbanisation rates compared to non-coastal regions (Merkens et al., 2018, Kummu et al., 2016, Neumann et al., 2015). Broad-scale coastal flood risk studies have shown that the world's coastline will experience more frequent flooding from ESLs and SLR, potentially leading to the displacement of hundreds of millions of people during the 21<sup>st</sup> century if no adaptation is in place (Hinkel et al., 2014). Adaptation in the form of hard/engineered and ecosystem-based coastal protection, accommodation, advancement, or retreat can reduce coastal flood risk by addressing one of the three risk components (vulnerability, exposure and/or hazards) (Abram et al., 2019). For instance, Lincke and Hinkel (2018) show that coastal protection is economically robust for 13% of the global coastline. This study illustrates that coastal flood risk and cost-efficient adaptation

are not uniform and vary significantly between regions and time. A common approach to identify and quantify the risk of coastal flooding and the benefits of adaptation are coastal flood risk assessments. In the following section, the need for broad-scale coastal flood risk assessments, their main advantages and constraints are discussed.

## 1.2 BROAD-SCALE<sup>1</sup> COASTAL FLOOD RISK ASSESSMENTS

Broad-scale assessments aim to analyse spatial patterns and temporal trends of coastal flooding on a continental to global scale. During the last decade, demand for broad-scale risk assessments under present and future conditions has grown (Vousdoukas et al., 2018a). These assessments can support international policymaking and organisations, such as the World Bank and the United Nations (UN), to identify coastal flood risk and adaptation hotspots and allocate international adaptation funds (Ward et al., 2013, McLeod et al., 2010) where action is required. Further, reinsurance companies, among others, require such assessments to evaluate current and future risk portfolios (de Moel et al., 2015). These assessments identify areas at risk from flooding and evaluate the effectiveness of coastal adaptation measures in reducing future coastal impacts (Ward et al., 2020). Their main advantage is the consistent methodological framework and underlying data over the entire region of interest, which enables comparative analyses of impacts and benefits of different adaptation measures in a standardised way, even in data-scarce countries (de Moel et al., 2015). Therefore, broad-scale assessments can help to gain a better understanding of the drivers of coastal flood risk and their potential implications for the natural and human system (hereafter referred to as 'impacts'). Despite recent advancements in coastal flood risk modelling research, only a few tools/modelling frameworks exist that are comprehensive, spatially explicit and assess all the different coastal flood risk drivers (namely hazard, exposure, vulnerability) in a combined manner on a broad scale (Tiggeloven et al., 2020). Besides the advantages of broad-scale coastal flood risk assessments mentioned, there are also a number of difficulties and limitations surrounding broad-scale assessments. The main challenges in modelling coastal flood risk on a broad scale are:

- (1) unavailability of consistent, open-access input data (Lichter et al., 2011, Vafeidis et al., 2008, McLeod et al., 2010);
- (2) depicting the dynamic coastal system into a data model that allows spatial information to be stored into a database (McFadden et al., 2007);

---

<sup>1</sup> In this thesis, broad-scale refers to continental to global scale coastal flood risk assessments.

- (3) combining datasets of different formats, reference systems and spatial/temporal resolution into consistent and detailed input data (Vafeidis et al., 2008);
- (4) developing models that are capable of resolving the dominant physical and human processes while remaining computationally inexpensive (Vousdoukas et al., 2018a, de Moel et al., 2015, Muis et al., 2015) as a large number of model runs are required to cover a range of scenarios; and
- (5) validating broad-scale assessment results due to the lack of spatially explicit and detailed information on relevant past events (de Moel et al., 2015).

Addressing these challenges requires making simplifications in coastal flood risk assessments and thus, affect the accuracy of assessment findings. However, most uncertainties involved are not fully quantified and their relative importance for coastal flood impacts assessments often remains unexplored (Vousdoukas et al., 2018a). This thesis contributes to improving our understanding of data uncertainties and addresses data limitations in broad-scale coastal flood risk assessments, specifically points 1-3 of the above mentioned constraints will be addressed. In the remainder of this section, I highlight the main data limitations and uncertainties of each coastal flood risk component and the associated implications for broad-scale coastal flood risk assessments. Section 1.3 discusses the individual components contributing to future coastal flood risk, with each section broken into two components: 1) a brief summary of the coastal flood risk component and its implementation in broad-scale coastal flood risk assessment, and 2) an overview of the main datasets used in broad-scale coastal flood risk assessment together with a discussion of the main current limitations or areas of uncertainty to illustrate their potential implications for coastal flood impact assessments.

## **1.3 DATA LIMITATIONS AND UNCERTAINTIES IN BROAD-SCALE COASTAL FLOOD RISK ASSESSMENTS**

### **1.3.1 Coastal flood hazards**

The first step in coastal flood risk assessments is the determination of the coastal flood hazard, including the assessment of the probability and intensity of a potential event (de Moel et al., 2015). ESLs and SLR are the two main hazards which contribute to future coastal flooding (Oppenheimer et al., 2019) and datasets of those two drivers are commonly used as input for assessing coastal impacts. ESLs can arise from different drivers, namely mean-sea level rise, storm surge, astronomical tide, wind waves, precipitation, river discharge and seasonal to interannual variability. Coastal flooding can occur from the superposition of these components. Coastal flood risk assessments theoretically require information on all ESL components and their potential future changes considering natural variability and climate change (even though



not all are used in broad-scale assessments). Climate change, for instance, will alter future ESLs mainly through rising sea levels and changes in storm activity (Rahmstorf, 2017).

### Sea-level rise projections

Sea-levels are rising due to global warming, which is a result of anthropogenic emissions of Greenhouse Gases (GHG) over the last century. The two primary factors leading to an accelerated sea level are the thermal expansion as seawater warms and the melting of land-based ice sheets and glaciers (Church et al., 2013). Therefore, one prerequisite to assess future coastal flood risk are sea-level rise projections that result from different future GHG concentration pathways. This involves combining different but uncertain components of sea level associated with climatic and non-climatic (for example vertical land movement) factors (Nicholls et al., 2014). A rise in global mean sea level (GMSL) in the future is certain but the rate and magnitude are subject to large uncertainties especially beyond 2050 (Oppenheimer et al., 2019). The largest uncertainties in sea-level projections are stemming from GHG emission scenarios and the estimation of future mass loss from the Antarctica and Greenland ice sheets (DeConto and Pollard, 2016) as our physical understanding of the dynamic response of the ice sheet is still very limited. The uncertainties in the remaining sea level (SL) components are much smaller and range in the order of 10 cm (van de Wal et al., 2019). According to the IPCC Fifth Assessment Report (AR5), GMSL is likely to rise by 0.26-0.55m under Representative Concentration Pathway (RCP) 2.6 (the lowest greenhouse gas concentration pathway) and 0.45-0.82m under RCP 8.5 (the highest greenhouse gas concentration pathway) in the period from 2081–2100 compared to 1986-2005 (Church et al., 2013). Recent studies suggest that future GMSL will be higher than reported in the IPCC AR5, which has not assessed probabilities beyond the likely range (67%) (Kopp et al., 2017, Horton et al., 2018). However, coastal decision-makers and planners with low uncertainty tolerance often require information on the upper bounds (low-probability) of SLR to assess worst-case scenarios that lead to high coastal impacts (Hinkel et al., 2019). As a consequence, many studies developed regional high-end SLR scenarios that do not focus on the median and central range projections but the upper bound of SLR (Jevrejeva et al., 2019). Many broad-scale flood impact assessments use those types of sea-level projections to account for the large uncertainty. Table 1-1 shows a summary of commonly used SLR projections in broad-scale coastal flood risk assessments.

Table 1-1: SLR projections used in broad-scale coastal flood impact assessment

<b>Study</b>	<b>GMSL rise by 2100 (RCP 8.5)</b>	<b>Modelling approach</b>	<b>Selected broad-scale assess.</b>
<b>Church et al. (2013) (IPCC: AR5)</b>	98 cm (83rd percentile)	process based models	-
<b>(Oppenheimer et al., 2019) (IPCC - SROCC, 2019)</b>	110 cm (83rd percentile)	process based models	-
<b>Jevrejeva et al. (2014)</b>	180 cm (95th percentile)	process based models and expert opinion	Tiggeloven et al. (2020)
<b>Hinkel et al. (2014)</b>	123 cm (95th percentile, across all models)	process-based models	Vousdoukas et al. (2017), Vafeidis et al. (2019)
<b>Kopp et al. (2014), Kopp et al. (2017)</b>	K14: 123 cm (95th percentile); 159 cm (99th percentile)  K17: 243 cm (95th percentile), 267 cm (99th percentile)	fully probabilistic, K14: process based models and expert opinion on ice sheet contributions,  K17: links physical models of ice sheet loss to the projection framework established in K14	Kulp and Strauss (2019), Reimann et al. (2018)
<b>Goodwin et al. (2017)</b>	105 cm (95th percentile, across all models), 112cm (99th percentile)	hybrid approach, containing a process-based thermosteric contribution and a semi-empirical ice-melt contribution	Brown et al. (2018), Nicholls et al. (2018)

Further, as the regional distribution of sea-level rise is not uniform in all regions of the world, due to spatially varying patterns caused by ocean (i.e. ocean circulation) and non-oceanic effects (e.g post-glacial rebound) (Bakker et al., 2017), most assessments use regional relative sea level projections. For instance, vertical land movement, which is the downward (subsidence) or upward movement (uplift) of the land relative to sea level, is an important component of regional sea levels. Subsidence often occurs in regions associated with alluvial sediments, such as deltas (Ericson et al., 2006) and groundwater extraction is one of the major sources contributing to subsidence. Most impact studies account for natural vertical land movement by using glacial isostatic adjustment datasets from, for instance, Peltier (2004), Peltier et al. (2015). However, human-induced subsidence is not considered in most studies even though it can reach several meters in some regions (Nicholls et al., 2018). One exception is the study of Tiggeloven et al. (2020) that included subsidence due to groundwater extraction on a broad-scale. Vertical land movement rates have a high spatial and temporal variability associated with local processes which makes the development of future vertical land movement projections extremely challenging. Thus, one source of uncertainty in existing coastal flood assessments remains the unavailability of comprehensive global datasets and projections of vertical land movement including natural and human-induced sources. A detailed overview on the current state of understanding of the processes that cause regional sea-level change and the remaining uncertainties is provided in Hamlington et al. (2020).

## Extreme sea-level models and datasets

Different definitions and approaches calculating ESLs exist, which makes the comparison of coastal flood risk studies very challenging (Table 1-2 shows a summary of the ESL datasets commonly used in broad-scale assessments). The product that most broad-scale impact studies use are return periods (or return water levels) of ESLs. These return water levels are generated by applying extreme value analysis approaches to hindcast or modelled extreme water levels (Wahl et al., 2017). Until recently, the DINAS-COAST ESL (DCESL) dataset was the only comprehensive and consistent global ESL dataset. DCESL was generated using a simple empirical model that depicts the following ESL components: mean high tide, storm surge and barometric pressure (Vafeidis et al., 2008, Muis et al., 2017). ESLs associated with different return periods are provided for 12,148 coastline segments of the Dynamic Interactive Vulnerability Assessment modeling framework (DIVA) that cover the whole world except Antarctica. Compared to observations, DCESL overestimates ESLs with a mean bias of 55cm for the 1 in 100-year extremes (Muis et al., 2017).

Recent computational advancements have paved the way for the first broad-scale hydrodynamic tide and storm surge model (GTSM = Global Tide and Surge Model). GTSM was forced with ERA-Interim reanalysis data to produce the Global Tide and Surge Reanalysis dataset (GTSR). This time series (1979-2014) is used to estimate the return water levels of ESLs (Muis et al., 2016) for all DIVA segments and tide gauge stations of the University of Hawaii Sea Level Center. GTSR ESLs are slightly underestimated with a mean bias of -19cm compared to ESLs from observations (1 in 100-year extremes). The bias is especially high in areas where tropical cyclones occur. This results from the low spatial and temporal resolution of the atmospheric forcing (ERA-Interim spatial resolution is  $\sim 79$  km at the equator, temporal resolution of 6h). The GTSR dataset does not consider wind waves, baroclinic effects, precipitation, river discharge or tide-surge interactions. For more details on the DCESL and GTSR datasets see Muis et al. (2017).

One study that incorporates future changes in ESLs on a broad-scale is the study of Vousdoukas et al. (2018c) (called thereafter JRC-ESL). Changes in storm surge, astronomical tide and wind wave characteristics that result from changes in mean sea level (MSL) and wind forcing under different climate scenarios are modelled using a Monte Carlo approach to generate probabilistic ESL projections. According to their study, regional MSL is the future dominant driver of increasing ESLs. Other flood drivers, such as storm surge or the wave component, show a very small increase on global average until the end of the century (Vousdoukas et al., 2018c). The study does not account for interactions between SLR, tidal flow, storm surge and waves. According to Vousdoukas et al. (2018c), the largest source of uncertainty influencing future ESLs changes is MSL change. However, the projection of future ESLs changes on a broad scale is still an ongoing research area.

Table 1-2: ESL datasets used in broad-scale coastal flood impact assessments

ESL dataset	ESL components included	Selected studies using the ESL dataset
<b>DCESL (Vafeidis et al., 2008)</b>	Mean high tide, storm surge and barometric pressure	Neumann et al. (2015), Hinkel et al. (2014), Hallegatte et al. (2013)
<b>GTSR (Muis et al., 2016)</b>	Mean high tide and storm surge	Tiggeloven et al. (2020), Vafeidis et al. (2019), Lincke and Hinkel (2018)
<b>JRC-ESL (Vousdoukas et al., 2018c)</b>	Mean sea level, tides, storm surges and wind waves	Vousdoukas et al. (2020a), Vousdoukas et al. (2018b)

Some uncertainties in the hazard component have been explored in the literature, but many remain unexplored. One major uncertainty in ESLs is that not all relevant drivers are implemented into broad-scale hydrodynamic ESL models, such as river discharge or waves (Jevrejeva et al., 2019). For instance, several studies have shown that waves are a significant factor affecting ESLs at the coast (Serafin et al., 2017, Vousdoukas et al., 2016, Melet et al., 2018). However, few studies to date have incorporated wave contribution (except Vousdoukas et al. (2016), Vousdoukas et al. (2018c) – but underestimated it by including wave setup) into the calculation of ESLs and thus into coastal flood impact assessment on a broad scale. Further, not accounting for the non-linear interactions of the different drivers of ESLs, such as tide-surge interaction, introduces uncertainty into the ESL values and thus, impact assessments. Arns et al. (2020), developed a statistical model that corrects the GTSR ESLs dataset for tide-surge-interactions. The study demonstrates that not accounting for these nonlinear interactions may lead up to 30% (or 70cm) higher ESLs and remains a source of uncertainty in broad-scale coastal flood impact assessments. Another uncertainty in current and future ESLs results from the statistical analysis of extreme values, which is influenced by the selected frequency analysis approach, distribution shape, and return period curve fitting. Wahl et al. (2017) estimated that uncertainties range from under 10cm up to more than 1m in the estimation of ESLs for the 1-100-year event (global average 22cm).

### 1.3.2 Coastal flood exposure

The second step in assessing coastal flood risk is the analysis of exposed land and population to current or future ESLs and SLR. The assessment of coastal flood exposure is often based on ESLs for specific return periods and future projections of SLR (as described in subsection 1.3.1). In the following section, the main data limitations and uncertainties in calculating future exposure of land and population are discussed.

#### Exposure of land

Potential coastal flood extent and depth is a fundamental element in broad-scale coastal flood risk assessments and there exist different approaches of varying complexity for assessing land

exposure. For all approaches, a digital elevation model (DEM) is the core spatial dataset to identify areas that are potentially affected by coastal flood hazards. DEMs are a gridded digital representation of the surface where each pixel value represents the elevation height above a datum (Hawker et al., 2018). All freely available DEMs with a near-global coverage, which is required for broad-scale coastal flood assessments, are digital surface models (DSMs) representing the Earth's surface height including surface objects, such as the roof of a house or the crown of a tree, and not the terrain. In other words, the elevation height value represents the first reflectance surface (Hawker et al., 2019). The most popular DEM used for broad-scale coastal flood impact assessments is the Shuttle Radar Topography Mission (SRTM) DEM obtained in 2000 by using Spaceborne Interferometric Synthetic Aperture Radar (InSAR) (Farr et al., 2007). Elevation values are given as integers. The accessibility of SRTM data, together with the vertical accuracy and fewer artefacts and noise compared to alternative broad-scale DEMs, such as ASTER, GTOPO30 and GLOBE, are some of the main reasons for the wide usage of SRTM in the past (Hawker et al., 2018). However, coastal flood risk assessments are very sensitive to height errors. SRTM has a reported vertical Mean absolute error (MAE) of around six meters (Rodriguez et al., 2006) and a Root-mean-square error (RMSE) of 9.73m ((Gesch, 2018); see Table 1-3). The recent release of products that correct SRTM, such as Multi-Error-Removed-Improved-Terrain (MERIT) DEM, NASADEM and the CoastalDEM (Kulp and Strauss, 2018), or the newly developed TanDEM-x-90, have an improved vertical accuracy compared to SRTM and thus, are most likely better suited to calculate coastal flood exposure. For instance, MERIT reduces the errors of SRTM by removing absolute bias, stripe noise, speckle noise and vegetation artefacts (but not buildings) leading to a significant improvement in flat terrain (Yamazaki et al., 2017) such as coasts. Unlike SRTM, elevation values are provided in floating-point numbers, which improves their suitability for coastal flood impact assessments. However, MERIT is basically built on SRTM and is thus limited by its errors (Hawker et al., 2018). CoastalDEM from Kulp and Strauss (2018), used Neural Networks to reduce SRTM errors. This correction leads to a reduction of the vertical bias in the order of decimeters in the US and Australia (see Table 1-3). The RMSE was reduced by half compared to SRTM (Kulp and Strauss, 2018). The vertical accuracies of the most commonly used DEMs in broad-scale coastal flood impact assessments are summarized in Table 1-3.

Table 1-3: Digital Elevation Model (DEM) used in broad-scale coastal flood impact assessments

DEM	Horizontal resolution	Vertical accuracy	Selected studies using the elevation data
<b>GTOPO30</b>	30 arc-seconds (~1 km)	18m (RMSE)*	Kummu et al. (2016), Lichter et al. (2011), Small and Nicholls (2003)
<b>GLOBE</b>	30 arc-seconds (~1 km)	18m (RMSE)**	Hinkel et al. (2014), Lichter et al. (2011)
<b>SRTM<sup>2</sup></b>	1 and 3 arc-seconds (~30 m and ~90 m)	9.73 (RMSE) <sup>#</sup> 5.57m (RMSE -U.S. LECZ) <sup>#</sup> ;	Vafeidis et al. (2019), Muis et al. (2017), Neumann et al. (2015), Lichter et al. (2011), McGranahan et al. (2007)
<b>MERIT</b>	3 arc-seconds (~90 m)	5.9m (RMSE) <sup>''</sup> 3.14 (RMSE -U.S. LECZ) <sup>#</sup>	Tiggeloven et al. (2020)
<b>CoastalDEM</b>	1 and 3 arc-seconds (~30 m and ~90 m)	2.46 m (RMSE - Australia) <sup>'</sup> 2.39m (RMSE - U.S.) <sup>'</sup>	Kulp and Strauss (2019)
<b>World DEM (TanDEM-X 90)</b>	3 arc-seconds (~90m), 0.4 arc-seconds (~12m)	6.08m (RMSE) <sup>#</sup> 1.69m (RMSE - U.S.) <sup>#</sup>	-

\*\*Hastings and Dunbar (1999)   '' O'Loughlin et al. (2016)   'Kulp and Strauss (2019)   #Gesch (2018) \*GTOPO30 Readme file (URL: [https://prd-wret.s3.us-west-2.amazonaws.com/assets/palladium/production/s3fs-public/atoms/files/GTOPO30\\_Readme.pdf](https://prd-wret.s3.us-west-2.amazonaws.com/assets/palladium/production/s3fs-public/atoms/files/GTOPO30_Readme.pdf))

The vertical error of elevation datasets often exceeds the range of projected SLR which makes the assessment of flood exposure very challenging (Poulter and Halpin, 2008). The error in broad-scale DEMs and the fact that global DEMs are surface models leads to large uncertainty in the estimation of coastal flood exposure. Hinkel et al. (2014) explore the uncertainty and sensitivity of DEMs in broad-scale flood impact assessments. They showed that the 1-100-year coastal floodplain is twice the extent when using GLOBE DEM compared to employing SRTM data. Lichter et al. (2011), analysed similar patterns by calculating the coastal area that lies below 2m. The authors found that the extent is halved when using SRTM data compared to using GLOBE or GTOPO DEMs.

Another source of uncertainty is introduced in broad-scale assessments due to the horizontal resolution of broad-scale DEMs. The horizontal resolution varies between 30 arc-seconds (approximately 1 km at the equator) and 3 arc-sec (approximately 90 m at the equator) in broad-scale DEMs, leading to simplifications and smoothing of the terrain as each pixel represents the average elevation height. This leads to, for instance, unresolved natural or artificial features, such as coastal protection elements, or added systematic bias (Poulter and Halpin, 2008, Vousdoukas et al., 2018a). Broad-scale coastal flood risk assessments can be sensitive to the employed spatial resolution. Vousdoukas et al. (2018a) resampled Light Detection And Ranging (LiDAR) elevation data and found that a lower spatial resolution leads to a greater extent of the coastal floodplain and accordingly to higher losses (the amount of

<sup>2</sup> Note: Different versions of SRTM exist

expected annual damage nearly tripled). The main reason for this was that the coastal protection of the dunes was not resolved in the lower resolution data. This could be a case-specific effect, and more research is needed to confirm and quantify this uncertainty. Still, the study gives an indication that, for instance, coastal protection is not resolved in broad-scale coastal flood impact assessments which potentially leads to an overestimation of future impacts. Poulter and Halpin (2008) showed that the horizontal resolution is especially crucial if low elevation increments are analysed, as results are more sensitive (1.1m SLR: 3% difference between 6 and 15m resolution, 0.3m SLR: 65% difference in the flood extent). However, as Lichter et al. (2011) point out, most types of assessments favour a higher resolution, which does not necessarily suggest that these datasets are more accurate and appropriate for specific assessments. More research on that topic is needed.

The third source of uncertainty arises from the obstacles in combining datasets of different formats, reference systems and spatial/temporal resolution. For the purpose of assessing coastal flood risk, one of the boundary conditions are ESLs for specific return periods which are referenced to MSL as the vertical datum. However, broad-scale DEMs are referenced to the geoid (e.g. SRTM - EGM96). The offset between those datasets can be up to 1.5m (Schaeffer et al., 2012). Only in recent years has this offset been corrected in broad-scale assessments (Muis et al., 2017) by using the mean dynamic ocean topography (MDT), which is the difference between MSL and the geoid over a specific period. However, whether this correction is the best approach to account for the offset is still an open research debate, as the MDT varies over time and the definition of the MSL of specific datasets is often not well documented, leading to further uncertainties. Implementing this vertical datum correction into broad-scale coastal flood impact assessments leads to an increase in the coastal flood extent between 16 and 20% for the 1-100 year event globally (Muis et al., 2017).

While improved broad-scale DEMs present a significant advancement in the estimation of broad-scale coastal flood impacts, there is still large variability on the extent of coastal flooding depending on the flood modelling approach used. This topic goes beyond the scope of the objectives of this thesis which focuses on data uncertainties and limitations. The sources of uncertainty in area exposure estimations described above should nevertheless be kept in mind. Another data limitation in broad-scale assessments is the lack of validation data that leads to uncertainties as coastal impact models/approaches cannot be accurately evaluated and validated. One reason for the difficulties in validating broad-scale assessments is the assessment scale, which is much larger than the scale of a single event. The broad-scale methods that exist simulate the hypothetical case that a specific event (e.g. 100-year event) occurs everywhere simultaneously. Given the rare occurrence of a coastal flood event, establishing a database for the whole globe would require hundreds of years of detailed observations during which boundary conditions change (de Moel et al., 2015). Even local historical data for single events rarely exist and constitute a major limitation in coastal flood assessments at all spatial scales.

## Exposure of people

Exposure of people threatened by current and future ESLs is commonly assessed by overlaying elevation data with spatially explicit population datasets and/or population projections.

### **Current exposure of people**

Five different gridded population products have been commonly used in broad-scale coastal flood risk assessment to estimate current exposure of people (Table 1-4 summarises them). The datasets that exist are based on national population and census data of varying years and resolution (Wardrop et al., 2018, Mondal and Tatem, 2012), which is a source of uncertainty in broad-scale coastal flood risk assessments. The main uncertainties in national population and housing census data stems from the fact that they are (1) often outdated, (2) inaccurate with regard to the quality, number and size of enumerated areas; (3) omit or undercount key groups or regions (e.g. people living in informal settlements), and (4) large variations exist in the frequency of data collection and the level of spatial detail that is provided between and within countries, leading to a potential misallocation of humans as they are not uniformly distributed within an areal/administrative unit in reality (Leyk et al., 2019, Wardrop et al., 2018). As a consequence, the research community developed different data products and strategies to overcome these inconsistencies and redistribute population counts to grids cells. The Gridded Population of the World (GPW v3 and v4) product uses a uniform allocation approach, called areal weighting, to redistribute the population of the source census data evenly across the land area within an administrative unit (Doxsey-Whitfield et al., 2015). This leads to irregular levels of detail in terms of size and extent of input population census data within and across different countries in the population data product (Leyk et al., 2019). Further, this approach leads to simplification as the population is not uniformly distributed within administrative units. A second, commonly used dataset is the Global Rural-Urban Mapping Project v1 (GRUMP), which is based on GPWv3 and is intended to capture and differentiate urban and rural locations and populations. GRUMP employs a dasymetric population disaggregation approach, which uses ancillary or covariate data to redistribute population by using functional relationships between population density and ancillary data (Leyk et al., 2019, Wardrop et al., 2018). The third dataset is the Global Human Settlement Layer - Population (GHS-POP) that is based on the residential population from GPWv4 and employs a dasymetric population disaggregation approach. The population is here reallocated using the distribution and density of built-up land provided by the Global Human Settlement Layer (GHSL) (Melchiorri et al., 2019). The fourth dataset is LandScan which represents an ambient (daytime) population distribution using a "smart interpolation" approach. The methods employ ancillary data, such as land cover, slope, roads or night-time lights to calculate a likelihood coefficient or weight for every cell according to their possible occurrence of the population (Leyk et al., 2019). Compared to the other three datasets, LandScan redistributes population based on their likely ambient location averages over a 24-hour period of typical days, weeks and seasons



(Dobson et al., 2000). The fifth dataset is the WorldPop population grid, which was produced with a weighted dasymetric approach that uses a random forest model to create a predictive weighting layer for dasymetrically redistributing population counts to raster cells (Leyk et al., 2019).

Table 1-4: Population datasets used in broad-scale coastal flood impact assessments

Population dataset	Reference year	Horizontal resolution	Disaggregation approach	Selected studies using the population data
<b>GRUMP</b>	1990, 1995, 2000	~1 km	Dasymetric (lightly modelled)	Merkens et al. (2016), Neumann et al. (2015), Hinkel et al. (2014), McGranahan et al. (2007), Lichter et al. (2011)
<b>LandScan</b>	1998, 2000 - 2018	~1 km	Smart interpolation (highly modelled)	Kulp and Strauss (2019), Hinkel et al. (2014), Lichter et al. (2011)
<b>GWP V3</b>	1990, 1995, 2000, 2005*, 2010*, 2015*	~5 km (V3)	Areal weighting (unmodelled)	Paprotny et al. (2018), Reimann et al. (2018), Jones and O'Neill (2016)
<b>V4</b>	2000, 2005, 2010, 2015*, 2020*	~1 km		
<b>GHS-POP</b>	1975, 1990, 2000, 2015	250 m & 1 km	Dasymetric refinement, proportional to built-up density** (lightly modelled)	-
<b>WorldPop</b>	2000-2020	100m & 1km	Statistical (random forest) /dasymetric	Mainly used in national assessments to date, e.g. Yang et al. (2019), Ramirez et al. (2016)

\* extrapolation \*\* Leyk et al. (2019)

To summarise, the main determinants that contribute to uncertainties in the final population data product are (1) the temporal and spatial quality/accuracy of the census input population data, (2) the implications of the methodological population redistribution approach applied, and (3) the quality and spatial/ temporal accuracies of the ancillary/covariate data used (Leyk et al., 2019). Further, the assessment of exposure of people to coastal flooding is based on combining spatially-explicit DEMs and population datasets. Thus, uncertainties through data inaccuracy propagate. Furthermore, offsets between DEMs and population data, for instance, due to different coastlines, could lead to systematic errors in the assessment of exposure (Lichter et al., 2011). Another source of uncertainties are inconsistencies in definitions of the global administrative units. Further, uncertainties arise from the daily dynamics of the population as this could lead to over- or underestimation of, for instance, urban settlements (Mondal and Tatem, 2012). All these factors influence the accuracy and characteristics of the output gridded population dataset. Knowledge of these characteristics is, however, crucial for analysing and interpreting coastal flood risk assessment results.

Only a few studies have quantified these input data uncertainties in coastal impact assessments. Among them, the studies of Kulp and Strauss (2019), Hinkel et al. (2014), Mondal and Tatem (2012) and Lichter et al. (2011) explored the sensitivity of coastal flood impact assessments by using different DEMs or population datasets. Kulp and Strauss (2019), calculated the exposure of people in the Low elevation coastal zone (LECZ, area below 10m elevation that is hydrologically connected to the ocean) using LandScan 2010 data combined with SRTM and CoastalDEM. They found that exposure to people is more than one third higher using the CoastalDEM compared to SRTM (SRTM+Landscan 2010 = 780 Mio People; CoastalDEM+LandScan 2010 = 1040 Mio People). Hinkel et al. (2014) used the GLOBE and SRTM DEM, and GRUMP and LandScan as population datasets to calculate the exposure of the 1-100-year coastal floodplain. The authors found that the coastal exposure of population is 7% (GLOBE) to 70% (SRTM) higher using GRUMP instead of LandScan depending on the DEM chosen. Lichter et al. (2011) calculated the LECZ using Landscan and GRUMP, and three different DEMs, namely GTOPO30, GLOBE and SRTM (ISciences). They found that the LECZ population was 20% higher using LandScan combined with GTOPO30 or GLOBE DEM, compared to GRUMP, whereas SRTM was 14% higher. The LECZ population was highest under both population data sets combined with SRTM data. Interestingly, they also analysed the population distribution below 1,2,3,4, and 5m and showed that LandScan distributes fewer people in close distance to the shoreline compared to GRUMP. The three studies mentioned above, highlight that the calculation of population exposure is very sensitive, not only to the population dataset chosen but even more to the selected DEM. In general, uncertainty due to the variation in population datasets is, therefore, small compared to DEMs.

The study of Mondal and Tatem (2012) provides insight into regional differences between LECZ population estimates using GRUMP and LandScan. They detect that small islands are the countries with the most substantial differences in the estimation of the LECZ population. In Europe and the US, differences between GRUMP and Landscan are small as both GRUMP and LandScan use similar input data, and the population distribution modelling approaches have only a small impact on the LECZ population estimates. In African countries, the input census data varies significantly in resolution and quality between and within countries, leading to much higher differences between the population datasets (GRUMP/LandScan) and therefore the LECZ population estimates.

### **Future exposure of people**

The future distribution of people is essential to assess coastal exposure of people by the end of the century. However, socio-economic development cannot be forecasted due to deep uncertainties (Merkens et al., 2018). Therefore, scenarios of plausible future conditions are applied to address and account for such uncertainties. Different socio-economic scenarios exist and have been applied to coastal flood impact assessments. Lately, the most commonly used scenarios in the coastal impact research community are the Shared Socioeconomic Pathways

(SSPs)<sup>3</sup>. Each of the five SSP scenarios consists of a qualitative (narrative) and quantitative (numerical quantification) dimension (O'Neill et al., 2017) describing key elements such as national population growth (Kc and Lutz, 2017), urbanization (Jiang and O'Neill, 2017) or economic development (Dellink et al., 2017). For this section, I focus on the future population projections.

Different approaches of applying the scenario assumptions on future population to coastal flood risk assessment exist (see Table 1-5). For instance, the main assumption in the study of Hinkel et al. (2014) is a homogenous population growth rate (national average everywhere). This approach neglects processes such as urbanisation, migration or the fact that coastal regions often grow faster than those inland (Merkens et al., 2018). In contrast, other spatially explicit population projections implemented varying growth patterns to account for such processes. One example is the study of Jones and O'Neill (2016). The authors analysed spatial, historical population development trends and used a parameterised gravity-based downscaling model to calculate future spatial population change. The model calculates a potential population surface that reflects attractiveness to allocate the projected urban and rural population change for all five SSPs, to develop spatially-explicit population projections. According to Merkens et al. (2018), population growth rates on subnational level vary indirectly between coastal and urban areas using the Jones and O'Neill (2016) approach. A second example of spatially explicit population projections is the study of Merkens et al. (2016), which focused on differences in spatial population patterns in coastal versus inland areas. The study analysed historical growth rates for coastal and inland regions and applied these in producing spatial population projections. Further, they extended the underlying SSP narratives to the coastal zone and implemented SSP-specific growth differences.

Table 1-5: Population projections used in broad-scale coastal flood impact assessments

<b>SSP spatially explicit population projection</b>	<b>Horizontal resolution</b>	<b>Selected studies using the population projections</b>
<b>Homogenous SSP growth rates per country</b>	Depends on baseline data used as input	Lincke and Hinkel (2018), Hinkel et al. (2014)
<b>Jones and O'Neill (2016)</b>	~14km, downscaled by Gao (2017) to ~1km	Vousdoukas et al. (2020b)
<b>Merkens et al. (2016)</b>	~1km	Merkens et al. (2018)

Little is known about the uncertainties in the projection of socio-economic development and hence, future population exposure. The main determinants that contribute to uncertainties in the future population exposure are (1) the base population data that is used as a starting point

<sup>3</sup> The thesis only reviews studies that use the SSPs

to create the spatially-explicit projections and estimate the historical growth patterns, (2) the regionalisation approach to distribute future population and estimate the future growth rates per grid cells. On a national level, population projections do not differ as the underlying population totals are the same. However, on a grid level the regionalisation approach can introduce large differences and hence uncertainties (Merkens et al., 2018). Another source of uncertainties (3) are the alternative SSPs that are used to span the range of uncertainties of future population change over the 21st century.

Only a few studies have quantified those factors mentioned above for the estimation of coastal flood risk. Merkens et al. (2018) found that the use of different SSPs can lead to up to 72% differences in the estimation of the LECZ population. Further, a comparison of different regionalisation approaches showed that the differences between a homogenous growth rate per country and the approach of Merkens et al. (2016), lead to up to 36% differences in the LECZ population estimates in 2100. For the Mediterranean region, Reimann et al. (2017) compared their coastal regionalisation population approach to Jones and O'Neill (2016) and Merkens et al. (2016). Compared to Jones and O'Neill (2016) differences regarding the LECZ population in 2100 have been up to 33% and up to 15% in comparison to Merkens et al. (2016).

### **Exposure of urban extent**

Population densification, in the form of urbanization or urban development affects coastal exposure and vulnerability (Oppenheimer et al., 2019). Changes in the spatial patterns and rate of urban development will be one of the main determinants of future coastal flood risk. Existing spatial projections of urban extent are, however, often available at coarse spatial resolution, local geographical scales or for short time horizons, which limits their suitability for broad-scale coastal flood impact assessments. Thus, the assessment of urban exposure has not been implemented into broad-scale assessment, which is one of the major shortcomings in coastal impact assessment to date (Muis et al., 2015).

### **1.3.3 Coastal flood vulnerability**

The third step in assessing coastal flood risk is the estimation of vulnerability to ESLs and SLR. Vulnerability is a multidimensional phenomenon that is dynamic in time and space (Abram et al., 2019) due to the complex social, demographic, cultural, economic, political and institutional patterns of societies (Roy and Blaschke, 2015). This complexity leads to difficulties in the accurate spatial representation of vulnerability and is one of the main drawbacks in broad-scale coastal flood risk assessments, to date (Jongman et al., 2012, de Moel et al., 2015). The assessment of vulnerability is therefore often restricted to the analysis of the vulnerability to

assets using depth-damage functions, and the consideration of coastal flood protection on a broad-scale. Even though the concept of vulnerability has a much broader meaning, a detailed assessment of vulnerability is often restricted by the unavailability of data, and a lacking understanding of its driving forces.

### Vulnerability of assets

The assessment of direct damages is commonly based on depth-damage curves in broad-scale coastal flood risk assessments (de Moel et al., 2015). Flood damage estimates often apply specific depth-damage functions for each type of landuse (Tiggeloven et al., 2020, Vousdoukas et al., 2020b, Vousdoukas et al., 2020a) or assets located in the flood-prone area (Hinkel et al., 2014). The aim is to calculate the total value of assets that would be lost by a specific inundation depth caused by ESLs and/or SLR. Therefore, first, the value of the maximum assets per square kilometre, house or population is estimated, and second, a depth-damage curve is applied, which is a function that reflects the relationship between flood inundation depth and direct damages (Vousdoukas et al., 2018b, Jongman et al., 2012). The main factors that introduce uncertainties using this approach are (1) the current and future estimation of the value of assets, (2) the depth damage function (which is often a normalized average), (3) the calculated flood extent and flood depth, (4) the elevation height of the exposed asset values, (5) the fact that not all processes that lead to flood damages are captured by only accounting for flood depth, as several other factors such as flow velocity, wave forces or duration influence direct flood damages (Huizinga et al., 2017), and (6) land cover change is often not taken into account. The influence of the uncertainties mentioned above to the assessment of coastal flood impacts has not been quantified in a systematic way on a broad scale. One exception is the study of Jongman et al. (2012) that analysed the methodological uncertainties in estimating assets exposure. On a global scale, they found that asset exposure varies by up to 71% in 2010 and increases to 98% in 2050 between different damage estimation methods. Further, the uncertainties of different depth damage curves have been analysed in detail on a local to national scale. For instance, de Moel et al. (2012) showed that the choice of the depth damage curve is the most influential parameter in the estimation of coastal flood damages at three beach locations in the Netherlands. However, on a broad-scale, such assessments are currently unavailable.

### Coastal flood adaptation

The implementation of coastal adaptation measures can reduce vulnerability (Oppenheimer et al., 2019). Coastal adaptation measures need to be implemented and reinforced to withstand future ESLs and SLR, and keep coastal flood damages constant in the future (Vousdoukas et al., 2018b). The implementation of coastal flood adaptation in the form of, for instance, coastal

protection into coastal flood risk assessment has a significant effect on model outcomes. This highlights the benefits of coastal adaptation but also the high sensitivity of model results (de Moel et al., 2015) and the substantial uncertainty that could be introduced in coastal flood risk assessments by excluding such coastal protection information (Tiggeloven et al., 2020, Paprotny et al., 2019, Paprotny et al., 2018, Hinkel et al., 2014).

Vousdoukas et al. (2018a) summarized three sources of uncertainties and errors in existing coastal protection datasets. The main uncertainties are (1) the way coastal protection is reported (i.e. in return periods which introduces artefacts), (2) the low level of detail that most coastal protection datasets provide, and (3) the lack of a consistent and centralized system to collect and update coastal protection information regularly on a broad scale (Vousdoukas et al., 2018a). Further uncertainties are introduced in the calculation of coastal adaptation cost, namely (4) the estimation of the unit costs of coastal flood protection which is site-specific (Lincke and Hinkel, 2018) and (5) the estimation of the coastal protection length needed to protect a coastal area which depends highly on the scale of the assessment (see chapter 2 of this thesis). Those uncertainties can modify expected annual damages between 30% to 60% in broad-scale coastal impact assessment (Vousdoukas et al., 2018a). Several coastal flood risk studies have shown that model results are most sensitive to the uncertainties in adaptation strategies (Paprotny et al., 2019, Hinkel et al., 2014) and thus, future research is needed to fill the gap of incomplete and missing data.

## 1.4. RESEARCH OBJECTIVES AND OUTLINE

This thesis aims at addressing some of the data limitations and associated uncertainties reviewed above. Specifically, the three main objectives of this thesis are:

- 1. To explore and quantify the effects of elevation, population and vertical land movement data uncertainties and assessment scale in coastal flood impact assessment**

The sensitivity of the global Dynamic Interactive Vulnerability Assessment (DIVA) modelling framework is investigated with regard to four uncertainty dimensions, namely (1) elevation, (2) population, (3) vertical land movement and (4) assessment scale in Emilia-Romagna (Italy).

- 2. To develop a consistent coastal database for the broad-scale assessment of coastal flood impacts and appropriate future interventions to SLR and ESLs**

A new open-access spatial data model and database for coastal flood risk assessment have been developed for the Mediterranean basin. The Mediterranean coast has been divided into homogeneous units in terms of impacts, vulnerability and adaptation needs to ESL and SLR. Around 13,900 coastal assessment units have been generated to which we spatially attributed 160 parameters on the characteristics of the natural and socio-economic coastal subsystems.

- 3. To develop spatially explicit urban extent projections to overcome data limitations in assessing future urban exposure on a broad scale**

Spatially explicit projections of urban extent for 10 Mediterranean countries with a spatial resolution of 100m have been developed. The urban extent projections are quantitatively and qualitatively consistent with the assumptions of the global Shared Socioeconomic Pathways (SSPs). A machine learning approach, namely Artificial Neural Networks, has been employed to develop an urban change model. The developed urban projections are then used for calculating future urban exposure to coastal flooding.

These objectives are addressed in the following four chapters of this thesis. The remainder of the thesis is structured as follows: Chapter 2 outlines analyses on the effects of elevation,

population and vertical land movement data uncertainties, and assessment scale in coastal flood impact assessment. Chapter 3 describes the development of the Mediterranean Coastal Database (MCD). In Chapter 4, urban extent projections are developed and the future urban exposure to coastal flooding is assessed for 10 countries in the Mediterranean. Chapter 5 contains a summary of the key findings of section 2 to 4. Further, recommendations for further research in the field are proposed.



# 2

## **EFFECTS OF SCALE AND INPUT DATA ON ASSESSING THE FUTURE IMPACTS OF COASTAL FLOODING: AN APPLICATION OF DIVA FOR THE EMILIA-ROMAGNA COAST**

This chapter is published as:

Wolff, C.; Vafeidis, A. T.; Lincke, D.; Marasmi, C. and Hinkel, J. (2016): Effects of Scale and Input Data on Assessing the Future Impacts of Coastal Flooding: An Application of DIVA for the Emilia-Romagna Coast. *Frontiers in Marine Science*, 3:41. doi: 10.3389/fmars.2016.00041

## ABSTRACT

This paper assesses sea-level rise related coastal flood impacts for Emilia-Romagna (Italy) using the Dynamic Interactive Vulnerability Assessment (DIVA) modeling framework and investigate the sensitivity of the model to four uncertainty dimensions, namely (1) elevation, (2) population, (3) vertical land movement, (4) scale and resolution of assessment. A one-driver-at-a-time sensitivity approach is used in order to explore and quantify the effects of uncertainties in input data and assessment scale on model outputs. Of particular interest is the sensitivity of flood risk estimates when using datasets of different resolutions. The change in assessment scale is implemented through the use of a more detailed digital coastline and input data for the coastline segmentation process. This change leads to a 35-fold increase in the number of coastal segments and in a more realistic spatial representation of coastal flood impacts for the Emilia-Romagna coast. Furthermore, the coastline length increases by 43%, considerably influencing adaptation costs (construction of dikes). With respect to input data our results show that by the end of the century coastal flood impacts are more sensitive to variations in elevation and vertical land movement data than to variations in population data in the study area. The inclusion of local information on human induced subsidence rates increases the relative sea-level by 60 cm in 2100, resulting in coastal flood impacts that are up to 25% higher compared to those generated with the global DIVA values, which mainly account for natural processes. The choice of one elevation model over another can result in differences of ~45% of the coastal floodplain extent and up to 50% in flood damages by 2100. Our results emphasize that the scale of assessment and resolution of the input data can have significant implications for the results of coastal flood impact assessments. Understanding and communicating these implications is essential for effectively supporting decision makers in developing long-term robust and flexible adaptation plans for future changes of highly uncertain scale and direction.

## 2.1 INTRODUCTION

Coastal flooding constitutes a major risk for coastal regions throughout the world and this risk is expected to worsen considerably during the twenty-first century with rising sea-levels and as future societal development increases the number of people and value of assets in the coastal floodplain (Hinkel et al., 2014). Therefore, there is a growing need of coastal communities and decision makers to access information on current and future risks as well as on strategies for managing and reducing risks. For instance, national and regional Mediterranean Coastal Administrations have expressed needs for improved methods to evaluate flood risk in Mediterranean coastal areas and to identify comprehensive plans to reduce these risks in recent years (Lupino et al., 2014).

Evaluating and managing coastal flood risk under climate change, as well as climate risk in general, requires to consider uncertainty about present and future risks as comprehensively as possible, because not considering uncertainty may only partially lead to maladaptation (Jones et al., 2014, Hinkel et al., 2015). For coastal flooding, uncertainty relates not only to

the amount or rate of sea-level rise (SLR) and socio-economic development, but also to the input data used in the analysis. While scenario uncertainty is generally explored in coastal impact assessments, data uncertainty has not received as much attention in the literature (Le Cozannet et al., 2015). Initial work carried out (Lichter et al., 2011, Mondal and Tatem, 2012) has shown that variations in estimates of area and population exposure are highly dependent on the input datasets. Hinkel et al. (2014) found that coastal flood impacts are much more sensitive to elevation data uncertainty than to, e.g., sea-level rise uncertainty stemming from the choice of climate model. Generally, a significant limitation of flood impact analysis on all scales is the unavailability of free high-accuracy datasets (Gesch, 2009, Mondal and Tatem, 2012, Neumann et al., 2015).

To our knowledge, there is, however, no study that has explored the uncertainty of coastal flood risk assessment with regard to the spatial scale of analysis and spatial resolution of input data. Scale is bound to be an essential parameter in flood risk analysis (de Moel et al., 2015) because different kinds of population, elevation and vertical land movement input data sets are available at different scales. Of particular interest thereby is the sensitivity of flood risk when switching from data sets with global coverage to local, high resolution ones, because the latter are more accurate but only available for a few regions. Comparing flood risk attained between global and local datasets thus helps to understand how accurate flood risk assessments are in regions where local high-resolution data are not available.

This paper contributes to improve our understanding of the above uncertainties in the context of global coastal flood risk assessment. We do this by taking the Dynamic Interactive Vulnerability Assessment (DIVA) flood risk module from Hinkel et al. (2014) and applying it to the Emilia-Romagna region in Italy using two scales of analysis: (i) a low resolution one based on the global coastline segmentation of Vafeidis et al. (2008) also used by Hinkel et al. (2014); and (ii) a newly developed high-resolution segmentation of the Emilia-Romagna region. The exercise is directly related to a policy process taking place within the EU-funded 'Coastal Governance and Adaptation Policies in the Mediterranean' (COASTGAP) project aiming at providing policy-relevant guidance on local coastal flood impacts of climate change.

Specifically, our research objectives are the following:

- (1) Explore the sensitivity of coastal flood risk estimates to the effects of different coastlines and segmentations
- (2) Explore the sensitivity of coastal flood risk estimates to different population and higher resolution elevation and vertical land movement input datasets

The remainder of this paper is structured as follows. Section 2.2 'Study Area, Methods, and Data' provides an overview of the study area, the coastal flood impact model, the segmentation process as well as the sensitivity analysis approach used in this Chapter. Furthermore, the underlying datasets as well as future climate and socio-economic scenarios will be described. Section 2.3 'Results' presents the sensitivity analysis from a selected number of simulation

outputs of impacts due to different input datasets and segmentations. Finally, key findings are evaluated and discussed in the 2.4 'Discussion' Section.

## 2.2 STUDY AREA, METHODS AND DATA

### 2.2.1 Overview

The determination of the effects of scale and sensitivity of impacts to different segmentations and input data follows a multi-level step procedure. The first step was the downscaling process of the assessment units using a more detailed coastline and segmentation process in order to create a data structure that enables the model to run and to be able to quantify the improvements of a more detailed coastline and segmentation. The second step was the calculation of exposure using different vertical land movement, elevation and population datasets, leading to the six datasets of various combinations of four uncertainty dimensions shown in Table 2-1. In a final step, the DIVA coastal flood module was used to assess potential flood impacts in terms of the following three parameters:

- (1) Potential floodplain extent of the 1-in-100-year extreme water level [in km<sup>2</sup>]
- (2) The average number of people flooded annually through extreme water level events [people/year]
- (3) The average annual damage caused by coastal flooding [in million US\$]

These model outputs are used in order to determine the sensitivity of the model.

**Table 2-1:** Datasets used to investigate the sensitivity of coastal impacts to the four uncertainty dimensions (coastline segmentation, elevation, population and vertical land movement).

<b>Coastline segmentation</b>	<b>Digital elevation model</b>	<b>Population</b>	<b>Vertical land movement</b>
<b>High-resolution segmentation</b>	LiDAR	LandScan	Peltier (2000) + 2mm/yr delta subsidence
	LiDAR	GRUMP	Peltier (2000) + 2mm/yr delta subsidence
	SRTM	LandScan	Peltier (2000) + 2mm/yr delta subsidence
	SRTM	GRUMP	Peltier (2000) + 2mm/yr delta subsidence
	LiDAR	LandScan	PInSAR
<b>Global segmentation</b>	SRTM	GRUMP	Peltier (2000) + 2mm/yr delta subsidence

## 2.2.2 Study Area

Emilia-Romagna is situated in the southern part of the Po basin in northern Italy (see Figure 2-1). It is inhabited by 4.4 million people and covers an area of 22,124 km<sup>2</sup>. The gross domestic product (GDP) per capita in Emilia-Romagna is 24,396 Euro (ISTAT, 2009), which is higher than the national average (20,043 Euro). The coastal strip is often higher in elevation than the hinterland, of which more than 100,000 ha are below sea-level (Preti et al., 2009). The low-lying coastal strip is characterized by different levels of human modification and development. The level of modification is ranging from natural to urbanized areas (93 km of the coast or 71% are urbanized). The coastline of urbanized regions has remained relatively stable due to human intervention such as hard shoreline protections or beach nourishment (Armaroli et al., 2012). Hard shore protection, mainly offshore breakwaters, protects 60% of the coastline from flooding and erosion (Nordstrom et al., 2015). The entire region is currently experiencing a sediment deficit which is a result of decreasing fluvial sediment transport caused by stabilization of slopes and hydraulic works along the river bed. Furthermore, there is a current interruption of long-shore sediment transport due to shore protection structures. More than 10 million m<sup>3</sup> of sediment was replenished to the beach of Emilia-Romagna between 1983 and 2012 (Montanari and Marasmi, 2014).

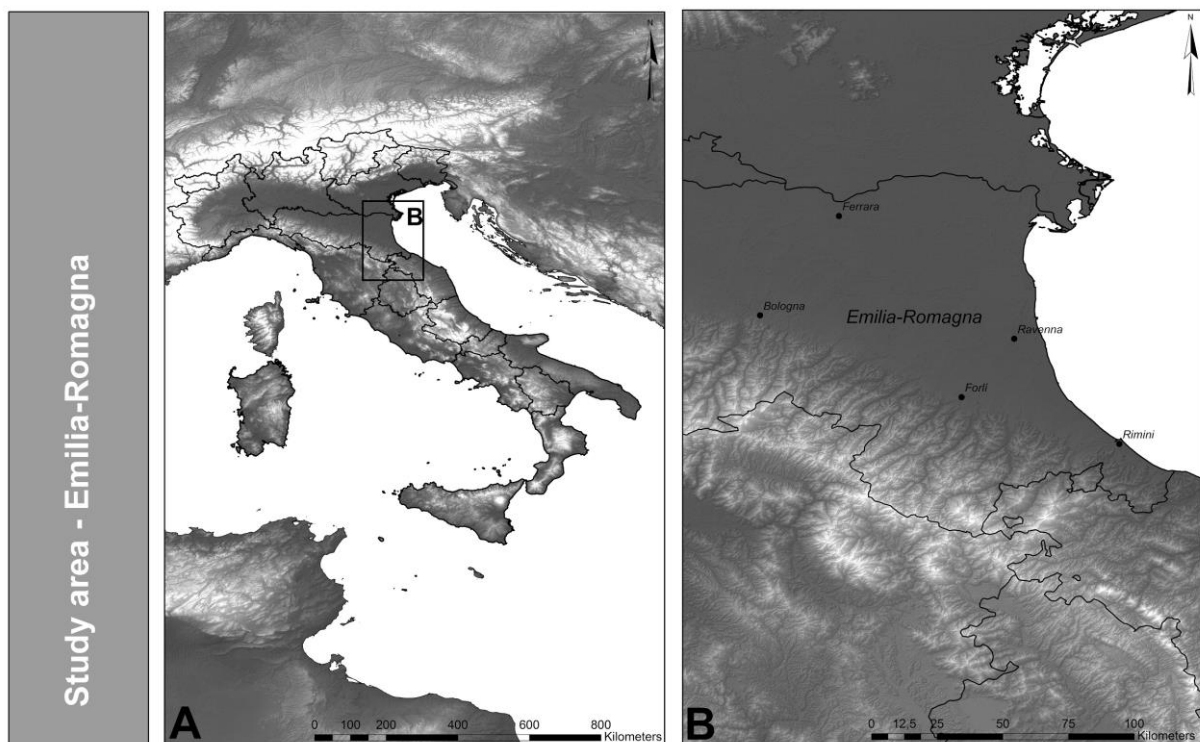


**Figure 2-1.** Study area—Emilia-Romagna. (A) Italy (B) Emilia-Romagna.

The dominant coastal type is considered to be sandy beach with an average width of 70 m (emerged beach). Wave energies are normally low in Emilia-Romagna. The wave height is

generally below 1.25m (91%), but storms from the south/southeast (Scirocco) and northeast (Bora) result in high waves and storm surge levels. According to Houtenbos et al. (2005), the relative sea-level rise is higher in Emilia-Romagna than the global eustatic component due to subsidence. Along the Emilia-Romagna coastal area, the degree of subsidence due to natural causes entails a few millimeters per year, while the anthropogenic subsidence has reached high speeds of 50 mm/ year in the 80's. Main drivers to cause anthropogenic subsidence include underground extraction of water and natural gas. The Integrated Coastal Zone Management (ICZM) effort in the Emilia-Romagna region started in 2002 and ended with the emanation of ICZM Guidelines approved by the Regional council in the beginning of 2005. They represent the tool to address all coastal activities toward economic, social and environmental sustainability, in compliance with EU Recommendation of the 30th May 2002. According to Preti et al. (2009), the touristic use dominates nearly 85 km of the coast. With more than 36 million overnight stays per year, Emilia-Romagna is one of Italy's most attractive tourist destinations.

## 2.2.3 Methods

### 2.2.3.1 Calculating Flood Risk

We used the DIVA (Dynamic Interactive Vulnerability Assessment) coastal flood module (Version 5.0.0) as presented in Hinkel et al. (2014) in order to calculate coastal flood impacts over the next century. The DIVA model operates on data attributed to coastline segments. Global applications of DIVA used a segmented coastline of the world, which comprises 12,148 units of variable length (average of 70 km) based on Vafeidis et al. (2008). Every segment represents a uniform response to SLR within the coastal system. More than 80 physical, ecological and socioeconomic parameters (e.g. uplift/subsidence in mm/year or coastal population) of the world's coastal zone (excluding Antarctica) are spatially referenced to these units. DIVA is driven by climatic and socioeconomic scenarios, which will be described in Section 2.2.4.1 'Sea-Level Rise Scenarios' and 2.2.4.2 'Socio-Economic Scenarios'. One important innovation introduced by DIVA is the explicit incorporation of a range of adaptation options, as impacts do not only depend on the selected climatic and socio-economic scenarios but also on the selected adaptation strategy. Possible adaptation strategies in the DIVA modeling framework in order to reduce coastal flood risk are the construction of dikes.

DIVA's flooding module uses a cumulative people and asset exposure function in order to estimate the potential socio-economic impacts of coastal flooding. In order to get the potential number of people living below a certain elevation level and therefore prone to flooding, a digital elevation model (DEM) was combined with a spatial population dataset (a more detailed description of the calculation can be found in Section 2.2.4.4 'Exposure Data'). Based on extreme water levels given for different return periods in the DIVA database (Vafeidis et al.,

2008) the potential exposed area and number of people living in these areas is calculated using a bathtub approach. The extreme water levels within the DIVA database were calculated based on the methodology described in Hoozemans et al. (1993). Relative sea-level rise is then added to the current extreme water level probability distribution, leading to shorter average return periods of flood levels. Hinkel et al. (2014) compute the number of people flooded by only making the binary distinction between flooded and not flooded. The estimation of the value of assets on a given elevation is done by multiplying the number of people with the GDP per capita times an empirically estimated GDP-to-assets ratio of 2.8 taken from Hallegatte et al. (2013). The amount of damage depends on the depth by which the asset is flooded. Hinkel et al. (2014) uses a depth-damage function in order to calculate the fraction of assets that will be damaged when flooded by a certain depth. The depth-damage function reflects the fact that the damage rate decreases with increasing water levels. It is assumed that a flood depth of 1 m destroys 50% of the assets. According to Hinkel et al. (2014), this assumption is a good indication based on the information available to date. If dikes are present, a damage of 0 is assumed for floods lower than the actual dike height. By default, a dike is constructed if at least 1 person per km<sup>2</sup> lives on the coast. The dike height is calculated based on a demand for safety function, which depends on the GDP per capita and population density. Following this function, dikes are built and upgraded for each coastline segment in each time step (5 years) until 2100. Future exposure is attained by applying national population and GDP growth rates of the socio-economic scenarios (Hinkel et al., 2014). A more detailed description of the coastal flood module used in this study can be found in Hinkel et al. (2014).

#### 2.2.3.2 Coastline Segmentation

In order to downscale the assessment scale of DIVA it was necessary to refine the existing coastline and segmentation. The segmentation is an essential step in order to generate a data structure that enables the model to run, and it defines the scale of assessment. The original DIVA segmentation was based on a digital global coastline data set (ESRI, 2002), with a cartographic scale of 1: 3,000,000. As this level of scale is too general for the purpose of a sub-national study due to the loss of important coastal features, a more detailed digital coastline was employed (see Section 2.2.4.3 'Coastline Segmentation Data'). This coastline was then segmented into units, based on the original concept of McFadden et al. (2007) and using the following parameters relevant for coastal-flood risk assessment and management (1) administrative boundaries, (2) the geomorphic structure of the coastal environment, (3) the expected morphological development of the coast given sea-level rise and (4) population density. We extended those parameters to also include (5) river mouths as these often have a much greater RSLR due to subsidence than other areas.

### 2.2.3.3 Sensitivity Analysis

A sensitivity analysis aims at exploring how much model outputs are affected by changes in input data (Saltelli et al., 2000). We used a simple One-Driver-At-a-Time (OAT) approach. This single factor approach is undertaken by modifying one input variable, e.g., the elevation data, while keeping all remaining inputs consistent. This enables us to explore and to systematically quantify the impacts of different assumptions on the calculated flood impacts. Sensitivity is calculated as the difference between the impacts in 2100. It is a useful method in order to identify key drivers which strengthen the understanding and interpretation of the DIVA modeling framework. In this study we do not quantify how interactions between input factors affect the variability of the model results, as the generation of input data for each point in the uncertainty space considered is computation and labor intensive. For each data point a large number of processing steps is required as the coastline needs to be segmented and the database needs to be populated with e.g., population, vertical land movement, and elevation data. Therefore, deriving more data points for conducting a general sensitivity analysis was not possible within the scope of this study.

## 2.2.4 Data

### 2.2.4.1 Sea-Level Rise Scenarios

We use regional SLR scenarios of Hinkel et al. (2014), which are based on the Representative Concentration Pathways (RCP) 2.6, 4.5, and 8.5 and comprise the following two main components:

(1) The steric contribution, produced by the Hadley Global Environment Model2–Earth System (HadGEM2-ES) (Collins et al., 2008).

(2) Land ice contribution consisting in the mass contribution of glaciers and ice caps, based on Marzeion et al. (2012). The mass contribution of the Greenland ice sheet and peripheral ice caps taken from Fettweis et al. (2013) and the mass contribution from the Antarctic based on Levermann et al. (2012). By combining the three mass contributions a low (5<sup>th</sup> percentile), medium (50<sup>th</sup> percentile) and high (95<sup>th</sup> percentile) land-ice scenario was created (see Table 2-2). These scenarios also consider gravitational, rotational and local land uplift effects that results from changes in ice masses and ocean circulations. To implement these effects, the model of Bamber and Riva (2010) was used which considers a uniform mass reduction over the ice sheets.



**Table 2-2:** Global mean sea-level rise in 2100 with respect to 1985-2005. (the median and, in parentheses, the 5% and 95% percentiles are provided) (Hinkel et al., 2014)

Scenario	Model	Steric [cm]	Mass [cm]				Total [cm]
			Glacier	Antarctica	Greenland	Sum	
RCP2.6	HadGEM2-ES	14	14 (14,15)	7 (2,23)	0 (0,0)	21 (16,39)	35 (29,52)
RCP4.5	HadGEM2-ES	18	17 (16,19)	8 (2,29)	7 (5,8)	32 (23,56)	50 (41,75)
RCP8.5	HadGEM2-ES	29	22 (20,26)	10 (2,41)	12 (10,14)	44 (31,81)	72 (60, 110)

For this study, we use three SLR scenarios that sample the full uncertainty space covered by Hinkel et al. (2014). A lower bound scenario (RCP2.6 combined with the 5% quantile of ice-melting projections), hereafter referred to as low SLR, a medium scenario (RCP 4.5 combined with the median), referred to as medium SLR, and an upper bound scenario (RCP8.5 combined with the 95% quantile), referred to as high SLR. The sea-level scenarios for Italy vary between 31 (low SLR scenario) and 122 cm (high SLR scenario) by the end of the twenty-first century (see Figure 2-2). For every coastline segment, the relative sea-level rise is generated by linking the regional sea-level rise values with the vertical land movement.

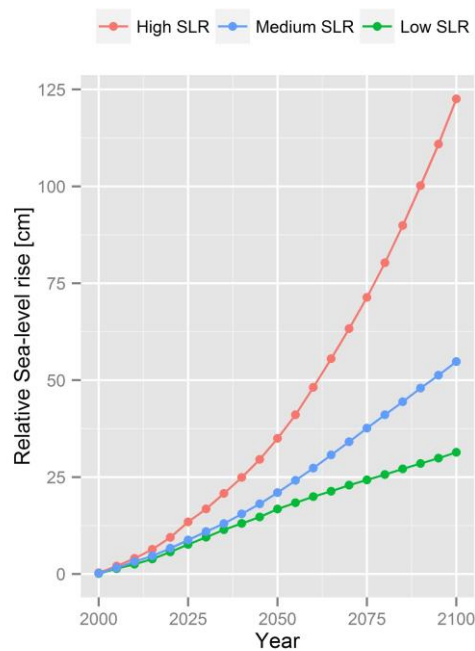


**Figure 2-2.** The average relative sea-level rise for Emilia-Romagna under all sea-level rise scenarios.

#### 2.2.4.2 Socio-Economic Scenarios

Three socio-economic scenarios have been used, based on the IPCC Shared Socio-economic Pathway (SSP) storylines (O'Neill et al., 2014), to present a range of potential future development directions in the Emilia-Romagna region. The SSP3 storyline assumes a high population growth and a slow economic development and represents a fragmented world. In

this storyline the world is separated into extreme poverty, moderate wealth and a bulk of regions that struggle to maintain living standards for a rapid growing population. The SSP5 represents a conventional development which is oriented toward economic growth. The population growth is generally low. SSP2 assumes medium growth in socio-economic development worldwide.

The amount of assets and people that will be located in the coastal zone determines the future exposure to coastal flooding. In DIVA the two variables population growth and GDP growth are the main drivers to determine future socio-economic development. The total population of Italy ranges between 22.8 and 75.4 million (see Figure 2-3) and the GDP per capita between 27,716 to 160,602 US dollar by 2100 (see Figure 2-4) following the SSP storylines. Those growth rates are applied to the exposure data in order to estimate future coastal flood impacts. According to the global flood risk assessment conducted by Hinkel et al. (2014), the flood costs are highest for SSP5 (economic growth) and lowest for SSP3 (security), reflecting the socio-economic growth rates developed by Kc and Lutz (2017). In order to cover the full range of uncertainty and future pathways, SSP3 and SSP5 have been chosen as well as SSP2 which reflects a world with medium assumptions.

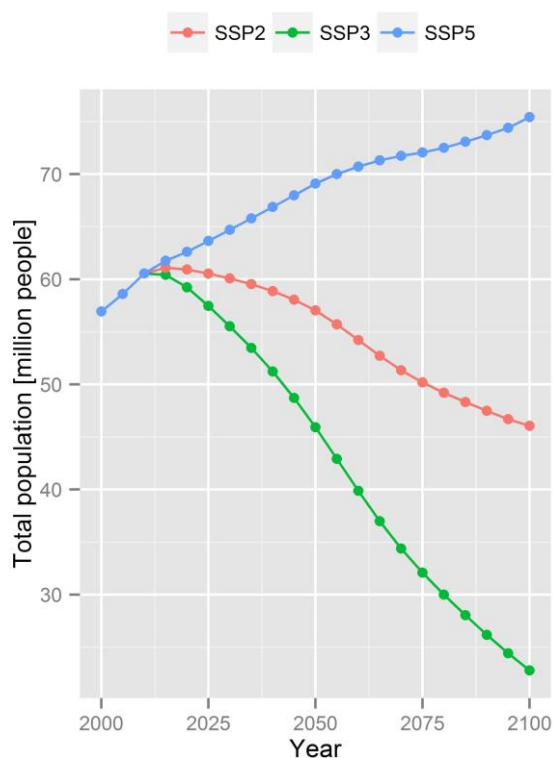


**Figure 2-3:** Total population of Italy for each Italy for storyline used in this study.

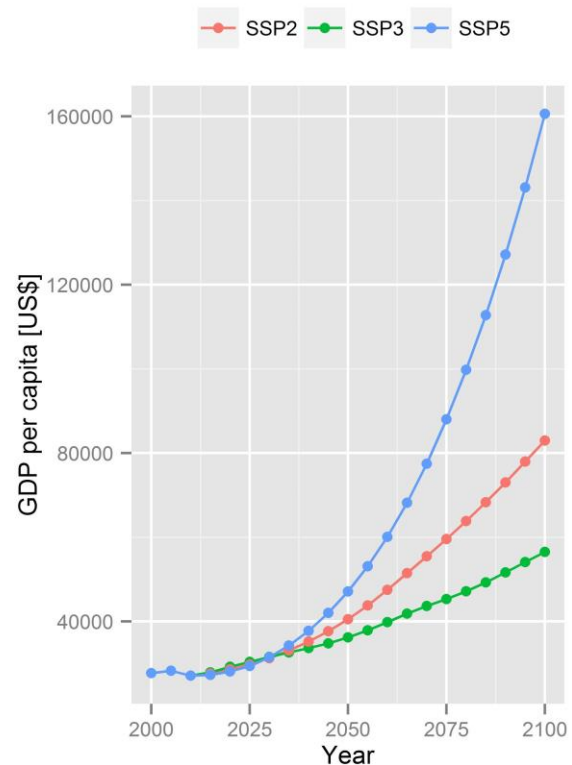


**Figure 2-4:** GDP per capita in each storyline used in this study.

### 2.2.4.3 Coastline segmentation data

For this study, the coast has been re-segmented using a more detailed digital coastline (see Appendix A - Supplementary Figure 2-1 for a comparison between the global and detailed coastline) and data. We selected the Global Administrative Areas (GADM, <http://www.gadm.org/>) level 01 coastline and corrected artifacts related to the format (e.g. “pixelization” of coastline) using a smoothing algorithm (polynomial approximation) and a tolerance of 100 m.

The availability of consistent datasets on coastal morphology and characteristics is a common limitation for global-, regional-, and national-scale impact assessments. Due to the lack of consistent coastal morphologies and geological characteristics data for the Emilia-Romagna region, an independent consistent data set was generated with Google earth. Google earth provides free satellite images and aerial pictures (Chang et al., 2009) for the whole study area. Based on the concept described in Scheffers et al. (2012), seven different classes [(i) sandy, (ii) unerodible, (iii) pebble, (iv) rocky with pocket beaches, (v) sandy with wave-breakers, (vi) muddy and (vii) fortified coast – see Figure 2-5B] have been classified based on visual interpretations of Google Earth imagery and location-tagged photographs from the web-service Panoramio which offers geographically tagged photographs from users. The coastline was split every time the type of coast changed.

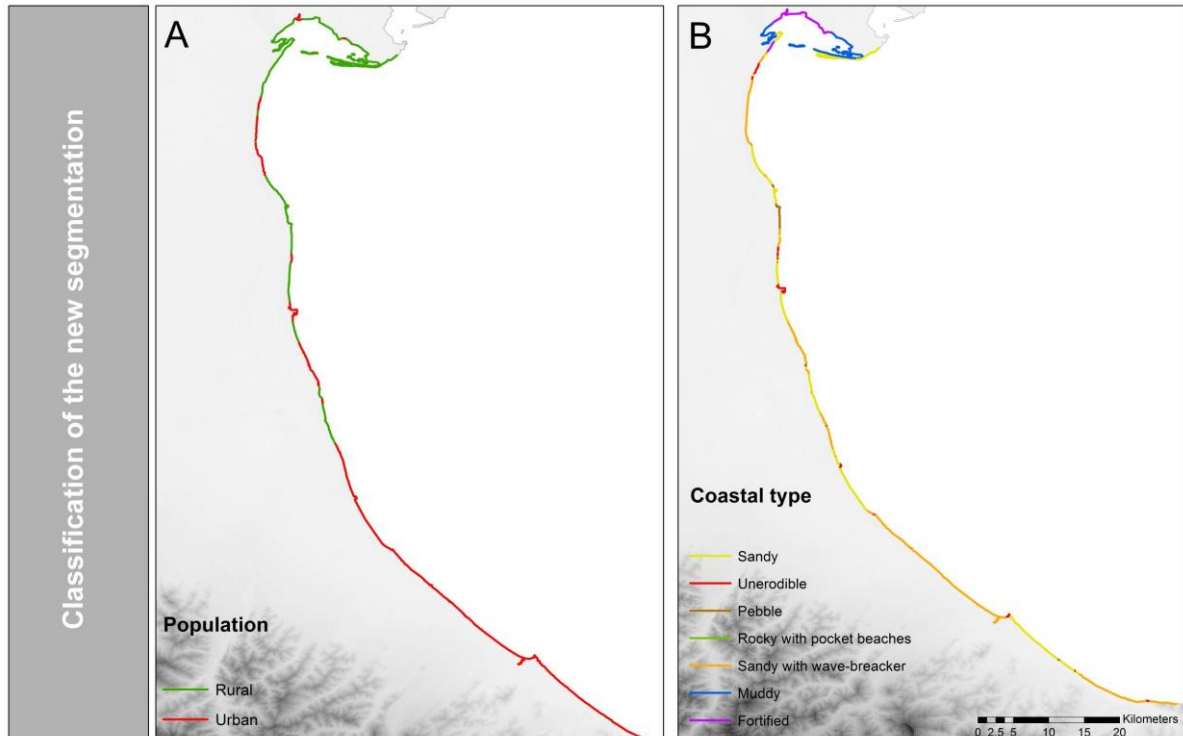


**Figure 2- 5:** Results of the high-resolution segmentation model. (A) Coastal settlements. (B) Coastal typology classification.

The coastal plain characteristics were segmented with the help of the geomorphic structure data developed by McGill (1958). The parameter provides information about the geomorphology and elevation of the coast. The third biophysical parameter is the river mouth layer. This layer was created with the help of Google earth as well. The population density information splits the coast into two classes, (i) urban/human settlements and (ii) rural (see Figure 2-5A). This indicates variations in the population distribution of the Emilia-Romagna coast which is essential for the assessment of vulnerability to SLR, as e.g. dikes are only built where people are actually living. This spatial dataset was derived with the help of satellite images from Google earth. Furthermore, according to (McFadden et al., 2007), institutional and governmental arrangements play an important role in defining the response of coastal systems to an accelerated sea-level. The inclusion of the political system (GADM level 03) is therefore important as different political and administrative controls react differently to SLR in terms of adaptation strategies. Finally, the created layers, described before, were overlaid in order to create segments that represent a uniform response to sea-level forcing.

#### 2.2.4.4 Exposure Data

The segmentation creates units for the analysis (data structure) to which information (e.g., elevation or population data) is attached. Hence, after the segmentation the DIVA database was populated and updated with the help of the data provided from the COASTGAP partners or with the DIVA data. Topography or elevation is one of the main parameters that determine the vulnerability of coastal zones to sea-level rise. In order to assess areas exposed to inundation, two different digital elevation models were used. First, the freely available (1) Shuttle Radar Terrain Mission (SRTM) digital elevation model (Jarvis et al., 2008). It has a vertical resolution of 1 m and spatial resolution of 03 arc seconds (~90 m at the equator). The SRTM (datum wgs84) employs an imaging radar system. It is important to note that the elevation represents the height of the first reflective surface. In open terrain, the SRTM elevation will represent the ground elevation, but in vegetated or urban areas the ground-elevation might be overestimated. According to Gesch (2009), this mix of ground elevation and non-bare ground elevation in SRTM data could be a source of error in inundation mapping in vegetated and urban areas (Baugh et al., 2013, Lewis et al., 2013, Griffin et al., 2015). The second data set used is the (2) Light Detection And Ranging (LiDAR) digital elevation model (datum wgs84) with a spatial resolution of 5 m and a vertical accuracy of ( $\pm$ )20 cm which was provided by the Emilia-Romagna region. LiDAR employs the airborne laser scanning technique which can resolve a point density of 2 points per m<sup>2</sup>. Both the 90 and 5m-resolution data have been used in order to calculate the exposure of areas. A simple 'bathtub approach' in which a grid cell becomes flooded if it is below a certain elevation has been used. In order to reflect surface flow connections, an eight-side-rule has been used, where the grid cell becomes a flooded grid cell if the cardinal and diagonal directions are connected. Following this approach, a mask that represents areas hydrologically connected to the sea was created. Afterwards, buffer zones per coastline segment have been produced in order to calculate the number of

pixels flooded per segment. The zones also extend seaward, in order to ensure the inclusion of population mismatching which is important in order to calculate exposure of people. As local population data was unavailable, two different global population data sets have been used in order to calculate the exposure of people. The population count datasets of LandScan (2006) (Bright et al., 2007) and the Global Rural Urban Mapping Project (GRUMP 2000) (Center for International Earth Science Information Network - CIESIN - Columbia University et al., 2011) were obtained. Both have a spatial resolution of 30 arc seconds and are based on census population counts. The main differences are the base year, administrative levels of input data and the modeling approach used to allocate and disaggregate these data (Mondal and Tatem, 2012). The total global population between those two population datasets varies by around 8% (Lichter et al., 2011), mainly due to the different base years. In this study, this deviation has been recalculated afterwards to the common base year 1995, using the growth rates of the SSP scenarios. The LandScan global population project allocated annual midyear population estimates, usually at province level, based on weightings derived from land cover, roads, slope, urban areas, and high-resolution imagery analysis. It represents an 'ambient' population distribution and hence, presents a highly modeled population distribution. In contrast to that, GRUMP was produced by population census data from administrative units and was originally developed in order to reallocate census population counts to urban and rural areas. People were not only redistributed based on areal weighting, but urban populations were also reallocated based on night-time light as GRUMP defines population distribution according to where people actually live (Mondal and Tatem, 2012). Exposure was calculated by combining the information on elevation data with the population distribution data. The number of people at risk was calculated by summarizing population per elevation per increment, per coastline segment. Those values were stored as attributes to the coastline segment.

#### 2.2.4.5 Vertical Land Movement Data

Vertical land movement is a downward (subsidence) or upward movement (uplift) of the land relative to sea level. Subsidence often occurs in regions associated with alluvial sediments, such as deltas (Ericson et al., 2006) as in the case of the study area, Emilia-Romagna. In this study we compare the vertical land movement of global modeled datasets, which are often used in flood risk assessment, with higher resolution local datasets, which are often not available for flood risk assessments because they are expensive to generate. In particular we consider a global model of glacial isostatic adjustment of Peltier (2000) together with an estimated 2mm/year subsidence for delta regions as used by Hinkel et al. (2014). Human-induced subsidence rates were not considered. However, it is an important parameter for regions such as Emilia-Romagna where human-induced subsidence due to extraction of water, oil and gas (Armaroli et al., 2012) is an issue. Data that include both natural and human-induced subsidence were available for this study through the COASTGAP partners. The data were generated from the Permanent Scatter Interferometric Synthetic Aperture Radar

(PSInSAR). According to Ferretti et al. (2001), the PSInSAR is a surface displacement observation technique based on conventional radar interferometry. The data was provided by the Emilia-Romagna region in a raster format with a spatial resolution of 100m. The coastal vertical land movement was calculated by combining the area below 3 m with the PSInSAR data. The coastal vertical land movement was calculated by averaging the rates per zone. Afterwards, the values were joined to the coastline segment. Table 2-3 shows the Peltier (2000) + 2 mm/year delta subsidence and PSInSAR values used in this study.

**Table 2-3:** Comparison between mean, maximum and minimum values of the globally modeled and locally measured vertical land movement data for the study area. Positive values indicate subsidence while negative values indicate uplift.

mm/year	Mean	Min	Max
Peltier (2000) + 2mm/yr delta subsidence	0,14	0,15	0,14
PSInSARs	4,88	0,59	19,62

## 2.3. RESULTS

### 2.3.1 Segmentation

For the Emilia-Romagna coastline the global segmentation produced three segments with an average segment length of 40 km (minimum length 5.5 km, maximum length 98.8 km, total: 121.5 km). In comparison, the high-resolution segmentation generated 113 segments with an average length of 1.5 km (minimum length is 0.03 km, maximum length is 11.2 km, total: 174.6 km). Thus, the coastline length increased by 43% (53.1 km). The high-resolution segmentation has a 28-fold increase compared to the global DIVA assessment scale referring to the average length of segments. In the global DIVA database, the entire coast of Emilia-Romagna was characterized by a sandy coastal morphology and urban settlements while in the new version a more detailed distinction (e.g. 57 segments or 86 km represents coastal settlements, 55km are classified as sandy plus 59 km as sandy with wave breaker - see Figure 2-5) was made. The comparison of the different segmentation models indicates that the new segmentation approach increased not only the length of the coast but also the spatial representation of impacts in the Emilia-Romagna region (see Figure 2-7).

### 2.3.2 Sensitivity to Segmentation

Using the high-resolution segmentation, the 100-year floodplain has an extent of 3309 km<sup>2</sup> (using the SRTM elevation model), assuming a high SLR, in 2100. That covers 15% of the entire area of Emilia-Romagna. The potential flood area extent differs by 789 km<sup>2</sup> depending

on the scale and resolution of assessment in 2100 (see Table 2-4). This situation shows that even if the underlying data (SRTM) remains the same, the total local values deviate due to the different scale of analysis. The main reason for that is the creation of buffer zones (see Appendix A - Supplementary Figure 2-2) which were used in order to calculate the exposure statistics per increment.

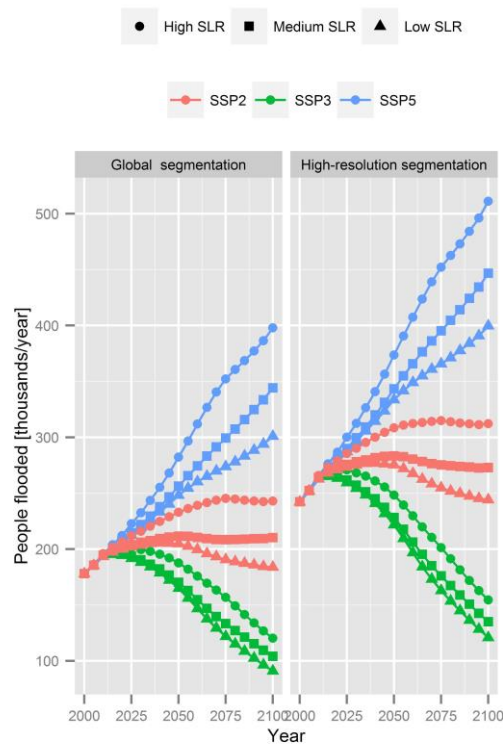


**Figure 2-6:** Average annual people flooded from 2000 to 2100 under all SLR scenarios.

The average number of people potentially flooded annually through extreme water level events is presented in Figure 2-6. The results depend on the coastal topography, population, and adaptation strategy, as well as sea-level rise and socio-economic developments. Assuming that there are no protection measures in place, the number of people flooded varies between 90,909 and 511,198 people in 2100, using different assessment scales.

**Table 2-4:** Sensitivity of coastal flood impacts to the four uncertainty parameters in 2100 (SSP5, high SLR). The impacts represent an average difference while only one of the listed parameters is modified at a time.

Uncertainty dimension	Area of the 100-year floodplain [km <sup>2</sup> ]	Number of people flooded annually	Flood cost [million/US\$]
Elevation	1,049 (46%)	119,839 (33%)	37,368 (49%)
Vertical land movement	93 (4%)	9,1458 (18%)	19,826 (26%)
Population	-	26,476 (08%)	576 (0.8%)
Segmentation	789 (31%)	113,349 (28%)	279 (0.2%)

In the worst case, the choice of one particular assessment scale over another can result in an additional difference of 2.6% concerning the total population of Emilia-Romagna at risk. The spatial distribution of the people at risk per coastline segment for both assessments scales is presented in Figure 2-7. The detailed coastline represents the spatial distribution of people at risk more realistically, due to the more refined assessment scale and the increase of units.

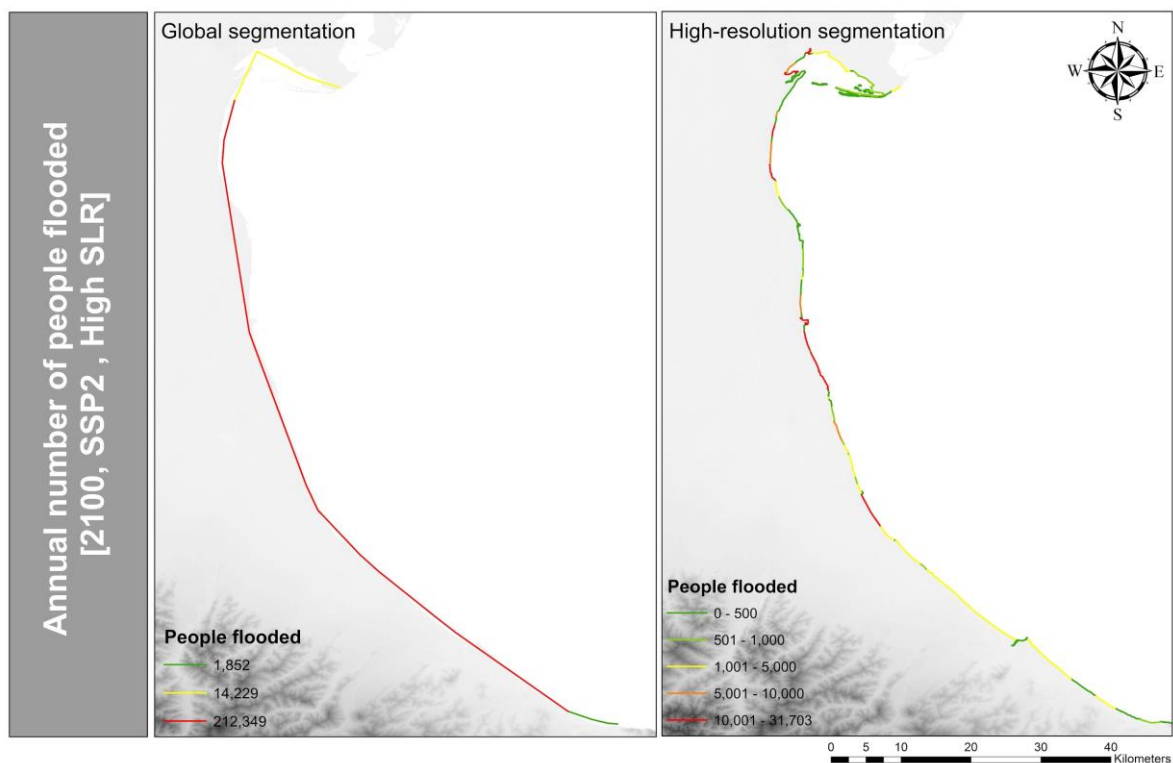


**Figure 2-7:** Comparison of the spatial distribution of the expected number of people flooded annually using the global and high-resolution segmentation in 2100 (SSP2, High SLR).

Impacts are also very sensitive to population density threshold that determines when dike building starts. Setting this threshold is a normative decision depending on the risk preferences of coastal societies. If this threshold is set to 1 person per km<sup>2</sup>, the entire coastline of the Emilia-Romagna is protected by dikes for both assessment scales (see Table 2-5). Considering



a dike construction threshold of 10 people per km<sup>2</sup>, 94% of the coast will be protected via dikes using the high-resolution segmentation assuming a medium SLR in 2100. In contrast, no change in the protection length was observed in the study area using the global assessment units. A threshold of 100 people per km<sup>2</sup> decreased the dike length by 36% using the detailed coastline and by 14% using the global coastline segmentation. The flood cost varies up to 279 million US dollar due to the change in the assessment scales. To conclude, the change in assessment scale, namely the increase of segments and length, showed a high sensitivity in this study (see Table 2-4).

**Table 2-5:** Protected coastline length and cost of dikes for different dike construction thresholds using two different assessment scales in 2100 (medium SLR).

<b>Dike building threshold</b>		<b>1 People/km<sup>2</sup></b>	<b>10 People/km<sup>2</sup></b>	<b>100 People/km<sup>2</sup></b>
High-resolution segmentation	Dike [km] (%)	174 (100%)	164 (94%)	112 (64%)
	Dikecost [millions US\$/year]	2.4	2.3	1.5
Global segmentation	Dike	121 (100%)	121 (100%)	104 (86%)
	Dikecost [millions US\$/year]	1.7	1.7	1.4

### 2.3.3 Sensitivity to Elevation Data

The coastal flood impact calculation showed the highest sensitivity to the change in the elevation data in this study (see Table 2-4). The estimated areas exposed to coastal flooding are smaller with LiDAR DEM than those calculated with the SRTM DEM. This leads to an increase in the exposed area and potential coastal flood impacts. The choice of one particular elevation model over another can translate to a difference of more than 1049 km<sup>2</sup> of the current potential 100-year floodplain (see Table 2-4). The floodplain increases by 4 to 26% in 2100 (referring to 2015), depending on the elevation model and sea-level rise scenario chosen. The differences of potential impacts using different digital elevation models decrease toward the end of the century when using a higher SLR scenario. This situation occurs due to the large differences between two elevation models in the area below 5 m. Those low-lying areas mainly influence the extent of the 100-year floodplain. Hence, the influence of the data sets used is higher under a low sea-level rise due to the fact that the elevation data differs the most at low elevations, as illustrated in Figure 2-8.

**Table 2-6:** 100-year floodplain under three different SLR scenarios using LiDAR and SRTM (today and in 2100). The sensitivity is calculated based on the difference between various potential flood areas.

Potential flood area (km <sup>2</sup> )	2015	2100		
		Low SLR	Medium SLR	High SLR
LiDAR	1,783	1958	2033	2260
SRTM	2,819	3060	3126	3309
Sensitivity	1,036 (58%)	1,102 (56%)	1,093 (53%)	1,049 (46%)

The potential of people exposed to annual coastal flooding and the average of annual damage caused by coastal flooding showed a high sensitivity to the change in elevation data (see Table 2-4). The potential impacts of coastal flooding are higher using the SRTM elevation model due to increasing areas at risk of coastal flooding (as shown in Table 2-6). The difference of 33% in the potential flood area leads to an increase of 49% in flood costs and to a 46% higher amount of people at risk compared to the impacts calculated with the LiDAR elevation model.

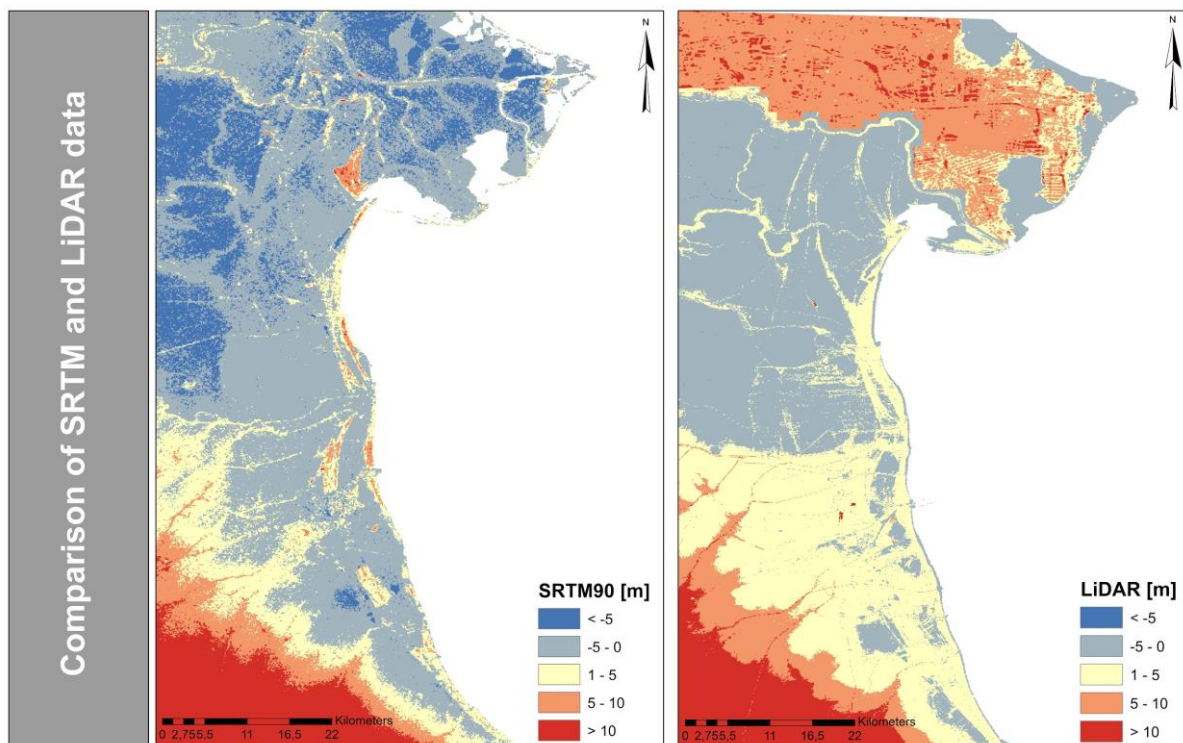


**Figure 2-8:** Comparison of the SRTM90 and LiDAR digital elevation data for the Emilia-Romagna region.

### 2.3.4 Sensitivity to Vertical Land Movement Data

The inclusion of measured data on human induced subsidence rates in the vertical land movement data led to an increase of relative sea-level rise (see Table 2-7). In 2100, an additional relative sea-level rise of 60 cm is reached, using the PSInSAR data which has a higher influence than the low and medium sea-level rise scenarios used in this study. This leads to a significant increase in the potential impacts as it increases the exposure of people and area to coastal flooding due to the landward displacement of the flood extent.

**Table 2-7:** Comparison of relative sea-level rise values using the old DIVA and the PSInSAR values.

RSLR [m]	Peltier 2000			PSInSAR		
	Low SLR	Medium SLR	High SLR	Low SLR	Medium SLR	High SLR
2000	0.00	0.00	0.00	0.03	0.03	0.03
2050	0.16	0.21	0.34	0.48	0.52	0.66
2100	0.31	0.54	1.22	0.91	1.15	1.82

The expected annual number of people flooded is highest using the PSInSAR vertical land movement data under SSP5, reflecting the highest population numbers, and a high SLR. The influence of the change in data is highest under the low SLR scenario and lowest under the high SLR scenario in 2100. Impacts intensify throughout the century under all socio-economic scenarios. Using the PSInSAR vertical land movement data, including human induced subsidence, impacts are up to 25% higher (e.g. flood cost) than those estimated using the DIVA values, which only account for natural processes.

### 2.3.5 Sensitivity to Population Data

Model outputs were least sensitive to variations of population data (see Table 2-4). The estimated number of exposed people using GRUMP is smaller than those calculated with LandScan. The total amount of population for Emilia-Romagna using the LandScan dataset is 0.7 % higher than using the GRUMP (total population of Emilia-Romagna using GRUMP: 4,016,951 and LandScan: 4,046,404). Due to the different reallocation methods and administrative levels of input data (explained in Section 2.4.4.3 'Coastline Segmentation Data') the number of estimated people exposed to coastal flooding differs with respect to the two datasets. In an area of around 15%, which represents the potential 100-year flood plain of Emilia-Romagna using the SRTM elevation model, approximately 10 % of the total population of Emilia-Romagna is living in the flood plain and therefore is potentially at risk to the 100-year surge. The expected number of people annually flooded due to the switch in datasets differs by 26 476 people (8 %) in 2100. The potential coastal flood cost differs by 576 million US dollar (0.8 %; see Table 2-4).

## 2.4. DISCUSSION

### 2.4.1 Effects of Different Coastlines and Segmentations to Coastal Flood Impact Assessment

Within the framework of the COASTGAP project and for the purpose of the current analysis, the DIVA assessment scale has been downscaled to be applicable at a sub-national scale. The distribution of features along the coast, the scale of the coastline and the defined classes for each parameter as well as available data used in order to segment the coast, determines the number of segments that were produced. The main effect due to the change in scale of the coastline was the increase in coastal length which influences adaptation cost (construction of dikes) considerably. The change in assessment units (segmentation), namely the increase of segments and the decrease of segment average length led to a high sensitivity of model outputs in this study. The main difference results from the creation of buffer zones which depend on the shape of the coast and segment (see Section 2.2.4.3 'Coastline Segmentation Data' and Appendix A - Supplementary Figure 2-2) that was used in order to calculate the exposure per segment. Using the global segmentation model and buffer zones, parts of the flood extent are potentially added to the neighboring administrative unit as the segments are quite large. Hence, one main improvement of the refined segmentation is the increased spatial accuracy of impacts on a sub-national scale as the number of segments and zones increase (see Figure 2-7). Thus, impacts are more concentrated and spatially accurate than before. This improves the assessment by making future predictions more realistic than before and suggests that the refined segmentation is more appropriate to be used when more detailed data (e.g. population) become available or underlying normative assumptions, such as dike building computation, are adopted for more detailed application. Thus, even if the underlying data improve, model algorithms/assumptions may also need to be adjusted to represent sub-national to local processes more realistically.

The aim of the COASTGAP project was to develop adaptation policies to reduce risk along the coast and to create new common tools and opportunities for coastal zone development in the Mediterranean. The developed approach can be used to support this development as it would enable consistent and comparable coastal flood impact assessments for local policy makers with limited data availability. The approach can also be useful for the implementation of the provisions of EC Directive 2007/60 in the assessment and management of flood risks which entered into force in 2007 (2007/60/EC). In particular, the Directive now requires Member States to assess if all water courses and coastlines are at risk from flooding, to map the flood extent, assets, humans at risk in these areas and to take adequate and coordinated measures to reduce this flood risk. These requirements can be realized by applying the DIVA modeling framework for the respective calculations. On a more refined scale it is more realistic to identify hot spots, for instance where people are at risk of coastal flooding (see comparison Figure 2-

7) or calculate adaptation needs. This simplifies the identification of priority regions that are highly vulnerable to SLR and need further research effort. Future work could be a scoping study in the Mediterranean using a downscaled version of the DIVA model in order to serve the need for basic information to politicians and decision-makers on the overall risk situation in the coastal zone and pinpoint hot spots. Finding the appropriate spatial scale which is most relevant for the objective of the research question or decision makers is highly important as vulnerability to SLR in the coastal zone is scale-dependent (Sterr, 2008, Fekete et al., 2010). It is important to keep in mind that a more detailed method to calculate coastal flood impacts requires more effort per unit of an area. The developed approach could be a starting point to close the gap and assess impacts and risk at an intermediate scale using a global coastal flood impact model. Furthermore, the link between different spatial scales could be a promising future research area as it would enable rapid coastal flood impact assessments with limited data and enable consistent and comparable coastal flood impact assessments worldwide (de Moel et al., 2015).

#### 2.4.2 Model Sensitivity to Input Data

Results of the study showed a high sensitivity to the change in elevation input data, which is consistent with previous studies (e.g. Poulter and Halpin (2008), Lichter et al. (2011), Hinkel et al. (2014)). Nevertheless, it is difficult to compare those studies as the estimates of area and population exposure in the coastal zone vary depending on the scale (global to local), input datasets (e.g. SRTM, Globe, Aster, LiDAR), methods (e.g. hydrological connectivity rule) and objectives of the study. According to Gesch (2009), the identification of areas exposed to a certain sea-level rise scenario improves considerably when higher-resolution and -accuracy data, such as LiDAR data, are used. He found the inundation area to be two times higher when the vertical accuracy of coarser elevation datasets, such as GTOPO30, is considered in the calculation of area exposure. In contrast to that, the LiDAR-based exposure calculation increases by only 14% when the accuracy of the elevation model is considered. Previous coastal impact studies have primarily used SRTM data due to the fact that these cover nearly the entire world and are freely available. The results of the present study showed a significant difference between the LiDAR (high resolution data) and SRTM digital elevation model. The SRTM data produced a much larger potential coastal floodplain than the LiDAR DEM, contrary to what was initially anticipated as the SRTM digital elevation model is a surface model and the elevation represents the height of the first reflective surface. In contrast to that, van de Sande et al. (2012) reported a four times smaller coastal floodplain using STRM data instead of LiDAR in a delta region in Nigeria (Lagos State and Lagos City). Therefore, it is important to evaluate and quantify data differences in order to improve our understanding of global digital elevation datasets and how these influence flood risk assessments.

If one compares the SRTM with land use data, such as the CORINE land use cover (see Figure 2-9), it becomes obvious that low elevation values occur over agricultural and low-vegetation

areas, while high-elevation values occur in forests and cities. This effect can be accounted for in local studies by, for example, reducing the elevation values of SRTM by the average height of vegetation derived on the basis of field measurements (Kaiser et al., 2011) or other sources of spatially distributed vegetation height data (Baugh et al., 2013). However, additional factors may also influence the elevation values of the model. Although the overestimation of elevation values, for instance in urban areas or vegetated terrain, is well documented in the literature (e.g. Hofton et al. (2006), Rodriguez et al. (2006)), some studies have found SRTM to underestimate elevation values (Jarvis et al., 2008). For example, in a study conducted in two vegetation-free areas in Iowa and North Dakota (USA) Kelldorfer et al. (2004) reported absolute errors of -4.0 and -1.1 m, respectively. Notably, most studies express the vertical accuracy in absolute values (e.g., Gorokhovich and Voustianiouk (2006), Berry et al. (2007)) and do not specify an over- or under-estimation of SRTM values. In this study, an overestimation of the potential coastal floodplain is observed using the SRTM elevation data, suggesting a negative bias in the data, which leads to much higher potential impacts. Understanding the effects of the use of elevation models of different resolution and accuracy would be of high value for coastal flood impact assessments as the choice of the digital elevation model can significantly influence the assessment of coastal flood impacts, as shown in this study. Importantly, high-resolution and -accuracy data cannot be employed for global or regional studies due to computational constraints and lack of such data.

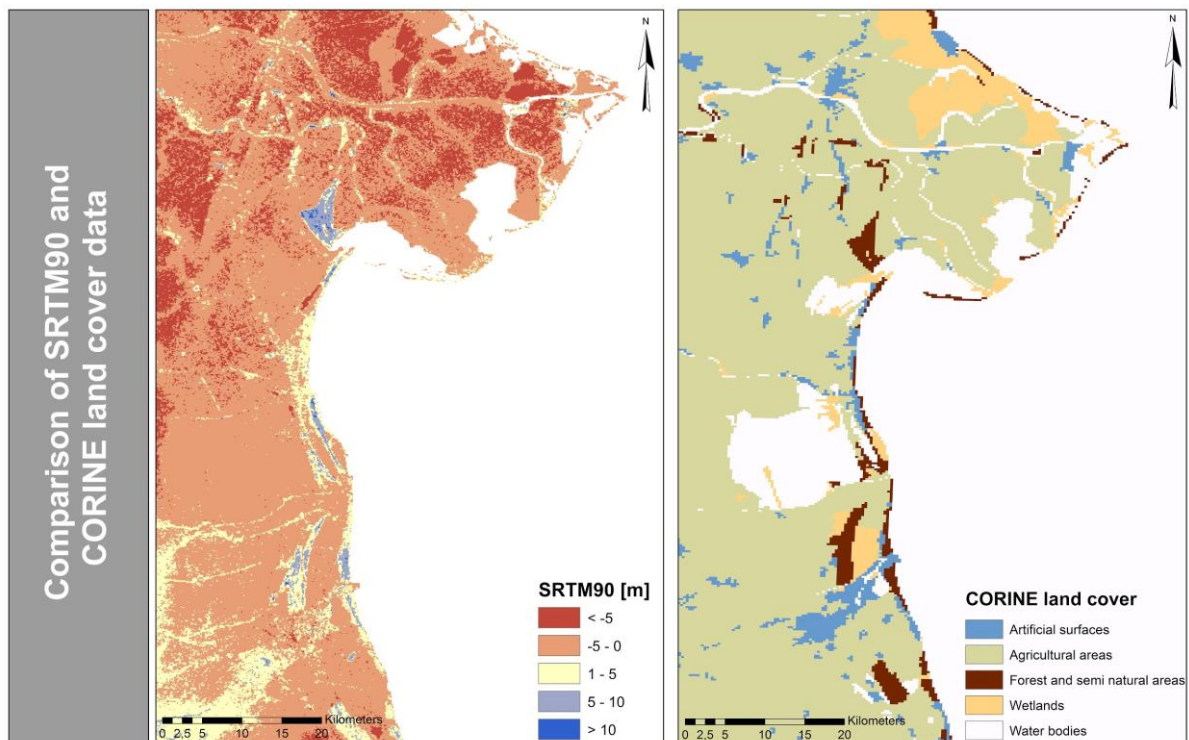


**Figure 2-9:** Comparison of the SRTM90 digital elevation data and CORINE land cover data in Emilia-Romagna.

Human-induced subsidence which leads to higher relative sea-level rates is a major source of uncertainty in coastal flood impact assessment as data is hardly available. The results indicate that the flood risk estimates for the region considered here have a moderate sensitivity to vertical land movement input data, as these can significantly influence the relative sea-level rise. In our study relative sea-level rise increased on average by 5 mm/year using data that include human-induced subsidence (PSInSAR data). This is in line with the study conducted by Syvitski et al. (2009), who estimated a relative sea-level rise of 4-60 mm/year, for the Po delta (the Po delta is the northern boundary of the study area). Furthermore, Taramelli et al. (2014) estimated coastal subsidence of 7-9 mm/year in the Ravenna coastal area and Bevano River. This study was undertaken in regions where there is intensive mining activity (freshwater or hydrocarbon) and the subsidence rates can be higher than a meter per century. This increase in relative sea-level rise leads to a significant increase in exposure of people and areas to coastal flooding due to the landward displacement of the flood extent, and thus in the exacerbation of potential impacts. This study indicates that the global results of Hinkel et al. (2014) using global vertical land movement data underestimates impacts due to the non-consideration of human induced subsidence even in non-delta regions like Emilia-Romagna.

In order to calculate potential coastal flood impacts a further uncertainty source is the distribution of people (and assets) along the coastline. Flood risk estimates showed a relevant but small sensitivity to changes in population input data. A similar trend was observed at global scale by Hinkel et al. (2014). Nevertheless, relative flood impact can differ substantially per segment, administrative unit or country, even if the total numbers do not differ significantly. The GRUMP model distributes people much more uniformly than the LandScan model. Figure 2-10 shows the comparison between the GRUMP and LandScan difference grid in comparison with the urban areas of the MODIS land cover data. Here, it can be seen that LandScan allocates higher population values in urban areas and human settlements. This explains why LandScan distributes more people to the coast than GRUMP in this study as popular tourist resorts, such as Ravenna and Rimini, are part of the floodplain. Thus, in order to interpret the flood risk estimates correctly it is important to keep the different representations/ assumptions of population distributions in mind. However, both population models seem to be useful in order to calculate coastal flood impact trends. For a more robust evaluation of the global datasets high-resolution data would be necessary.

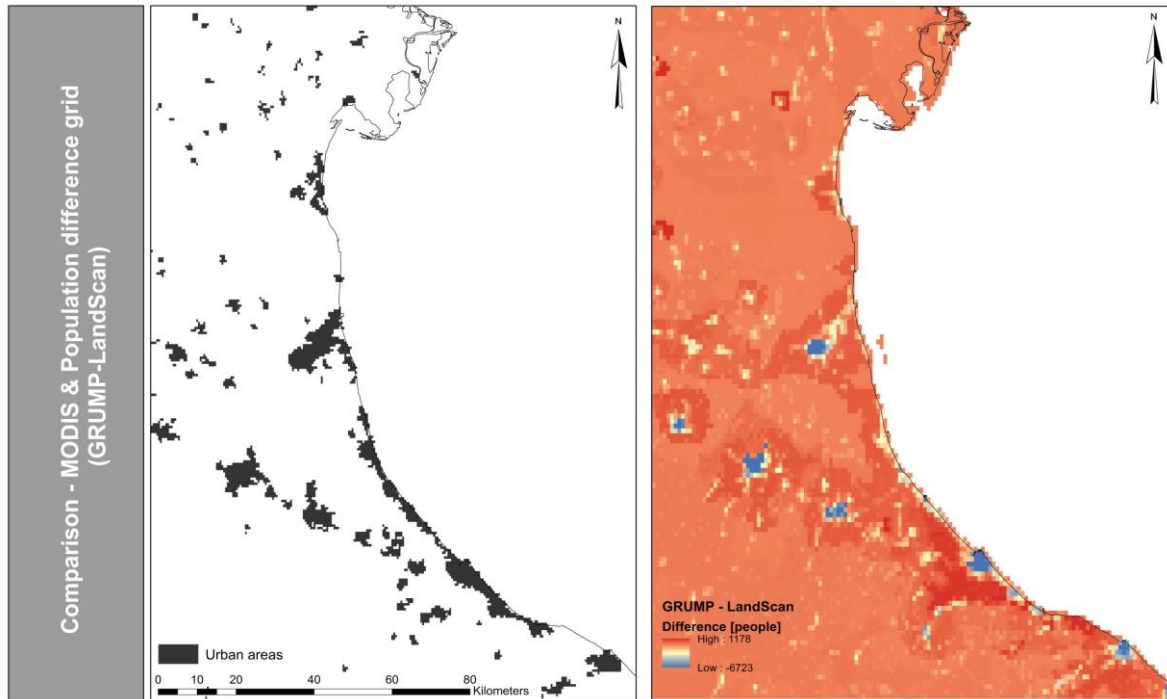


**Figure 2-10:** Comparison of the GRUMP-LandScan difference grid to the urban areas of the MODIS land cover data.

Overall, the largest uncertainty when looking at the present-day situation is the elevation data, as shown in previous work (Lichter et al., 2011, Hinkel et al., 2014). Different elevation datasets can have substantial effects, increasing or decreasing the floodplain area by factor 2 to 3. Our analysis confirms these findings. In our case study the DEM is the most important factor for assessing current exposure and risk. For assessing the future impacts of coastal flooding, sea-level rise is the most important factor, which is also in accordance with Hinkel et al. (2014). Nevertheless, in our case study sea-level rise is strongly influenced by human induced subsidence, which, as shown by previous work (Nicholls, 1995), is usually a local phenomenon often occurring in megacities. Thus, a further insight from our study is that exposure and risk are increasing in the heavily subsiding broader Emilia-Romagna region, although no major city is located in this region.

## 2.5 CONCLUSION

This study presented an assessment of sea-level rise impacts on the coastal region of Emilia-Romagna using different input datasets and assessment scales. The first objective of the study was to explore the potential benefits of the use of a more refined coastline and segmentation. The high-resolution segmentation improves the potential coastal flood impact representation as future predictions are more concentrated and spatially explicit. This study is a first approach to downscale the DIVA assessment scale and data for sub-national applications and refines



the existing segmentation model and database; and a first step to downscale global coastal flood impact assessments for specific areas. Downscaling global coastal flood impact models could be a promising future research area as it would enable rapid coastal flood impact assessments for local policy makers with limited data and resource availability. Furthermore, identifying links between spatial scales can enable consistent and comparable coastal flood impact assessments and would constitute a useful tool for global actors (e.g., Re-insurers, European flood directive, World Bank).

The second objective of the study was to explore the model sensitivity to different input data on elevation, population and vertical land movement when assessing coastal flood impacts. This study indicates that the lack of high-accuracy elevation and vertical land movement data remains a significant constraint in global coastal flood impact analysis. We must also note that coastal flood impact assessment also includes other sources of uncertainties that should be investigated in future work, such as the spatial (Lewis et al., 2013) and temporal variability (Quinn et al., 2014) of extreme water levels and their implications in coastal flood impact assessment. Understanding the whole range of uncertainties and communicating their implications is essential for the development of long-term robust and flexible adaptation plans for future changes of highly uncertain scale and direction. Further work aims to assess the sensitivity of different input datasets and scale of analysis in different regions, in order to gain a more complete understanding of the use of global datasets in flood-impact modeling and the sensitivity of the DIVA flooding module to input data and scale.

## **ACKNOWLEDGEMENT**

CW, ATV and CM were supported by the COASTGAP project (1CAP-MED012-08) which was co-financed by the European Regional Development Fund (ERDF). DL and JH have been supported by the EU-funded projects, RISES-AM (Grant Nr: 603396) and GREEN-WIN (Grant Nr: 642018). The authors would also like to thank Dr. Eva Papaioannou who assisted in the implementation of the coastline segmentation.



# 3

## **A MEDITERRANEAN COASTAL DATABASE FOR ASSESSING THE IMPACTS OF SEA- LEVEL RISE AND ASSOCIATED HAZARDS**

This chapter is published as:

Wolff, C.; Vafeidis, A. T.; Muis, S.; Lincke, D., Satta, A.; Lionello, P.; Jimenez, J.; Conte, D. and Hinkel, J. (2018): A Mediterranean coastal database for assessing the impacts of sea-level rise and associated hazards. *Scientific Data*, 5:180044. doi: [10.1038/sdata.2018.44](https://doi.org/10.1038/sdata.2018.44)

## ABSTRACT

We have developed a new coastal database for the Mediterranean basin that is intended for coastal impact and adaptation assessment to sea-level rise and associated hazards on a regional scale. The data structure of the database relies on a linear representation of the coast with associated spatial assessment units. Using information on coastal morphology, human settlements and administrative boundaries, we have divided the Mediterranean coast into 13,900 coastal assessment units. To these units we have spatially attributed 160 parameters on the characteristics of the natural and socio-economic subsystems, such as extreme sea levels, vertical land movement and number of people exposed to sea-level rise and extreme sea levels. The database contains information on current conditions and on plausible future changes that are essential drivers for future impacts, such as sea-level rise rates and socio-economic development. Besides its intended use in risk and impact assessment, we anticipate that the Mediterranean Coastal Database (MCD) constitutes a useful source of information for a wide range of coastal applications.

### 3.1 BACKGROUND & SUMMARY

The Mediterranean basin is characterized by a squeezed coastal area with a high concentration of people and assets and by rapid demographic, social, economic as well as environmental change (Sánchez-Arcilla et al., 2010, UNEP/MAP, 2016). Between 1960 and 2010, the population of the Mediterranean has doubled from 240 million to 480 million (European Environment Agency, 2014) and the urban population has increased by 20% (UNEP/MAP, 2016). This human pressure is further amplified by international tourism. Around one third of the global tourist arrivals in 2011 have been registered in Mediterranean countries, predominantly along the coast. The number of arrivals is expected to increase further, and could reach 637 million per year by 2025 (European Environment Agency, 2014). The Mediterranean coastal zone is not only increasingly under pressure from local human activities, but also subject to future global environmental change. In particular, sea-level rise and associated hazards (Conte and Lionello, 2013) are expected to have significant impacts in Mediterranean nations during the 21<sup>st</sup> century (Casas-Prat and Sierra, 2010, Jimenez et al., 2017, Vousdoukas et al., 2017).

To address these pressures and to underpin future coastal management and adaptation policies, such as those included in the Integrated Coastal Zone Management (ICZM) Protocol of the Barcelona Convention (UNEP/MAP/PAP, 2008), policy makers and coastal administrations in Mediterranean nations require impact and vulnerability assessments. Such integrated assessments are cross-sectorial studies that require information from various fields and disciplines. A prerequisite for coastal impact assessment and for the planning of appropriate future interventions is the availability of consistent information on the physical, ecological and socio-economic characteristics of the Mediterranean coastal zone. Despite an increasing demand of decision-makers, planners and coastal researchers from various

disciplines for such consistent scientific data (Malvarez et al., 2015, Santoro et al., 2014) there is currently no source of readily available information for the 22 countries that surround the Mediterranean basin. Due to the lack of such data only a limited number of studies exist that have analyzed the impacts of sea-level rise for the entire region (Santoro et al., 2014, United Nations Environment Programme/Mediterranean Action Plan (UNEP/MAP)-Plan Bleu, 2009). Collecting and organising such data is a challenging task as consistent information on socio-economic and physical characteristics, both on current conditions as well as on future developments, of the coast is needed.

The developed MCD aims to meet these needs through the provision of an open access spatial database, that provides consistent information (in terms of format, resolution, quality, accuracy) for the entire region and that is based on a lean data model. The coastal database contains 160 parameters that characterize the natural and socio-economic systems of the Mediterranean coast. It relies on the structure that was originally designed for the Dynamic Interactive Vulnerability Assessment (DIVA) modeling framework (Hinkel et al., 2014, Hinkel et al., 2013, Spencer et al., 2016), following the concepts described in Vafeidis et al. (2008) and McFadden et al. (2007). However, we have downscaled and extended these approaches by introducing spatial coastal assessment units that capture the spatial structure of population, assets and land exposed to coastal hazards. Further we have enhanced the transparency of the process of attribution of spatial data to the segments and coastal assessment units in order to make the database more user friendly. The developed coastal database is intended for use in regional scale analyses and provides a robust basis for all types of comparative coastal studies to future change as it allows results to be comparable across the entire region.

In this data descriptor we describe the generation of coastal segments and associated spatial coastal assessment units; the methods that we have used to attribute around 160 different parameters on current and future conditions in various formats to the coastal units; and the development of consistent data for the Mediterranean coasts.

## **3.2 METHODS**

### **3.2.1 Coastal data model**

Finding a data model to represent coastal space for vulnerability, impact and adaptation assessment is not a straightforward task as coasts are highly dynamic and complex in terms of process interactions (Brown et al., 2014). This introduces challenges when trying to depict this system into a format that allows spatial information to be stored into a database. A linear representation of the coastal zone has often been used in coastal studies due to the common perception of the coast as a linear boundary between the sea and the land (Bartlett, 2000). The main advantage of a linear data model is its computational efficiency, which is essential for being able to conduct the large number of model runs needed in impact and adaptation

assessments as a result of the large number of plausible sea-level rise, socio-economic or adaptation scenarios available. However, there is no direct way to attribute spatial data, such as the number of people living in the low-elevation coastal zone or landuse covering the coastal space, to a linear feature without losing spatial information. Therefore, a main disadvantage of a linear data model is that the explicit spatial structure of the system is lost (Brenner et al., 2006). The alternative data model frequently applied in order to preserve coastal spatial information is a grid. The disadvantage of this model is, however, that data volumes are large and computationally expensive for use in impact and adaptation assessments at broader geographic scales.

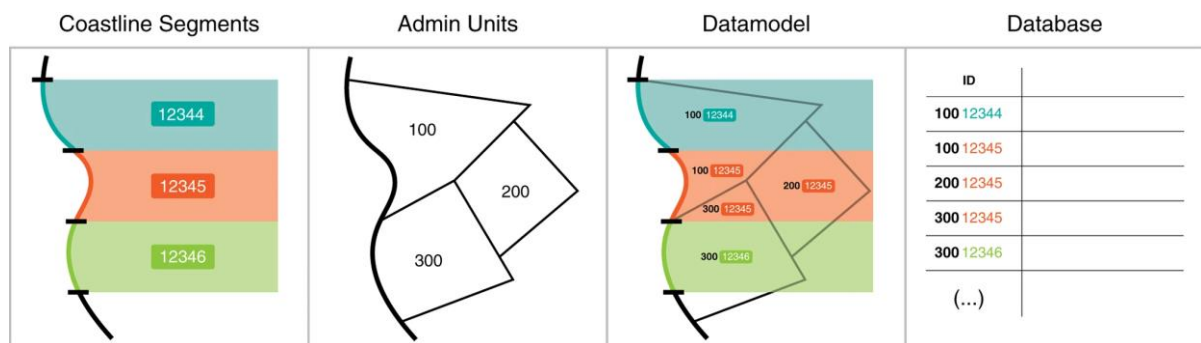


**Figure 3-1:** Workflow of the data model generation for the Mediterranean Coastal Database.

To address this challenge, we have created a data structure that combines the linear representation of the coast with spatial coastal assessment units that extend inland (Figure 3-1). Thus, we combined the advantages of a linear data model with a spatial representation of the coastal zone. To create such a data model, the first step was to divide the coast into homogenous segments in terms of impacts, vulnerability and adaptation to sea-level rise. For each segment, we then created a set of spatial coastal assessment units according to administrative boundaries and extent of land up to 20m of elevation above mean sea level. Our aim was to generate assessment units that will respond uniformly to sea-level rise and can be treated as single units for the purpose of adaptation planning in the future. In the following section, we describe the data model and present the computational data processing that was undertaken for populating the database.

### Coastal segments

Following the concept of Vafeidis et al. (2008) and Wolff et al. (2016), we generated coastal segments of variable length, each segment representing parts of the coast with a uniform vulnerability to sea-level rise at a regional scale. As differences in vulnerability to sea-level rise are driven by variations in both socio-economic as well as geomorphic/physical characteristics

of the coastal zone (McFadden et al., 2007), we used four parameters covering both these domains in the segmentation decision. Every time one of the four parameters changed in value, a new segment was started (Figure 3-2).

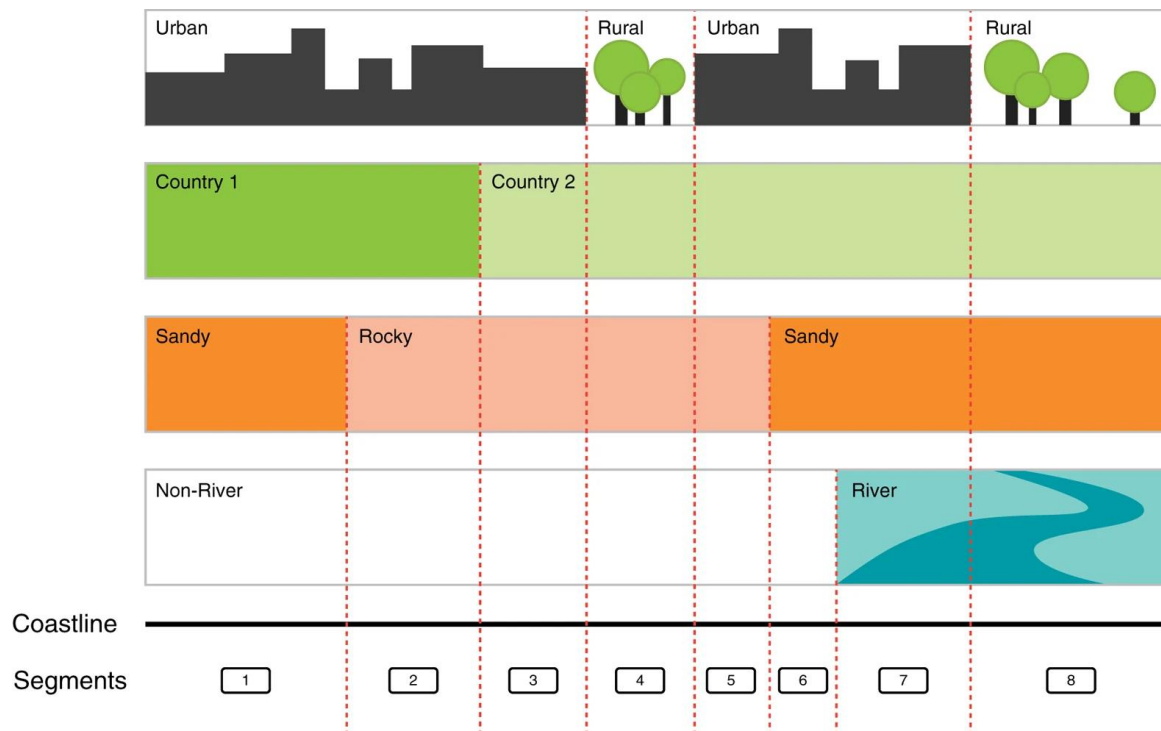


**Figure 3-2:** Schematic segmentation procedure for the Mediterranean Coastal Database.

We employed the coastline of the Global Administrative Areas database level 01 (Global Administrative Areas (GADM), 2015) as the base layer for the segmentation for the Mediterranean countries (Figure 3-2) and corrected artefacts related to the format (e.g., “pixelization” of coastline) using a smoothing algorithm (polynomial approximation) and a tolerance of 100 meters.

The first social system parameter included in the segmentation were (1) administrative boundaries. This parameter was included, because society’s capacity to respond to sea-level rise differs across jurisdictions. In this study, we used the GADM level 02 dataset (see Table 3-1).

The second social system parameter we used in the segmentation was the (2) distribution of assets and people distinguishing the coast into two classes, (a) urban and (b) rural. This parameter is relevant for the segmentation, because population and asset density influence vulnerability by both determining the exposure to sea-level rise and storm surges, as well as by influencing society’s capacity to adapt (Hinkel et al., 2014). We classified the coast using satellite imagery and photos from Google Earth and the Moderate Resolution Imaging

Spectroradiometer (MODIS) global map of urban extent dataset with a spatial resolution of 500m (Schneider et al., 2009). Classification decisions were based on visual interpretation of Google imagery and on the MODIS data, where urban areas are defined as places with predominantly built environment. That includes all non-vegetative, human-constructed elements, such as buildings, roads, runways and are greater than 1km<sup>2</sup> (Schneider et al., 2009). All pixels with a coverage greater than or equal to 50% built environment according to the MODIS dataset were classified as urban. As we were particularly interested in all human settlements that are lying directly on the coast, we refined the classification using Google Earth in order to also include smaller human settlements. Therefore, settlements with a maximum distance of 300m to the shoreline and a minimum extent of 300m x 300m, predominantly covered by residential buildings, were defined as urban. Harbours were excluded from the urban classification, as they will require specific adaptation measures in the future.

The first geomorphological parameter we considered in the segmentation was the (3) coastal material. The material of the coast has a significant impact on the large-scale response to sea-level rise (McFadden et al., 2007). One of the major impacts of sea-level rise is long-term erosion and land loss due to permanent inundation (Hinkel et al., 2013). For instance, sandy beaches will respond differently than rocky coasts to a rising sea level. We created a typology of four different geomorphic classes that respond differently to rising sea level and will require different adaptation measures. For the Mediterranean, no such dataset on coastal morphology and geological characteristics was available at that time. Four different classes, namely (a) sand, (b) unerodible, (c) mud and (d) rock with pocket beaches have been classified based on visual interpretation of Google Earth imagery and location-tagged photographs from the web-service Panoramio which offers geographically tagged photographs from users (Scheffers et al., 2012). A similar method has been used in Wolff et al. (2016) and Scheffers et al. (2012).

The second geomorphological parameter that we included in the segmentation process is (4) river mouths. This parameter was included because deltas and estuaries are among the most vulnerable coastal geomorphic features to sea-level rise (Wong et al., 2014). We classified 47 river mouths for the Mediterranean region based on Google Earth imagery.

Finally, those layers with the four different parameters were combined to create the coastline segmentation for the Mediterranean. Overall, there are 11,975 segments with an average length of 4.5 km.

### **Spatial assessment units**

The spatial assessment units expanding inland were created by generating inland buffer zones for every coastline segment and overlaying them with elevation data and the administrative boundaries (resolution: 3 arc second). We only account for the low-lying part of the coastal zone that is hydrologically connected to the sea and lies above 20m from mean sea level. The low-lying part of the coast is particularly at risk due to higher extreme sea levels in the future



(Nicholls et al., 2014, Muis et al., 2015). We decided to extend the LECZ (Low Elevation Coastal Zone = Area below 10m (Lichter et al., 2011, Neumann et al., 2015, McGranahan et al., 2007)) up to 20m in order to account for all plausible scenarios of changes in mean sea level and associated hazards, including high-end scenarios, as well as to allow exploring different adaptation strategies such as coastal retreat. Every coastal assessment unit was linked to a coastal segment with a unique identifier code. The coastal segment unique identifier code consists of eight digits. The first three represent the administrative unit and the last five digits represent the coastline segment (Figure 3-1). The generated coastal data model forms the basis for the subsequent compilation of the database.

### 3.2.2 Extreme sea levels and waves

The MCD includes two extreme sea level datasets. The first dataset included is derived from the Global Tide and Surge Reanalysis (GTSR) dataset. GTSR is the first near-coast global reanalysis of storm surges and is based on global hydrodynamic modelling combined with meteorological forcing from ERA-Interim (1979-2014). A Gumbel extreme value distribution was fitted to the annual maximum to derive extreme sea levels for various return periods. GTSR generally provides extreme sea levels for the centroids of the coastal segments of the global database used in the DIVA model. However, for the MCD we increased the spatial resolution and saved the outputs for the 11,975 centroids of the Mediterranean coastline segments (GTSR-MED). The general methodology is described in detail in Muis et al. (2016).

The second dataset that we included in the MCD is the DINAS-COAST Extreme Sea Levels (DCESL). This dataset has been the first global extreme water level dataset and was developed with the use of a simple empirical model described in detail in Muis et al. (2017) and Hunter et al. (2017).

Besides the data on extreme sea levels, we have also included information on mean wave heights for the period 1971-2000 for the Mediterranean basin. The wave data have been computed using the wave model WAM (Hasselmann et al., 1988) at a resolution of 0.25 degrees, resolving the spectrum using 12 directions and 25 frequencies. The wind meteorological forcing was generated using the hourly meteorological fields produced by the regional climate model COSMO-CLM at a resolution of 0.12 degrees. The model framework has been validated by Lionello and Sanna (2005) and Lionello et al. (2008). These mean wave heights should be considered representative of offshore conditions, before depth induced wave breaking and interaction with the bottom in the near shore zone occur.

### 3.2.3 Computational data processing

The database was developed with the use of ArcPy, which is a site-package that builds on the ArcGIS scripting module. It enables users to perform geographic spatial data analysis, data conversion and data management with the programming language Python. One main

advantage is that every Python script constitutes a precise documentation of the computational data processing that was conducted. The input spatial data were available in various formats depending on the information that they represented. Therefore, we used different methods to attribute the data to the coastline segments and spatial assessment units.

Data processing differed according to two characteristics of the input data, namely: (1) whether the data were originally in vector or raster format; and (2) whether we attributed them to the coastline segment or to the assessment units (e.g. data representing information that extends several kilometres inland). For instance, the extreme sea level data were available in a vector (point) format representing extreme sea levels for different return periods directly at the coast. We spatially joined the nearest extreme sea level data point to the centroid of every segment in order to have a common attribution approach. Every coastal assessment unit obtained the extreme sea level information of the corresponding coastline segment (Figure 3-1). Another example for the attribution of raster data to the coastal assessment units is the information about the distribution of people in the coastal zone. For this purpose, a gridded population dataset was combined with gridded elevation data in order to calculate the number of people below a certain elevation (in 1 m increments, up to 20 m). Then we calculated the zonal statistics for every coastal assessment unit in order to get the number of people per elevation increment. A detailed documentation for every step employed for attributing the different parameters to the coastal units can be found in the Python scripts (Table 3-1 and Table 3-2).

The database consists of various parameters about current conditions of the coastal zone. In addition, the database provides information on plausible future changes that will drive future impacts, such as sea-level rise or socio-economic development scenarios. Table 3-1 and Table 3-2 summarizes all parameters that are included in the database; their source; a short description and the name of the python code where the detailed computational data processing steps are documented. With the exception for the extreme sea level datasets and the wave data, we only used datasets that are publicly available.

**Table 3-1:** Summary of the parameter and data included in the Mediterranean Coastal Database on a segment level.

Label	Description	Data source	Code
ISO	ISO alpha-3 codes, Standard country codes for statistical use	International Organization for Standardization (International Standard ISO 3166-1, 2006)	
country_name	Country borders	GADM database of Global Administrative Areas, version 2.8 (Global Administrative Areas (GADM), 2015)	
admin_name	Administrative borders and their associated names	GADM database of Global Administrative Areas, level 02, version 2.8 (Global Administrative Areas (GADM), 2015)	
admin_id	Administrative unique identifier code associating each segment/assessment unit with the corresponding administrative information	-	
urban	Distinguishes the coast into two classes, (1) urban and (0) rural.	Google Earth imagery and location-tagged photographs from the web-service Panoramio; MODIS 500-m global map of urban extent dataset (Schneider et al., 2009)	
Coast_material	Four different coastal material classes, namely (1) sand, (2) unerodible, (3) mud and (4) rock with pocket beaches have been classified.	Google Earth imagery and location-tagged photographs from the web-service Panoramio	
length	Coastline segment length [in km], the Equidistant conic (world) projection was used.	-	
lati	Latitude of the midpoint of the coastline segment [in decimal degrees]	-	
longi	Longitude of the midpoint of the coastline segment [in decimal degrees]	-	
locationid	Unique numerical identifier code which links each coastline segment to the attributed data	-	
coastalass_unit	Indicates the coastal assessment unit that belongs to the segment and lies directly at the coast. (Segments that are smaller than the resolution of the assessment units (~ 90m) do not have an assessment unit. Those coastal assessment units are indicated with 999 as the first three digits)	-	
gdpc_year	GDP per capita in current international \$ for 1995, 2000, 2005, 2010, 2015 (For countries where records are missing we used the values from GBR for GIB, FRA for MCO; for LYB and MNE we used the gdpc growth rates from IIASA to calculate 1995, There is no data for SYR (all years) and LBY (2015) provided by the World bank)	World Bank (2016)	
gdpcGRSSPx_year	Annual average growth rate per capita [%] for every SSP on a country level from 2000 -2100 (5yr time steps). For small countries, no SSP data exists. Therefore, we used for GIB the values of GBR, MCO – FRA and PSE – ISR.	International Institute for Applied Systems Analysis (IIASA) - SSP Database (International Institute for Applied Systems Analysis, 2015, Crespo Cuaresma, 2015)	

popGRSSPx_year	Annual average population growth rate [%] for every SSP on a country level from 2000 -2100 (5yr time steps). For small countries, no SSP data exists. We used for GIB the values of GBR, MCO – FRA and PSE – ISR.	International Institute for Applied Systems Analysis (IIASA) - SSP Database (International Institute for Applied Systems Analysis, 2015, Kc and Lutz, 2017)	
river	Includes the main estuaries and deltas of the Mediterranean, Non-river segment (0), river segment (1)	Derived from google earth	
river_name	Name of the river mouth		
GTSR_rp1 (2,5, 10,25, 50, 100, 250, 500, 1000)	1 in 1, 1 in 2, 1 in 5, 1 in 10, 1 in 25, 1 in 50, 1 in 100, 1 in 250, 1 in 500, 1 in 1000 year surge height (in base year) respectively, Height above mean sea level, [in m]	Based on the global reanalysis of storm surges and extreme sea level (GTSR) dataset (Muis et al., 2016)	surges.py
DCESL_rp1 (10,100,1000)	1 in 1, 1 in 10, 1 in 100, 1 in 1000 year surge height (in base year) respectively, Height above mean sea level, [in m]	Vafeidis et al. (2008)	surges.py
waves	Mean wave height [in cm]	Dataset produced as part of the RISES-AM project by CMCC (Euro-Mediterranean Center on Climate Change) (Conte and Lionello, 2013, Lionello et al., 2008)	waves.py
cst	Topographic coastal slope [in degrees] derived from GEBCO [30 arc-seconds resolution]	GEBCO (Weatherall et al., 2015)	cst.py
maxhw	Max High Water [in m]	Pickering et al. (2017), Pickering (2014)	tide.py
mhw	High Water [in m]	Pickering et al. (2017), Pickering (2014)	tide.py
minlw	Minimum Low Water [in m]	Pickering et al. (2017), Pickering (2014)	tide.py
mlw	Low Water [in m]	Pickering et al. (2017), Pickering (2014)	tide.py
mtr	Mean Tidal Range [in m]	Pickering et al. (2017), Pickering (2014)	tide.py
VerticalMovement04	Average uplift/subsidence [in mm/yr] along the segment from estimates of glacio-isostatic adjustment.	Peltier (2004)	uplift2004.py
VerticalMovement14	Average uplift/subsidence [in mm/yr] along the segment from estimates of glacio-isostatic adjustment.	Peltier et al. (2015), Argus et al. (2014)	uplift2014.py
saltmarshes	Area of salt marsh within a coastal segment [in km <sup>2</sup> ]	UNEP-WCMC (McOwen et al., 2017)	wetland.py
RCP26(45,85)_1995(-2100)_hig	Regionalized SLR scenarios, which account for regional gravitational and rotational effects due to changes in ice mass distribution and steric changes. Mean sea-level rise relative to 1985-2005 [m] for RCP 2.6, 4.5 and 8.5 for a high ice-sheet melting scenario.	Hinkel et al. (2014)	SLR_hig.py
RCP26(45,85)_1995(-2100)_med	Regionalized SLR scenarios, which account for regional gravitational and rotational effects due to changes in ice mass distribution and steric changes. Mean sea-level rise relative to 1985-2005 [m] for RCP 2.6, 4.5 and 8.5 for a medium ice-sheet melting scenario.	Hinkel et al. (2014)	SLR_med.py
Tour_arryear	International tourism, number of arrivals on a country level form 1995-2014, 0 equals NoData	World Bank (World Tourism Organization et al., 2014)	
MDT	The MDT is the difference between the mean sea surface and the geoid over the 1993-2012 period	Rio et al. (2014)	MDT.py

	[in m]. This parameter can be used to correct the offset for instance between extreme water levels and elevation data31		
--	---	--	--

**Table 3-2:** Summary of the parameter and data included in the Mediterranean Coastal Database on at coastal assessment unit level.

Parameter	Label	Description	Data source	Code
Area below 1...20m	area1...20	Hydrological connected area [in km <sup>2</sup> ] at elevation increment x, corresponding to every coastal assessment unit. In order to calculate the earth surface area we generated a 'real' area grid based on the spheroidal approximation of the Earth surface (Santini et al., 2010) and overlaid it with the SRTM data.	Shuttle Radar Terrain Mission (SRTM) data, 90m resolution (Jarvis et al., 2008)	area.py
Population living in area 1...20m	popx_gpw2000	Total population living in elevation increment x based on the gridded population of the world, version 4. UN-adjusted population estimates for 2000. The resolution is 30 arc-seconds, or ≈1 km at the equator.	Center for International Earth Science, Information Network, Columbia University (Center for International Earth Science Information Network - Columbia University, 2016)	gpw00.py
	popx_gpw2010	Total population living in elevation increment x based on the gridded population of the world, version 4. UN-adjusted population estimates for 2010. The resolution is 30 arc-seconds, or ≈1 km at the equator.	Center for International Earth Science, Information Network, Columbia University (Center for International Earth Science Information Network - Columbia University, 2016)	gpw10.py
	popx_gr2000	Total population living in elevation increment x based on the Global Rural-Urban Mapping Project, Version1 (GRUMPv1). The resolution is 30 arc-seconds, or ≈1 km at the equator.	Center for International Earth Science Information Network, Columbia University (Center for International Earth Science Information Network - CIESIN - Columbia University et al., 2011)	gr00.py
Landuse	ForestArea (UrbanArea, ArableArea, OpenArea)	The Globcover data includes 22 land cover classes defined by the United Nations (UN) Land Cover Classification System (LCCS). We reclassified this classification to 4 classes, namely forest, urban, arable land and open space. For every assessment unit the area for every class is calculated [in km <sup>2</sup> ].	Global Land Cover Map for 2009 European Space Agency and Université Catholique De Louvain (2009)	landuse.py
	PC_forest (PC_Urban, PC_arable, PC_open)	Percent of every assessment unit that is covered by one of the landuse classes.	Global Land Cover Map for 2009 European Space Agency and Université Catholique De Louvain (2009)	landuse.py
Coastal parameter	coastal_zone	Indicates if a coastal assessment unit is lying directly at the coast (true) or inland (false)	-	

SSP	GR_SSP1(-5)_2010(-2100)_med	Spatial Population growth rates for the Mediterranean Coastal Zone per coastal assessment unit and SSP. These are based on Regionalized Shared Socioeconomic Pathways which are based on GPWv4.	Reimann et al. (2017)	SSPs_med.py
	GR_SSP1(-5)_2010(-2100)_global	Global spatial Population growth rates per coastal assessment unit and SSP. These are based on global gridded population projections for the coastal zone under the Shared Socioeconomic Pathways. Based on GRUMP 2000.	Merkens et al. (2016)	SSP_global.py
	SSP1(-5)_2010(-2100)_med	Total population numbers generated for every time step from Regionalized Shared Socioeconomic Pathways. Based on GPWv4	Reimann et al. (2017)	SSPs_med.py
	SSP1(-5)_2010(-2100)_global	Total population numbers generated for every time step from global gridded population projections. Based on GRUMP 2000.	Merkens et al. (2016)	SSP_global.py

### 3.2.4 Code availability

The python code to populate the Mediterranean coastal database is available to download in the figshare repository. The code consists of ArcPy commands, which can be used if an ArcGIS for Desktop license is installed. Each script is internally documented with explanation of the different data processing steps. The internal documentation of the scripts should be used in combination with this manuscript.

## 3.3 DATA RECORDS

The developed Mediterranean coastal database described in this article is publicly and freely available through the figshare repository. We have included csv files with all the information on a segment (MCD – coastal segment level) and assessment unit level (MCD – coastal assessment unit level) into the repository. Furthermore, we provide the coastal segments and administrative boundaries in a shapefile format as well as the coastal assessment unit in a tiff format in the repository. The database will be updated and expanded as new and improved data become available.

## 3.4 TECHNICAL VALIDATION

The database presented here has been created using a number of publicly available datasets, which are thoroughly documented and described in reports or scientific articles (Table 3-1 and

Table 3-2). Thus, these datasets have undergone rigorous quality controls and/or validation. In addition, for those parameters where consistent information for the entire basin did not exist, new datasets were generated. Technical validation therefore has focused on the evaluation of these new datasets (i.e. the coastal material, GTSR-MED extreme sea levels); and on the correct attribution of data to the assessment units.

### 3.4.1 Geomorphological classification

The geomorphological classification dataset was compared to the recently compiled geomorphological dataset of the Mediterranean Sea and Coast Foundation (MEDSEA, 2017) which was developed independently, using a similar methodological approach. Further validation for some of the Mediterranean countries, where this was possible, was undertaken based on expert judgement and on national digital datasets of coastal morphology.

Comparing different coastal classification datasets can be a challenging task as the number and type of classes used can differ substantially, depending on factors such as scale or user requirements (Burrough and McDonnell, 1998 p.267). The MEDSEA data included similar classes to our dataset, namely: (1) sandy beach and beach with uncertain grain size; (2) river, deltas; estuaries and soft sedimentary strands; (3) artificial structures and artificial frontage; (4) soft rock shores; and (5) hard rock shores (see Table 3-3). 23% of the coast were classified as sandy in both datasets. The MCD class 'unerodible' includes rocky coasts and artificial structures. When comparing the MCD class (2) and the MEDSEA classes (3) and (5), the datasets show good agreement, accounting for 46 (MCD) and 40 (MEDSEA) percent of the total coastline. The remaining classes ("rocky with pocket beaches" and "soft rock shores" from MCD and MEDSEA respectively) are not directly comparable. Overall, the two datasets are in agreement for around 70 percent of the Mediterranean coast. The spatial patterns of coastal types are similar in the southern and eastern Mediterranean basin. In the north western part of the basin differences in the classification are visible as the MEDSEA dataset indicates a higher extent of hard and soft rock shores. However, this difference is primarily due to the difference in the definition of the classes for the two classification schemes.

**Table 3-3:** Comparison of coastal morphology classification

MCD	Length [km]	Percent of total coastline length	MEDSEA	Length [km]	Percent of total coastline length
(1) Sandy	12,493	23.0	(1) Sandy beach and beach with uncertain grain size	11,929	23.8
(2) Unerodible	25,051	46.1	(2) River deltas, estuaries and soft sedimentary strands	1,802	3.6
(3) Muddy	3,570	6.6	(3) Artificial structures and artificial frontage	4,936	9.8
(4) Rocky with pocket beaches	13,181	24.3	(4) Soft Rock shores	16,163	32.2
			(5) Hard Rock shores	15,322	30.5
Total coastline length	54,296	100	Total coastline length	50,153	100

Local experts from Spain, Greece and Croatia undertook additional checks, based on visual inspections and on national or local datasets. For Spain, there was agreement for 75% of the coast. For the remaining 25%, we implemented changes based on the expert suggestions and additional checks with Google Earth. For Croatia, we compared our dataset to a national spatial dataset on the distribution of sandy beaches provided by the Ministry of Environmental and Nature Protection and found that all sandy beaches were included. Further qualitative tests based on expert judgement and visual assessment were carried out for Greece for approximately 100 randomly selected segments, indicating an agreement for approximately 85% of the inspected segments. Accordingly, discrepancies were checked and corrected based on Google Earth and expert suggestions. Finally, further comparisons were carried out for the districts of Lazio and Emilia-Romagna with available classifications used in previous analyses (Wolff et al., 2016).

It must be noted that despite the extensive evaluation of the geomorphological classification and the agreement with all employed data sources, some errors may still exist. These errors can result from numerous factors, such as differences in the quality of Google Earth imagery for the entire region; differences in scale; errors in the location of Panoramio photographs; coverage of location-tagged photographs varying considerably between the Northern and Southern part of the basin; errors in classification; or differences due to subjectivity in class definition. Nevertheless, the dataset will continue to be updated as new data become available. We are currently exploring options for extending the validation using crowd sourced data from the project Coastwards (<http://coastwards.org/>) in order improve our current classification.

### 3.4.2 Extreme sea level datasets

Here we compare the two datasets of extreme sea levels against observations. First, we evaluate GTSR-MED and DCESL which include tides and surges. Figure 3-3a shows a



comparison of the modelled and observed extreme sea level with a 10-year return period for the GTSR dataset. Extreme sea levels are generally in the range of 0.15 m and 1.24 m. Off the coast of Tunis, the Strait of Gibraltar, and near Venice extreme sea levels are relatively high. This is corresponding with the relatively high tidal range in these areas. For example, the Gulf of Gabes off the coast of Tunisia has a tidal range of nearly two meters, while tides are generally small in other parts of the basin. Muis et al. (2016) evaluated the GTSR extreme sea levels against observed sea levels from the archive of the University of Hawaii (<http://uhslc.soest.hawaii.edu>). However, the set of tide gauges used for the global validation has a very limited number of tide gauges available in the Mediterranean basin. Therefore, we performed additional validation using the GESLA-2 dataset (<http://gesla.org>), which includes data from many more tide gauges (Woodworth et al., 2016). Here we use the estimates of the return periods of extreme sea levels from Wahl et al. (2017). They processed the raw data and fitted a Gumbel distribution to the annual maxima using all stations that contain at least 20 complete years that is less than 25% missing data. For the Mediterranean region, this resulted in 17 observation stations. To evaluate the performance of the GTSR-MED extreme sea levels, we calculate the mean bias and the mean absolute error between the modelled and observed extremes. The modelled extreme sea levels are generally characterized by a negative bias. For a 10-year return period the mean bias is -0.21 m (s.d. 0.20 m), whereas for a 100-year return period the mean bias is -0.34 m (s.d. 0.41 m). As extreme sea level are generally below 1.5 m, the relative differences exceeds 25% for a number of locations. This is depicted in Figure 3-3a-c. The relatively strong negative bias may be due the fact that in semi-enclosed basins, such as the Mediterranean Sea, extreme sea levels are largely controlled by local conditions and mesoscale dynamics. Hence, the representation of the global bathymetry and the resolution of the global tide and surge model may not be sufficient in this region. Moreover, in areas with a complex orography, such as the Adriatic Sea, global climate reanalysis data can have difficulties in reproducing local winds (Wakelin and Proctor, 2002). Unfortunately, almost all tide gauges are located in Portugal, Spain and Italy. Hence, the eastern and the southern part of the Mediterranean Sea are under-represented. Therefore, we were not able to assess the performance of the model for the entire basin.

The DCESL data have been validated by Hunter et al. (2017). The study concluded that the return periods of DCESL are generally too high, compared to observed return periods from GESLA-2. Muis et al. (2017) compared the GTSR and DCESL against UHSCL observations. They found that both GTSR and DCESL capture the spatial variability of extremes. However, DCESL generally overestimates the extreme sea levels, whereas GTSR generally underestimates the extreme sea levels, but with smaller errors compared to observations.

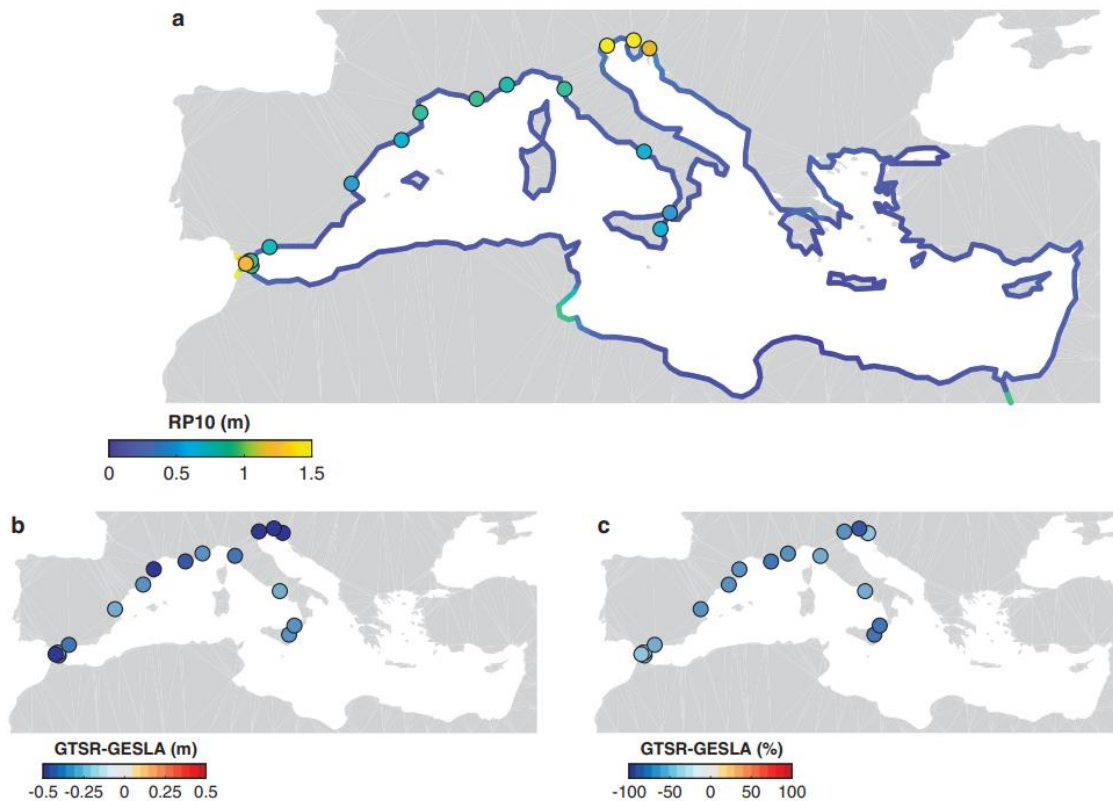


**Figure 3-3:** Performance of the GTSR-MED extreme sea levels for the Mediterranean Sea for the 10-year return period. Observed extreme sea levels are taken from the GESLA dataset. (a) GTSR-MED and GESLA extreme sea levels. (b) The difference of GTSR-MED with GESLA in m. (c) Relative differences of GTSR-MED and GESLA.

However, this comparison included only few stations in the Mediterranean. The comparison of GTSR and DCESEL by Wahl et al. (2017) is based on the GESLA-2 dataset and includes more stations. It shows that DCESEL overestimates the 100-year return period values by more than 0.5 m. If we compare the DCESEL return periods against the GESLA-2 stations used for the GTSR-MED validation (see above), the mean bias is 0.16 m (s.d. 0.43 m), 0.17 m (s.d. 0.59 m), and 0.20 m (s.d. 0.76 m), respectively for the 10-, 100-, and 1000-year return periods. For specific stations the bias is up to 1.5 m, whereas for other stations the bias of DCESEL is less than a few centimetres. Hence, although the performance is variable, DCESEL generally also overestimates extreme sea levels in the Mediterranean basin. Again, there is no information to assess DCESEL for the eastern and the southern part of the Mediterranean Sea.

We would like to highlight that due to the limited numbers of observations it is difficult to assess the overall performance of the extreme sea level datasets. However, we recommend users that would like to perform an analysis on a regional scale to use the GTSR-MED extreme sea levels as the standard deviation (observed vs modelled) is smaller. Users that are interested in a specific location may be more interested in the DCESEL dataset as the mean bias is smaller than for the GTSR-MED dataset, which indicates that the modelled extreme sea levels may be closer to the observed values in some locations. Users interested in coastal flood

risk assessment to extreme sea levels should be aware that both datasets do not include waves. Omitting waves could lead to an underestimation of potential impacts (see Vousdoukas et al. (2016)).

### 3.4.3 Data attribution

The attribution of data to the coastal units involved several processing steps, which varied depending on the type of dataset (as documented in the python scripts, see methods section). Every parameter of the database was then checked manually in a Geographic Information System, by at least two different users, to ensure correct attribution. This validation process was introduced to ensure internal consistency and, to identify and correct errors or mismatches in the database compilation process.

## 3.5 USAGE NOTES

We envisage that academics, managers and planners will use the developed database for coastal applications. We emphasize that the database is designed for regional-scale applications. Caution is required when using the database for local applications.

## ACKNOWLEDGEMENTS

A.T.V., D.C., S.M., J.H., D.L., and J.A.J. were funded by the European research project RISES-AM (grant agreement 603396). The authors thank Thomas Wahl for providing the extreme sea-level return periods based on the GESLA-2 observations. We acknowledge financial support by Land Schleswig-Holstein within the funding programme Open Access Publikationsfonds.



# 4

## **FUTURE URBAN DEVELOPMENT EXACERBATES COASTAL EXPOSURE IN THE MEDITERRANEAN**

This chapter is published as:

Wolff, C.; Nikolettopoulos, T.; Hinkel, J. and Vafeidis, A. T. (2020): Future urban development exacerbates coastal exposure in the Mediterranean. *Scientific Reports*, 10:14420. doi: [10.1038/s41598-020-70928-9](https://doi.org/10.1038/s41598-020-70928-9)

## ABSTRACT

Changes in the spatial patterns and rate of urban development will be one of the main determinants of future coastal flood risk. Existing spatial projections of urban extent are, however, often available at coarse spatial resolutions, local geographical scales or for short time horizons, which limits their suitability for broad-scale coastal flood impact assessments. Here, we present a new set of spatially explicit projections of urban extent for ten countries in the Mediterranean, consistent with the Shared Socioeconomic Pathways (SSPs). To model plausible future urban development, we develop an Urban Change Model, which uses input variables such as elevation, population density or road network and an artificial neural network to project urban development on a regional scale. The developed future projections for the five SSPs indicate that accounting for the spatial patterns of urban development can lead to significant differences in the assessment of future coastal urban exposure. The increase in exposure in the Extended Low Elevation Coastal Zone (E-LEcz = area below 20m of elevation) until 2100 can vary, by up to 104% depending on the urban development scenario chosen. This finding highlights that accounting for urban development in long-term adaptation planning, e.g. in the form of land-use planning, can be an effective measure for reducing future coastal flood risk on a regional scale.

## 4.1 INTRODUCTION

The urban extent in low lying coastal areas is increasing faster than in other regions (Seto et al., 2011), thus leading to increased exposure to sea-level rise and associated hazards. Societies' risk from these hazards will, therefore, not only depend on the physical drivers of change but also on the rate and pattern of urban growth which will be guided, to a large extent, by policies on future urban development (Song et al., 2017). One way to investigate how urban development influences future coastal flood risk is by accounting for spatiotemporal urban land cover change with the use of spatially explicit future urban projections in coastal impact assessments. Spatially explicit future urban extent scenarios are, however, currently often not available on a regional scale, which is one of the major shortcomings in coastal impact assessments to date (Muis et al., 2015). Until recently, most studies have considered physical drivers of future change, partly accounting for population and economic development (Vousdoukas et al., 2020b) but have neglected changes in the spatial extent of urban agglomerations, where most impacts occur. Large scale urban change models can help to better understand how a non-climatic driver, namely urban development, influences future risk.

Different concepts and methods have been developed for modelling future urban change. Consequently, there now exists a vast diversity in modelling approaches, concepts, and models striving to describe and understand the mechanisms of land cover change. These approaches include, among others, the use of Cellular Automata (Feng et al., 2011), Monte Carlo simulations (Güneralp and Seto, 2013), Artificial Neural Networks (Iizuka et al., 2017), as well as process-based and empirical models (e.g. CLUE) (Verburg and Overmars, 2007). To date, most spatially explicit urban extent studies involve local applications (Song et al., 2017, Iizuka et al., 2017, Pijanowski et al., 2014, Pijanowski et al., 2002b), and few broad-scale studies exist. Examples of regional-scale applications of urban change models include the studies of Seto et al. (2012), Zhou et al. (2019) and Gao and O'Neill (2020). Seto et al. (2012) used the land change model GEOMOD and a Monte Carlo simulation approach using projected GDP and urban population to develop spatially explicit probabilistic forecasts of urban land cover change until 2030 with a resolution of  $\sim 5$  km. Zhou et al. (2019) used the SLEUTH Urban Growth model to develop urban land cover projections between 2012 and 2050 based on urban maps generated from LandScan population data at a resolution of 1 km. SLEUTH is an abbreviation that stands for all the inputs used in the model, which are slope, land cover, excluded regions, urban land cover, transportation and hill shade (Zhou et al., 2019). Recently, Gao and O'Neill (2020) developed an empirical model based on spatial data, the Spatially Explicit Long-term Empirical City development (SELECT) model, to project urban land cover over the 21 century with a resolution of  $\sim 14$  km. All the studies mentioned above are too coarse, in terms of spatial resolution, for regional coastal applications while in most cases the time horizon of the projections is too short for long-term coastal impact assessments.

In this paper, we address this gap by developing spatially explicit projections of urban extent for 10 Mediterranean countries with a resolution of 100 m, which is 10 to 140 times finer than existing gridded urban extent projections. For this purpose, we couple a Multilayer Perceptron (MLP) with a Geographic Information System to generate spatially explicit urban extent projections, for a range of socio-economic scenarios, until 2100. MLP is one of the modelling tools that has recently been used in the attempt to explore the complexity of interactions that govern the patterns in which urban extent changes and evolve (Basse et al., 2014, Chen et al., 2020). An MLP has the ability to quantify complex behaviour and patterns (Pijanowski et al., 2002a) by taking into account non-linear relationships between the input and output variables and generalise in the presence of noisy or incomplete data (Mas and Flores, 2008).

Our projections are quantitatively and qualitatively consistent with the assumptions of the global Shared Socioeconomic Pathways (SSPs), which have been developed to support vulnerability and impact assessment studies. The SSPs comprise narratives that describe five different plausible pathways of societal development and also include information on future urban outcomes (see Table 4-1) (Jiang and O'Neill, 2017). In specific, urbanisation in SSP1 and SSP5 is rapid, although it is less well managed in SSP5 (Jones and O'Neill, 2016), leading to higher urban sprawl. In SSP3 urbanisation proceeds slowly with mixed spatial patterns,

particularly in developing countries, which are characterised by inequality and fragmentation. Urban settlements are poorly planned, and limited urban employment opportunities lead to unattractive urban centres and slow urbanisation rates in SSP3. However, population growth is rapid under SSP3 (Kc and Lutz, 2017) (except for the wealthier OECD countries) leading to high demand for urban space. A rapid urbanisation rate characterises SSP4 in medium and low-income countries, and central urbanisation rate in high-income countries with mixed spatial patterns, mainly driven by a lack of rural employment opportunities. Population growth is low in Mediterranean countries. SSP2 describes a world with a development that occurs at rates consistent with historical patterns of urbanisation and spatial patterns (Jones and O'Neill, 2016).

**Table 4-1:** Summary of the Shared Socioeconomic Pathway assumptions underlying urban development (based on Jones and O'Neill (2016); Jiang and O'Neill (2017) and KC and Lutz (2014))

SSP	Urbanisation rate	Urban spatial patterns	Population growth	GDP growth
SSP 1	Rapid	Urban expansion well managed (compact)	Global population growth is relatively low; fertility is medium in wealthier OECD countries	High-income growth, but slower economic growth over the longer term
SSP 2	Central	Historical spatial patterns	Global population growth is moderate and levels off in the second half of the century	Medium income growth
SSP 3	Slow	Mixed urban spatial patterns	Population growth is rapid (except for the wealthier OECD countries) leading to high demand for urban space	Low-income growth
SSP 4	Rapid in medium and low-income countries, central in high-income countries	Mixed spatial patterns	Population growth is low in Mediterranean countries	Low-income growth
SSP 5	Rapid	High urban sprawl, urban expansion is not well managed (compared to SSP1)	Population growth is high in wealthier OECD countries, low population growth in developing countries	Rapid growth of the global economy

In a final step, we use the developed scenarios to investigate how coastal exposure changes in the future. We choose the Mediterranean region as it is considered a hotspot of urban development globally. Between 1960 and 2010, the urban population increased by 20% (UNEP/MAP, 2016). A large share of urban development takes place along the coast where most of the industry and services are located (European Environment Agency, 2014). According to Seto et al. (2012), the region is expected to experience a 160% increase in urban extent between 2000 and 2030. Therefore, many Mediterranean cities will be potentially exposed to climate-related hazards such as coastal flooding and erosion. Even though the current level of risk is not high in the Mediterranean, it is likely to increase in the future (Cramer



et al., 2018, Reimann et al., 2018), also due to socio-economic development. Thus, the Mediterranean region can be considered as an adaptation hotspot (Hallegatte et al., 2013).

## 4.2 RESULTS

### 4.2.1 Spatially explicit projections of urban extent

At the Mediterranean scale, we find substantial differences in future urban development rates and patterns until 2100 between the different projections (Figure 4-1 and 4-2). The difference between the high and low urban extent projection ranges between 25% (HRV) and 115% (FRA) within the countries in the year 2100. Under all SSPs, urban extent increases during the century (Figure 4-1).

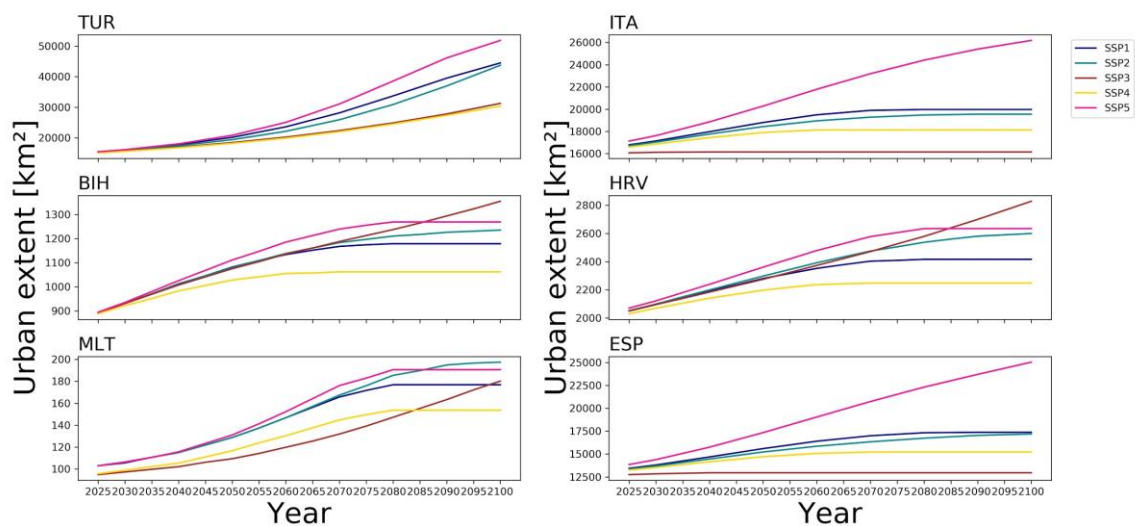


**Figure 4-1:** Temporal development of urban extent for six selected countries from 2025 to 2100. Note that the scales on the y-axis are different for each graph

Until 2085, SSP5 produces the highest urban extent in all countries, reflecting the underlying narrative of a high urbanisation rate combined with urban sprawl. Interestingly, for some countries, the urban extent under SSP3 is, towards the end of the century, higher than under SSP5 (see Figure 4-1 - HRV and BIH). Rapid population growth in lower-income countries seems to be the main driver for urban land demand after 2085.

SSP3 is characterised by a low fertility rate and declining population in most of the developed world (Kc and Lutz, 2017), leading to limited growth in urban extent in the wealthier European Mediterranean OECD countries (France, Greece, Italy, Slovenia, Spain) as well as in Turkey and Malta until 2100. In contrast, in the same scenario, the urban extent is highest in Bosnia-

Herzegovina, Croatia, and Cyprus due to rapid population growth in those countries under SSP3. SSP5 shows the highest urban extent in wealthier European Mediterranean OECD countries and second highest in the rest of the countries (except for Malta). SSP5 is characterised by a high population growth driven by optimistic economic outlooks leading to a high GDP in high-income countries (O'Neill et al., 2017). At the same time, in the rest of the countries, rapid development causes slower population growth compared to SSP3 (Jones and O'Neill, 2016). SSP1 is characterised by fast urbanisation rates and concentrated spatial patterns (Jiang and O'Neill, 2017) in all countries but a relatively low population increase. This leads to the second-highest urban extent in the wealthier European Mediterranean OECD countries and Turkey. In contrast, the increase in urban extent is relatively low in Malta, Bosnia-Herzegovina, Cyprus, and Croatia, where the population seems to be the primary driver of future urban extent in 2100. In all countries (except for Malta) SSP2 represents a middle-of-the-road urban future with moderate urban development (Figure 4-1 and Appendix B - Supplementary Table 4-1 and Supplementary Figure 4-1.)

Ranking the SSPs according to their total urban extent in 2100 from lowest to highest (see Appendix B - Supplementary Table 4-2) shows that the wealthier European Mediterranean OECD countries follow the same patterns, with SSP3 having the smallest extent and SSP5 the highest. Bosnia-Herzegovina, Cyprus, and Croatia form a second group with similar patterns, this time with SSP4 having the lowest urban extent and SPP5 the highest, leading to up to 28% differences in the urban extent between the scenarios in 2100. Turkey and Malta seem to develop differently. Malta is highly urbanised, thus having the highest urban share of all countries (one-third of the nation is urban). The greatest urban extent for Malta occurs under SSP2, reflecting the historical pattern of urbanisation. Malta's high historical urban development rates combined with a high GDP under SSP2 lead to the highest urban extent. The high urban share in Malta leads to very few rural pixels that can convert in the future to urban. We investigated that the spatial allocation of future urban land may be plausible but somewhat unrealistic in Malta. We argue that such a high urban development rate in such a small country illustrates the challenges of urban land allocation in the future if urban development will be rapid and not well managed.

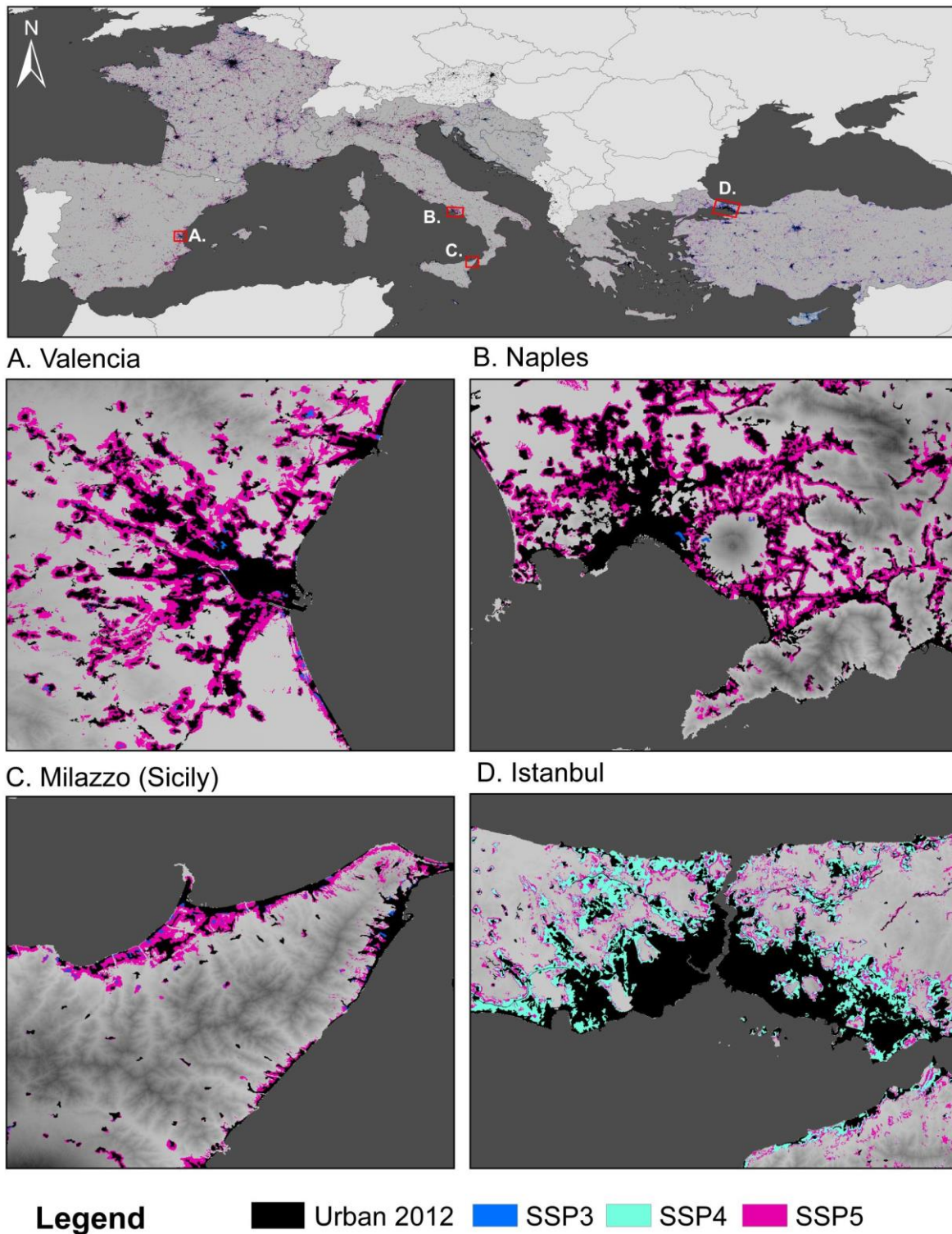


**Figure 4-2:** Spatially explicit urban extent in 2100 for different SSPs. European Mediterranean Countries included in the study are highlighted in darker shades of grey in the upper panel. For four selected regions, we present the spatially explicit urban extent scenarios that produce the highest and lowest urban extent.

#### 4.2.2 Future coastal urban exposure in 2100

Depending on the urban development scenario chosen the urban extent increases in the E-LECZ (area below 20m) between 2012 and 2100, for instance, by 67% (2075km<sup>2</sup>) for Italy, 104% (2331km<sup>2</sup>) for France (Mediterranean coast only) and 86% (691km<sup>2</sup>) for Greece (Figure 4-3 and Appendix B - Supplementary Table 4-3).

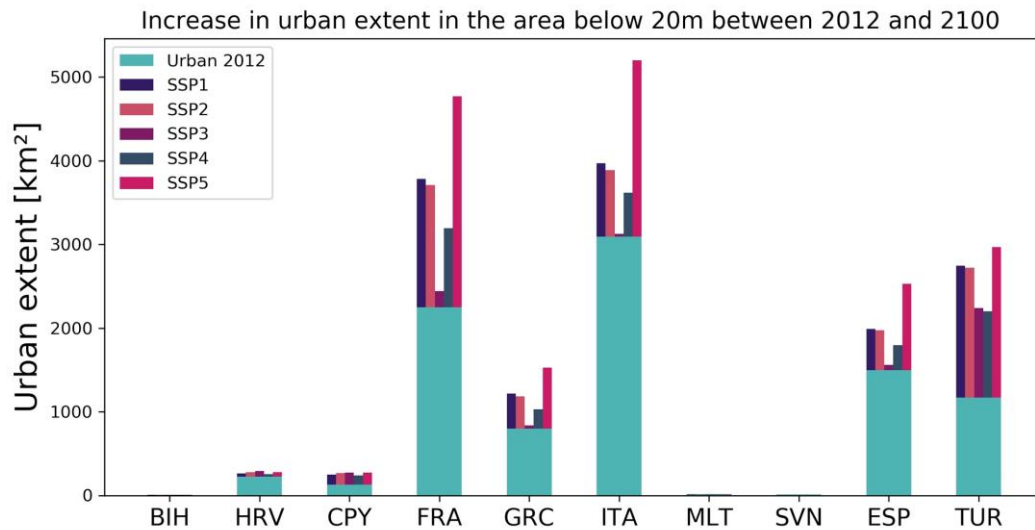


**Figure 4-3:** Country-specific increase in urban extent in the E-LECZ between 2012 and 2100 [in km<sup>2</sup>] for the five SSPs.

The urban extent scenario that leads to the highest urban exposure in the E-LECZ is the one that also produces the highest total urban extent in 2100 (see Section 4.2.1 "Spatially explicit projections of urban extent") reflecting that the model simulates high urban development in the E-LECZ. Figure 4-4 shows the spatial difference between 2012 and 2100 for four selected regions under SSP5. Compared to the year 2012, the urban extent increases in the floodplain in all regions leading to a significant increase in coastal exposure. Our results, therefore, show that accounting for the spatial patterns of coastal development can lead to significant differences in future exposure.

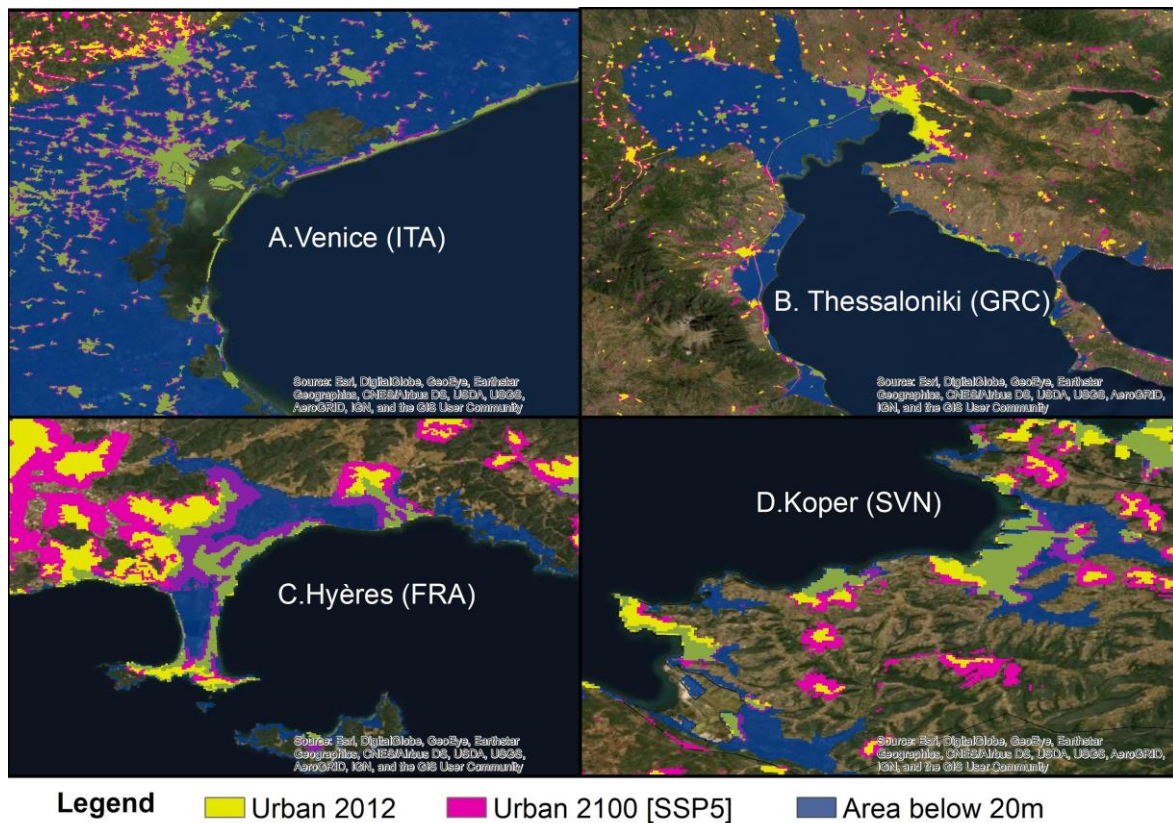


**Figure 4-4:** Potential urban development in four selected coastal regions under SSP5. In dark blue, the area that lies below 20 m is indicated.

### 4.3 DISCUSSION

The ability to project future urban development enables researchers and policymakers to anticipate better the consequences of specific actions, e.g. in the context of urban planning (Song et al., 2017), or to plan appropriate future interventions that can reduce exposure to future climate-related hazards such as coastal flooding. The spatially explicit urban extent scenarios offer, therefore, the possibility to analyse different urban futures and designate future priority areas for coastal adaptation in the Mediterranean. In this context, the results of this study can inform the development of future coastal management and adaptation policies on a regional scale (Haasnoot et al., 2019), such as those outlined in the Integrated Coastal Zone Management (ICZM) protocol of the Barcelona Convention (UNEP/MAP/PAP, 2008).

Our study shows that one of the most effective measures to reduce future exposure will be to reduce future urban development inside the coastal floodplain. The ICZM Protocol prescribes the implementation of a 100m setback zone that restricts further development within this zone (Rochette et al., 2010). Spatial planning in the form of setback zones or even retreat can be one of the most effective interventions to reduce future exposure (Lincke et al., 2020) and lead to a more sustainable Mediterranean future urban development. However, coastal urban development could also entail positive effects to reduce future vulnerability to natural hazards and hence increase the overall adaptive capacity of cities (Garschagen and Romero-Lankao,

2013). Even if future urban exposure increases, the coastal vulnerability could decrease if actual adaptation action (e.g. in the form of hard protection) and disaster management are effectively implemented. Hence, we argue that the concentration of people and assets could also increase the efficiency and effectiveness of adaptation measures in the future. Future urban extent scenarios could be useful to explore these avenues and inform adaptation and spatial planning authorities what mix of adaptation strategies for different regions could be most effective.

Several studies of European cities had shown that even when population decreased, urban extent increased (Kasanko et al., 2006, Barranco et al., 2014). This trend is also reflected in our developed spatially explicit urban extent scenarios, where urban extent increases with time under all scenarios, albeit at lower rates in those cases where population declines. The urban projections reflect that urban development is linked to GDP growth in high-income countries. In contrast, in lower-income countries, urban development is more driven by population growth towards the end of the century. This pattern has also been reported in other studies (e.g. see meta-analysis of global urban land expansion from Seto et al. (2011)).

### **Model performance and limitations**

Evaluating our country-specific urban change models against historical data indicates that these are capable of reproducing historical spatial patterns of urban development on a regional scale. We observed that the models of those countries with a high urban share and/or uniform urban sprawl patterns (see Table 4-2), such as Croatia, Slovenia, France or Cyprus, perform best. This indicates that the MLP model can better generalise on countries where a large enough sample of urban change is provided. As the extent of urban areas is small in comparison to that of rural areas, we have an imbalanced dataset due to an uneven distribution of classes (much more rural pixel, than urban). This poses a challenge from a Machine Learning perspective since models are harder to train with imbalanced training sets. This issue has been tackled by under-sampling the majority that is the rural class in our case, to create a more balanced training set. For most countries, the model performed best with an under-sampling ratio of 10 (1:10, Urban: Rural) (the undersampling ratio used for every country can be found in Appendix B - Supplementary Table 4-4). Further, we improved the performance of the MLP model by using data augmenting which creates additional training data. At the same time, the MLP is challenged when trying to reproduce inhomogeneous settlements, where urban development is fragmented with clustered and contrasted patterns. Such an example is Spain, where the performance of the MLP was the lowest (Table 4-2).

**Table 4-2:** Performance measures of the MLP for predicting urban extent in 2012 for every country.

Country	Overall accuracy	Precision	Recall	Negative predictive value	Specificity	F1-score
BIH	0.997	0.901	0.888	0.998	0.998	0.894
CYP	0.992	0.955	0.951	0.995	0.996	0.953
ESP	0.986	0.745	0.635	0.991	0.995	0.680
FRA	0.992	0.967	0.892	0.994	0.998	0.928
GRC	0.993	0.893	0.852	0.996	0.997	0.871
HRV	0.996	0.950	0.937	0.998	0.998	0.939
ITA	0.993	0.970	0.890	0.994	0.998	0.927
MLT	0.999	0.999	0.999	0.999	0.999	0.999
SVN	0.999	0.980	0.977	0.999	0.999	0.978
TUR	0.992	0.788	0.731	0.995	0.996	0.759

The explanatory potential of the input variables was analysed by using entropy and mutual information (Theodoridis, 2015). Mutual information measures the dependencies between each feature and the output. It quantifies the information content of two variables in classification problems by considering the input-output statistics without any reference to a specific model. Mutual information should be interpreted relative to the entropy. The mathematical explanations of the two metrics can be found in Appendix B. Supplementary Table 4-5 (in Appendix B) shows the mutual information and entropy values for every input variables and country. High mutual information means that the input feature is suitable in explaining the output. In nearly all countries, distance to urban land cover and the population density have the highest mutual information, reflecting the fact that new urban development is expected to grow near existing urban agglomerations. However, the order of magnitude between the variables is often similar, thus we believe that all input variables are useful for our MLP. The entropy of a country can be interpreted as a measure of urbanisation in this study. In countries where the distribution of urban and rural pixels is more balanced (e.g MLT 29% Urban; 70% Rural), the entropy is high (for MLT 0.8).

We must note that the validation measure 'overall accuracy' alone does not necessarily mean that the urban change model has high predictive power. Pontius and Malanson (2005) discuss several reasons why 'percent correct' alone is not enough to validate a model. Importantly, they state that a null model that predicts pure persistence between two-time steps often leads to more than 90% correct due to the temporal autocorrelation between the time steps. Additionally, the merit is not appropriate for imbalanced datasets (Jeni et al., 2013). Therefore,

it is essential to consider the f1-score, precision, recall and a visual assessment of the spatial performance of the urban change model to assess the performance.

Future research could improve and extend this work in a number of ways. First, in our study, we assume a constant pattern of the input variables throughout the century due to lack of data. Hence, one central assumption of the study is that similar processes drive future urban development. For instance, urban development will change as a response to a changing road network but information on the future development of the road network is currently not available for most countries. The MLP model would be able to incorporate such processes if input data for all variables become available in the future, which would allow us to dynamically model future urban expansion from one time step to another. Second, the developed urban change model only considers spatial aspects and does not account for non-spatial elements such as demographic characteristics, spatial planning policies or tipping points that are unpredictable (such as natural hazards) which is a major challenge in urban land change models (Pijanowski et al., 2002a). Future work could further expand the urban scenarios by accounting for policy interventions such as coastal adaptation measures in the form of setback zones that restricts future urban development in flood-prone areas or include vertical growth of cities into the scenarios. Last, a time interval of more than 12 years between the input and target data could lead to improved training of the MLP by providing a larger number of urban pixels that change from one time step to another. However, the lack of a consistent land cover time series with a high resolution that can be used as input (e.g. distance to forest, grassland) and output data (urban) to train the MLP is currently not available at this scale.

#### **4.4 CONCLUSION**

Urban growth rates and spatial patterns of urban development will determine society's exposure and vulnerability to extreme events, sea level, and other climate-related hazards. Urban development is a dynamic and complex process (Schneider et al., 2015) that is influenced by physical, socio-economic and political conditions. Hence, how urban development influences future risk has not yet been quantified and is not well understood (Song et al., 2017). Spatiotemporal land cover analysis and future urban land cover projections can help improve our understanding of these processes.

We have produced urban extent projections that cover a plausible range of uncertainty with a resolution of 100m, spanning from 2025 to 2100. The developed urban projections are based on the global SSPs and thus depict five different plausible urban development scenarios. Across all SSPs, we observe a continued increase in urban areas in the coastal zone, which leads to an increase in coastal exposure, even though the rates and spatial patterns of urban development vary between the different scenarios. We anticipate that the developed urban



extent scenarios will be employed in a wide range of impact assessments to climate change-related hazards beyond coastal applications.

## 4.5 METHODS

To model plausible future urban extent, we developed a set of country-specific urban change models (see Figure 4-5) as the rate and pattern of urban development can vary considerably across countries and years (Li et al., 2019). First, we employ an MLP artificial neural network for modelling the likelihood of urban transformation (see Figure 4-5a). In a second step, we calculate, for each SSP, the future urban land demand in 5-year time steps until 2100 (see Figure 4-5b). Finally, we create the urban extent scenarios by classifying the MLP model outputs accordingly (see Figure 4-5c). These projections are then employed for calculating future exposure to coastal flooding (see Section 4.5.2 'Future coastal flood exposure').



**Figure 4-5:** Workflow of the urban change model

### 4.5.1 Urban change model

#### Step a: Likelihood of urban transformation

We used an MLP to generate a predictive spatially explicit model of urban development for 10 Mediterranean countries where data were available (MLT, CYP, GRC, SVN, ITA, BIH, HRV, FRA, ESP, TUR). An MLP is a computational model often used for complex, non-linear behavior, and patterns of unknown input-output relations (Iizuka et al., 2017, Pijanowski et al., 2009). Every MLP is composed of one input layer, one or several hidden layers, and one output layer. For a detailed description of MLPs see Theodoridis (2015).

The MLP was trained using input data from 2000 to reproduce CORINE urban land cover data from 2012 (<https://land.copernicus.eu/>). In this study, we define urban areas as locations dominated by artificial surfaces, which corresponds to the artificial surface class (code 1) from CORINE that includes residential, industrial, commercial, transport and green urban areas.

The input layer of our MLP consists of nine input variables (Table 4-3). The input variables have been selected based on literature review and data availability. Elevation and slope have been selected to reflect the topography, which influences urban development as steep areas, and areas of high elevation are less likely to develop (Iizuka et al., 2017). Distance to roads has been included because areas that are easy to access are more likely of being developed (Tayyebi et al., 2011) as it is correlated to people's mobility (Iizuka et al., 2017), which influences where people decide to settle. As the study focuses mainly on the exposure of urban areas to sea-level rise and climate-related hazards such as storm surges, we decided to also include the distance to the coast as an input variable. Low elevation coastal zones are developing faster than the hinterland (Li et al., 2019) and therefore distance to the coast can be an important predictor. We also included the Euclidean distance to urban areas, arable land, grassland, and forest to account for the effect of other types of land use on urban development. Finally, we used population density as an input variable to reflect socio-economic driving forces, as numerous studies show that these constitute underlying drivers of urban development.

The output layer consists of a single variable giving the likelihood that a pixel will turn urban in the next time step. To define the best MLP architecture for every country (i.e. the number of neurons in each layer, the connection patterns between the layers, the activation function and the learning methods) we conducted a sensitivity analysis using between 6-10 different network architectures. An overview of the best model architecture per country can be found in Appendix B - Supplementary Table 4-4.

**Table 4-3:** Summary of data used for input and output variables of the MLP

Variables		Source	Spatial resolution	Pre-processing notes
Input	Distance to forest	CORINE 2000	100m	Corine classes used: 311, 312, 313, Euclidean distance to forest
	Distance to grassland	CORINE 2000	100m	Corine classes used: 321, 322, 323, 324, Euclidean distance to grassland
	Distance to urban	CORINE 2000	100m	Corine classes used: 111, 112, 121, 122, 123, 124, 131, 132, 133, 141, 142, Euclidean distance to urban 2000
	Distance to arable land	CORINE 2000	100m	Corine classes used: 211, 212, 213, 221, 222, 223, 231, 241, 242, 243, 244, Euclidean distance to arable land 2000
	Distance to roads	Open Street Map		We used the main roads (fclass: primary motorways, secondary), Euclidean distance to roads
	Population density	GPW v4 2000	1km	Total population in 2000 per km <sup>2</sup> , resampled to 100m
	Elevation	SRTM	30m	Elevation in m, resampled to 100m
	Slope	Derived from SRTM	30m	Percent increase in slope, resampled to 100m
	Distance to coast	Based on CORINE coastline	100m	Euclidean distance to coastline
Output	Urban	CORINE 2012	100m	Reclassification of CORINE data to Urban = 1, Rural = 0; Corine classes used: 111, 112, 121, 122, 123, 124, 131, 132, 133, 141, 142

### **Step b: Future urban land demand**

In the second step, we calculated the future urban land demand for every country, SSP and time step. For this purpose, we used the relative changes in total urban extent for every country between 2020 and 2100, obtained from Li et al. (2019). This study developed (non-spatial) country-specific urban extent growth models using data from an urban extent time series, spanning from 1992 to 2013 (22 years) based on satellite observations, and historical socio-economic indicators, namely Population and GDP. These country-specific models were then used to project future urban growth under the Shared Socioeconomic Pathways until the end of the 21st century using the population and GDP data from the SSP database. The reported mean accuracy for Europe compared to fine resolution land cover data was 95% (Li et al., 2019). In our model, we used the relative changes of Li et al. (2019) to calculate the total number of future urban grid cells.

### **Step c: Spatial classification**

Finally, the future urban land demand per time step was used to reclassify our MLP outputs. The highest urban transformation likelihoods were reclassified according to the total number of future urban grid cells (see Figure 4-5). We used CORINE 2012 as a starting year to create high-resolution spatially explicit urban extent scenarios that are consistent with the global SSP assumptions, in 5-year time steps until 2100. We produced scenarios for 10 European Mediterranean countries where global SSP assumption and CORINE data exist.

## **4.5.2 Future coastal flood exposure**

Using the spatially explicit urban extent projections, we then assessed future coastal exposure for the Mediterranean coast in 2100. For this purpose, we calculated the low-lying part of the coastal zone that is hydrologically connected to the sea and lies above 20m of mean sea level (E-LECZ). We decided to use the E-LECZ to account for all plausible future changes in mean sea level and associated extreme water levels (Wolff et al., 2018). The exposed area was overlaid with the developed urban extent projections to analyse the exposure of future urban extent for all SSPs.

## **4.5.3 MLP performance**

We used a confusion matrix to evaluate the model performance (see Figure 4-6) and find the MLP model architecture that best approximates the input-output relationships. The confusion matrix is a way to investigate the percentage of correct and incorrect classified pixels and is a measure for analysing the goodness of fit for a specific classification model architecture. The overall accuracy reflects the overall correct classified pixels. However, this metric is very

sensitive to imbalanced datasets and can be misleading when measuring the MLP performance (Jeni et al., 2013) as our dataset contains few urban pixels compared to the rural class. A more appropriate merit to assess the performance of binary classification problems with a skewed dataset is, therefore, the F1-score. The F1 score is used to represent the balance between precision (Positive predictive value - the percentage of pixels that are classified as urban and are, in reality, urban) and recall (True positive rate - the ratio of the pixels that are correctly classified in relation to the total positive (target) pixels). It can be viewed as the harmonic mean of precision and recall. The results per country are presented in Table 4-2.

CONFUSION MATRIX		GROUND TRUTH		
		RURAL	URBAN	
PREDICTED	RURAL	True Negative (TN)	False Positive (FP)	<b>SPECIFICITY:</b> TN / (TN+FP)
	URBAN	False Negative (FN)	True Positive (TP)	<b>RECALL:</b> TP / (TP+FN)
<b>F1 SCORE:</b> $2 \times \frac{\text{PRECISION} * \text{RECALL}}{\text{PRECISION} + \text{RECALL}}$		<b>NEGATIVE PREDICTIVE VALUE:</b> TN / (TN+FN)	<b>PRECISION:</b> TP / (TP+FP)	<b>OVERALL ACCURACY:</b> TP + TN / (TP+FP+TN+FN)

**Figure 4-6:** Confusion matrix

The urban change models can reproduce the observed patterns of past urban development between 2000 and 2012 with an F1-score between 68 and 99 % in all countries (see Table 4-2). This indicates that the country-specific urban change models capture past patterns of urban development. However, the confusion matrix is not very useful in assessing spatial patterns. For instance, if a pixel is misclassified, regardless of whether the correct class is found in a neighbouring pixel, it is presented as incorrect (Pontius and Malanson, 2005). Therefore, a visual assessment was conducted by overlaying the simulated and CORINE 2012 maps using a Geographic Information System to explore the spatial and qualitative patterns of the predicted model outputs (see Appendix B - Supplementary Figure 4-2 for an example).

## 4.6 DATA AVAILABILITY

The urban extent projections are available at the figshare repository (<https://figshare.com/s/8fc878cbf3597c6574e1>). Further, we provide the python code to set up the MLP model and create the urban extent projection in the figshare repository.

## ACKNOWLEDGEMENTS

We thank George Vafeidis for useful discussions on the use of ANNs and under-sampling. Open access funding provided by Projekt DEAL.



# 5

## SYNTHESIS

## 5.1 SUMMARY OF THE MAIN RESEARCH FINDINGS

There are different limitations and constraints inherent in broad-scale coastal flood risk assessments. The aim of this thesis has been to address data limitations and improve our understanding of data uncertainties in broad-scale coastal flood risk assessments. This research, in particular, contributes in the following ways to the overarching aim. It (1) addresses data availability, consistency and reproducibility constraints, (2) extends existing coastal data models and increases the level of detail of assessments, and (3) explores and quantifies data uncertainties in broad-scale coastal flood risk assessment for the Mediterranean coastal region. This final chapter summarizes the main findings and lessons learned. It then discusses the remaining data challenges and ways forward in broad-scale coastal flood risk assessment.

### 5.1.1 Data availability, consistency and reproducibility

This thesis contributes to overcoming data limitations for broad-scale coastal flood risk assessments. Using the Mediterranean coastal region as a case study, we developed a consistent, open-access, spatial coastal database that consists of 160 parameters on the characteristics of the natural and socio-economic coastal subsystems. The Mediterranean Coastal Database (MCD) contains information on current conditions and plausible future changes, such as sea-level rise and socio-economic development. In Chapter 3, we demonstrate that the database is designed for broad-scale analysis and provides a robust basis for different types of comparative coastal studies as it contains consistent information in terms of resolution, quality, accuracy and format for the entire region. Further, we enhance the transparency and reusability of the database by documenting and providing open-source code for all data processing steps in an online repository.

Further, as described in chapter 4, we have developed a new set of spatially explicit projections of urban extent for ten countries in the Mediterranean with a resolution of 100m, which is 10 to 140 times finer than existing gridded urban extent projections on a broad-scale. To produce the urban extent projections, we developed an urban change model for every country independently. The modelling approach could be applied to different regions where land use data for different time steps and ancillary data are or become available in the future. The urban extent projections spanning from 2025 to 2100 and the python code to set up the urban change model are freely and publicly available in an online repository.

In Chapters 2 and 3 we also produced independent consistent datasets on the geomorphological structure of the coast, deltas and the distribution of assets and population for the Mediterranean and Emilia-Romagna coast, as consistent data were not available. We



developed a method to classify the coast into homogenous units by using Google Earth, which provides satellite images and location-tagged pictures that can be used to visually interpret and distinguish the coastal type.

### 5.1.2 Coastal data model and assessment scale

This thesis extends the spatial representation and data structure of coastal space for broad-scale coastal flood risk assessment. We have created a new coastal data model with a data structure that combines the linear representation of the coast with spatial coastal assessment units that capture the spatial structure of exposed land and administrative boundaries for the Mediterranean region. Both Chapter 2 and 3 achieved the goal of downscaling a global coastal database by using a refined coastline and coastal assessment units that divide the coast into homogeneous segments in terms of impacts, vulnerability and adaptation needs to ESL and SLR. With the segmentation methods and results presented in this thesis, broad-scale coastal flood risk assessment results can be presented in a more detailed manner and impact indicators such as adaptation costs, for instance in the form of dike construction, are more accurate compared, for instance, to the global DIVA data model. In Chapter 2, for instance, we show that a more detailed coastline leads to an increase in coastline length by 43%, thus, considerably influencing adaptation costs in Emilia-Romagna. Further, a comparison of the different segmentation models indicated that not only does the length of the coast increase, but the spatial representation of coastal flood impacts is also more realistic due to the more refined assessment scale and the increase in the number of assessment units. The applied methods (e.g. data model, segmentation process) are transferable and can be applied in other regions.

### 5.1.3 Data uncertainties

This thesis improves our understanding of data uncertainties in broad-scale coastal flood risk assessments in two ways. First, chapter 2 shows that coastal flood risk assessments are most sensitive to variations in elevation and vertical land movement data compared to variations in population data. Results show significant uncertainties in global elevation datasets that affect coastal impact assessment results, a finding that is consistent with previous studies (e.g. Poulter and Halpin (2008), Lichter et al. (2011), Hinkel et al. (2014)). Contrary to what is often reported in the literature, this thesis shows that the estimated areas exposed to coastal flooding are smaller with LiDAR DEM than those calculated with the SRTM DEM. In this thesis, an overestimation of the potential coastal floodplain is observed using SRTM elevation data, suggesting a negative bias in the data, which leads to higher potential coastal flood impacts

in Emilia-Romagna (~45% higher coastal flood extent, ~50% higher coastal flood damages). The largest differences between the DEMs were found in the area below 5m. Further, the inclusion of local information on human-induced subsidence rates increased the relative sea-level rise by 60cm in 2100, resulting in coastal flood impacts that are 25% higher compared to assessments where we mainly account for natural processes. These results indicate that broad-scale coastal flood risk assessments underestimate impacts due to the non-consideration of human-induced subsidence even in non-delta regions such as Emilia-Romagna.

Second, this thesis also improved our understanding of data uncertainties in broad-scale coastal flood risk assessments through novel urban extent projections that cover a plausible range of uncertainty spanning from 2025 to 2100. Existing spatial projections of urban extent are often available at coarse spatial resolutions, local geographical scales or for short time horizons, which limits their suitability for broad-scale coastal flood impact assessments. The developed urban projections are based on the global SSPs and thus depict five different plausible urban development scenarios and enable the assessment of coastal urban exposure under deep uncertainties on a broad-scale. Across all SSPs, we observe a continued increase in urban areas in the coastal zone, which leads to an increase in coastal exposure, even though the rates and spatial patterns of urban development vary between the different scenarios. The increase in exposure in the Extended Low Elevation Coastal Zone (E-LECZ = area below 20m of elevation) until 2100 can vary, by up to 104% depending on the urban development scenario chosen. This finding highlights that accounting for urban development in the assessment of coastal flood risk can be an important driver in the estimation of future coastal flood damages on a broad scale. Further, the results emphasise that adaptation planning in the form of land-use planning (e.g. setback zones, retreat) could be an effective measure for reducing future coastal flood risk on a broad-scale.

## 5.2 RECOMMENDATIONS FOR FUTURE RESEARCH

The outcome of this thesis highlights that data limitations and uncertainties are one of the major restrictions in broad-scale coastal flood impact assessments. There are various data related challenges and possible ways forward in improving broad-scale coastal flood impact assessments that go beyond the work conducted in this thesis. Some key prioritizing topics that require further research which targets data related challenges in broad-scale coastal flood risk assessments are listed in the following seven recommendations:

### **1. Better science through better data: Increase the availability of open-access, well-documented data and modelling techniques**

Broad-scale coastal flood risk assessments benefit from high-quality, well-documented, consistent and freely available data and modelling techniques. At the same time, the availability of such data is one of the major constraints. The provision of thorough and detailed descriptions of the methodological approaches and underlying assumptions (metadata) of all published scientific data products and results provide information on how research was produced and what it contains. Further, metadata enables researchers to independently verify the data product, incorporate modifications and build upon it. For this to happen, the research community would need to share the data and code available in an easy-to-use and open format. There are several reasons why sharing benefits everyone in the research community:

- (1) It forces us to document data work and code well, enabling researchers to replicate studies faster.
- (2) Reproducibility increases trust in scientific work.
- (3) We can get scientific credit for the effort we put into the data work. This is often one of the most time-consuming and less rewarding tasks of research even though it is a fundamental part of science.
- (4) We can make the life of the next researcher much easier, which will advance science even faster in the long run.

The Alan Turing Institute handbook for reproducible data science called 'The Turing Way' which is an open-source community-driven guide to reproducible, ethical, inclusive and collaborative data science (The Turing Way Community et al., 2019), could be a way to support scientists to develop the necessary skills to produce publications including the underlying data and analysing code to foster this transition.

## **2. Use of new data sources: Collecting and analysing information on characteristics of coasts and coastal flood components using crowd-sourced and citizen science projects could improve coastal flood risk assessments**

As described in chapter 1, there is a clear need for consistent and harmonised information on all components of coastal flood risk (hazard, exposure, vulnerability). New technologies and approaches, such as crowd-sourced or citizen science projects, could be useful to, for instance, monitor and keep track of past hazards and their impacts (Ward et al., 2020), which would provide data for model validation and development. The rapid development of mobile applications and internet platforms, such as Open Street Maps, has made it possible to produce and acquire data online. One main appeal of social media, such as Twitter, for research is that humans effectively act as sensors, providing a high volume of data at potentially high spatial and temporal resolution, in real time (Muller et al., 2015). Such high accuracy data could significantly improve our understanding of the temporal and spatial evolution of all components of coastal flood risks. For instance, Twitter has been used as an event detection medium for river or coastal flooding (Arthur et al., 2018, Barker et al., 2019) and for the creation of a global database of historical flood events including a web platform for real-time monitoring of flood events (de Bruijn et al., 2019).

Another example is the citizen science project Coastwards ([www.coastwards.org](http://www.coastwards.org)) which collects information on coastal material globally. Everyone can contribute to the development of the global database of coastal types by providing close-up images of coasts and classifying the image. These data could be used to validate, for instance, coastal classifications as outlined in Chapter 3.

Research has made use of some of the new technologies mentioned. However, most opportunities have been explored to a limited extent, but a growing demand can be expected for these research directions as the provision of extensive, real-time information with technologies that are of low cost are promising for coastal flood risk assessments, especially for improving the data availability in data-scarce regions.

## **3. Provide clearer guidance and recommendations for input dataset selections**

The research community should foster studies that assist developers and scientists in the review, selection and implementation of datasets for risk assessments. A good example is the POPGRID Data Collaborative that created a report, entitled 'Leaving No One off the Map: A Guide for Gridded Population Data for Sustainable Development' which aims to support users by selecting the most suitable gridded population dataset for the intended use. The report presents an overview, comparison, analysis and recommendation for seven gridded population datasets including an analysis of the underlying data, methods and basic assumptions, and the corresponding strengths and limitations of each dataset. Such reports or reviews address many of the misconceptions around the datasets and

provide guiding criteria to aid users in their selection process. A similar study, for instance, analysing the underlying methods of global DEMs and validating the DEMs for different regions around the world would be of high value for coastal impact assessments. It is important to instruct and educate data users on the underlying assumptions and existing uncertainties (Leyk et al., 2019).

#### **4. Urban extent projections could advance future population modelling and damage estimations**

The research community requires detailed settlement footprints and future projections of these urban environments to advance future population redistribution modelling and hence, coastal flood risk estimates. Data on urban land cover is often used as the main ancillary parameter in population modelling using dasymetric refinement approaches (Leyk et al., 2020). Hence, spatial urban extent projections provide a unique opportunity to advance future population modelling. Projections of future population, such as the coastal SSP of Merkens et al. (2016) and Reimann et al. (2017) currently do not consider urban expansion, which is a relevant process in coastal areas. Thus, including urban extent projections into population modelling could further improve future population projections, which may lead to more plausible estimates of future coastal exposure.

Further, the projected urban extent could strengthen the methodology of damage estimates. To calculate direct flood damages, depth-damage functions are used for different land cover data (Vousdoukas et al., 2018b). So far, damages have been assessed in a static manner in broad-scale coastal flood impact assessments, assuming no land cover change during the 21st century. Using urban extent projections, damages could be estimated in a dynamic way from time step to time step.

Future steps in research should focus on the creation of settlement footprints with higher temporal resolution and the inclusion of demographic variables as well as housing-related attributes to enable more in-depth insights into human settlements and its population (Leyk et al., 2020).

#### **5. Validation data on past coastal (extreme) events are of high value to thoroughly assess, calibrate and evaluate model results**

Validation of coastal flood assessments is often lacking at all spatial scales (de Moel et al., 2015, Paprotny et al., 2019). One main reason is the challenging circumstances to collect these data because of the rare occurrence of coastal extreme events as well as the fact that obtaining ground observations and information during an actual event is not a straightforward task. Currently, few examples of data that have been collected

immediately or shortly after specific events exist (e.g. Ramirez et al. (2016), Voudoukas et al. (2016)). However, all these data have a limited spatial and temporal coverage and thus, do not allow to thoroughly calibrate, validate and thus improve the performance of coastal flood risk assessments to date. Therefore, coastal flood risk assessments are difficult to advance without the availability of such data. Coastal authorities and scientists should create coastal observatories or observing networks (Toimil et al., 2020) that collect data on all components of coastal flood risk during an extreme event in a systematic way and make these data available to the research community.

## **6. Improvements in the spatial representation of coastal vulnerability would enhance the quality of coastal flood risk assessments**

Vulnerability is a multidimensional phenomenon with complex connections and patterns (Abram et al., 2019) and SLR impacts and risk are not evenly spread within and between coastal communities (Oppenheimer et al., 2019). This complexity is geographically and temporally dependent (Bevacqua et al., 2018) and leads to difficulties in the accurate spatial representation of vulnerability in broad-scale coastal flood impact assessments. In broad-scale coastal flood impact assessments, vulnerability is mainly related to physical assets in the sense of how assets get damaged by extreme sea levels and sea-level rise (de Moel et al., 2015). However, vulnerability has a much broader meaning as the population is not uniformly vulnerable to coastal hazards. To determine social vulnerability, unique and subjective aspects of people's behaviour, perspective, values, as well as sociodemographic determinants such as welfare, living conditions, gender, health-care, age or religion are important. Further, vulnerability is not a static phenomenon as it is important to determine temporal variations, for instance, between day and night. However, to obtain such sociodemographic data at a relevant spatial scale is extremely challenging, especially in developing countries (Bukvic et al., 2020). Therefore, the representation of social vulnerability is one of the main drawbacks in broad-scale coastal flood risk assessments to date (Jongman et al., 2012, de Moel et al., 2015). One promising research direction is the development of heterogeneity modelling to project age-structure, gender, race and ethnicity of future population (e.g. Hauer (2019) for the U.S counties).

## **7. Systematic uncertainty analyses are of high value to develop robust and useful broad-scale coastal flood risk information**

Understanding and quantifying uncertainty is a fundamental step in providing useful coastal risk information and improving coastal flood risk assessments. However, the relative importance of each source of uncertainty in the assessment of coastal flood risk has rarely been quantified in broad-scale assessments (Le Cozannet et al., 2015). One approach that could be promising is the variance-based global sensitivity analysis (GSA)

that facilitates identifying which source of uncertainty contributes to which extent to the output variability (Saltelli and Annoni, 2010). Future research should focus on developing approaches that enable systematic analysis and objective validations of data products and methodological choices to further refine and improve the accuracy and utility of broad-scale coastal flood risk assessments.





## REFERENCES

- ABRAM, N., GATTUSO, J.-P., PRAKASH, A., CHENG, L., CHIDICHIMO, M. P., CRATE, S., ENOMOTO, H., GARSCHAGEN, M., GRUBER, N., HARPER, S., HOLLAND, E., KUDELA, R. M., RICE, J., STEFFEN, K. & VON SCHUCKMANN, K. 2019. Framing and Context of the Report. In: IPCC Special Report on the Ocean and Cryosphere in a Changing Climate *In: PÖRTNER, H.-O., ROBERTS, D. C., MASSON-DELMOTTE, V., ZHAI, P., TIGNOR, M., POLOCZANSKA, E., MINTENBECK, K., ALEGRÍA, A., NICOLAI, M., OKEM, A., PETZOLD, J., RAMA, B., WEYER, N. M. & (EDS.)* (eds.).
- ARGUS, D. F., PELTIER, W. R., DRUMMOND, R. & MOORE, A. W. 2014. The Antarctica component of postglacial rebound model ICE-6G\_C (VM5a) based on GPS positioning, exposure age dating of ice thicknesses, and relative sea level histories. *Geophysical Journal International*, 198, 537-563.
- ARMAROLI, C., CIAVOLA, P., PERINI, L., CALABRESE, L., LORITO, S., VALENTINI, A. & MASINA, M. 2012. Critical storm thresholds for significant morphological changes and damage along the Emilia-Romagna coastline, Italy. *Geomorphology*, 143-144, 34–51.
- ARNS, A., WAHL, T., WOLFF, C., VAFEIDIS, A. T., HAIGH, I. D., WOODWORTH, P., NIEHUSER, S. & JENSEN, J. 2020. Non-linear interaction modulates global extreme sea levels, coastal flood exposure, and impacts. *Nat Commun*, 11, 1918.
- ARTHUR, R., BOULTON, C. A., SHOTTON, H. & WILLIAMS, H. T. P. 2018. Social sensing of floods in the UK. *PLoS One*, 13, e0189327.
- BAKKER, A. M. R., LOUCHARD, D. & KELLER, K. 2017. Sources and implications of deep uncertainties surrounding sea-level projections. *Climatic Change*, 140, 339-347.
- BAMBER, J. & RIVA, R. 2010. The sea level fingerprint of recent ice mass fluxes. *Cryosphere*, 4, 621-627.
- BARKER, J., BARKER, J. L. P. & MACLEOD, C. J. A. 2019. Development of a national-scale real-time Twitter data mining pipeline for social geodata on the potential impacts of flooding on communities. *Environmental Modelling and Software*, 213-227.
- BARRANCO, R. R., SILVA, F. B. E., MARIN HERRERA, M. & LAVALLE, C. 2014. Integrating the MOLAND and the Urban Atlas Geo-databases to Analyze Urban Growth in European Cities. *Journal of Map & Geography Libraries*, 10, 305-328.
- BARTLETT, D. J. 2000. Working on the frontiers of science: applying GIS to the coastal zone. *In: WRIGHT, D. J., AND BARTLETT, D.J.* (ed.) *Marine and Coastal Geographical Information Systems*. London: Taylor and Francis.
- BASSE, R. M., OMRANI, H., CHARIF, O., GERBER, P. & BÓDIS, K. 2014. Land use changes modelling using advanced methods: Cellular automata and artificial neural networks. The spatial and explicit representation of land cover dynamics at the cross-border region scale. *Applied Geography*, 53, 160-171.
- BAUGH, C. A., BATES, P. D., SCHUMANN, G. & TRIGG, M. A. 2013. SRTM vegetation removal and hydrodynamic modeling accuracy. *Water Resources Research*, 49, 5276-5289.
- BERRY, P. A. M., GARLICK, J. D. & SMITH, R. G. 2007. Near-global validation of the SRTM DEM using satellite radar altimetry. *Remote Sensing of Environment*, 106, 17–27.

- BEVACQUA, A., YU, D. & ZHANG, Y. 2018. Coastal vulnerability: Evolving concepts in understanding vulnerable people and places. *Environmental Science & Policy*, 82, 19-29.
- BRENNER, J., JIMENEZ, J. A. & SARDA, R. 2006. Definition of homogeneous environmental management units for the Catalan coast. *Environmental Management*, 38, 993-1005.
- BRIGHT, E. A., COLEMAN, P. R. & KING, A. L. 2007. LandScan 2006. 2006 ed. Oak Ridge, TN: Oak Ridge National Laboratory.
- BROWN, S., HANSON, S. & NICHOLLS, R. J. 2014. Implications of sea-level rise and extreme events around Europe: a review of coastal energy infrastructure. *Climatic Change*, 122, 81-95.
- BROWN, S., NICHOLLS, R. J., GOODWIN, P., HAIGH, I. D., LINCKE, D., VAFEIDIS, A. T. & HINKEL, J. 2018. Quantifying Land and People Exposed to Sea-Level Rise with No Mitigation and 1.5°C and 2.0°C Rise in Global Temperatures to Year 2300. *Earth's Future*, 6, 583-600.
- BUKVIC, A., ROHAT, G., APOTSOS, A. & DE SHERBININ, A. 2020. A Systematic Review of Coastal Vulnerability Mapping. *Sustainability*, 12.
- BURROUGH, P. A. & MCDONNELL, R. 1998. *Principles of geographical information systems*, Oxford University Press.
- CASAS-PRAT, M. & SIERRA, J. P. 2010. Trend analysis of wave storminess: wave direction and its impact on harbour agitation. *Nat. Hazards Earth Syst. Sci.*, 10, 2327-2340.
- CENTER FOR INTERNATIONAL EARTH SCIENCE INFORMATION NETWORK - CIESIN - COLUMBIA UNIVERSITY, INTERNATIONAL FOOD POLICY RESEARCH INSTITUTE - IFPRI, THE WORLD BANK & CENTRO INTERNACIONAL DE AGRICULTURA TROPICAL - CIAT 2011. Global Rural-Urban Mapping Project, Version 1 (GRUMPv1): Population Density Grid. Palisades, NY: NASA Socioeconomic Data and Applications Center (SEDAC).
- CENTER FOR INTERNATIONAL EARTH SCIENCE INFORMATION NETWORK - COLUMBIA UNIVERSITY 2016. Gridded Population of the World, Version 4 (GPWv4): Population Count Adjusted to Match 2015 Revision of UN WPP Country Totals. Palisades, NY: NASA Socioeconomic Data and Applications Center.
- CHANG, A. Y., PARRALES, M. E., JIMENEZ, J., SOBIESZCZYK, M. E., HAMMER, S. M., COPENHAVER, D. J. & KULKARNI, R. P. 2009. Combining Google Earth and GIS mapping technologies in a dengue surveillance system for developing countries. *International journal of health geographics*, 8, 49.
- CHEN, G., LI, X., LIU, X., CHEN, Y., LIANG, X., LENG, J., XU, X., LIAO, W., QIU, Y. A., WU, Q. & HUANG, K. 2020. Global projections of future urban land expansion under shared socioeconomic pathways. *Nature Communications*, 11, 537.
- CHURCH, J. A., CLARK, P. U., CAZENAVE, A., GREGORY, J. M., JEVREJEVA, S., LEVERMANN, A., MERRIFIELD, M. A., MILNE, G. A., NEREM, R. S., NUNN, P. D., PAYNE, A. J., PFEFFER, W. T., STAMMER, D. & UNNIKRIISHNAN, A. S. 2013. Sea Level Change. In: STOCKER, T. F., D. QIN, G.-K. PLATTNER, M. TIGNOR, S.K. ALLEN, J. BOSCHUNG, A. NAUELS, Y. XIA, V. BEX AND P.M. MIDGLEY (ed.) *Climate Change 2013: The Physical Science Basis. Contribution of Working Group I to the Fifth Assessment Report of the*

- Intergovernmental Panel on Climate Change*. Cambridge, United Kingdom and New York, NY, USA: Cambridge University Press,.
- COLLINS, W. J., BELLOUIN, N., DOUTRIAUX-BOUCHER, M., GEDNEY, N., HINTON, T., JONES, C. D., LIDDICOAT, S., MARTIN, G., O'CONNOR, F., RAE, J., SENIOR, C., TOTTERDELL, I., WOODWARD, S., REICHLER, T. & KIM, J. 2008. Evaluation of the HadGEM2 model.: Met Office Hadley Centre Technical Note no. HCTN 74.
- COMMUNITY, T. T. W., ARNOLD, B., BOWLER, L., GIBSON, S., HERTERICH, P., HIGMAN, R., KRYSTALLI, A., MORLEY, A., O'REILLY, M. & WHITAKER, K. 2019. The Turing Way: A Handbook for Reproducible Data Science.
- CONTE, D. & LIONELLO, P. 2013. Characteristics of large positive and negative surges in the Mediterranean Sea and their attenuation in future climate scenarios. *Global and Planetary Change*, 111, 159-173.
- CRAMER, W., GUIOT, J., FADER, M., GARRABOU, J., GATTUSO, J.-P., IGLESIAS, A., LANGE, M. A., LIONELLO, P., LLASAT, M. C., PAZ, S., PEÑUELAS, J., SNOUSSI, M., TORETI, A., TSIMPLIS, M. N. & XOPLAKI, E. 2018. Climate change and interconnected risks to sustainable development in the Mediterranean. *Nature Climate Change*, 8, 972-980.
- CRESPO CUARESMA, J. 2015. Income projections for climate change research: A framework based on human capital dynamics. *Global Environmental Change*.
- DE BRUIJN, J. A., DE MOEL, H., JONGMAN, B., DE RUITER, M. C., WAGEMAKER, J. & AERTS, J. 2019. A global database of historic and real-time flood events based on social media. *Sci Data*, 6, 311.
- DE MOEL, H., ASSELMAN, N. E. M. & AERTS, J. C. J. H. 2012. Uncertainty and sensitivity analysis of coastal flood damage estimates in the west of the Netherlands. *Nat. Hazards Earth Syst. Sci.*, 12, 1045-1058.
- DE MOEL, H., JONGMAN, B., KREIBICH, H., MERZ, B., PENNING-ROUSELL, E. & WARD, P. J. 2015. Flood risk assessments at different spatial scales. *Mitigation and Adaptation Strategies for Global Change*, 20, 865-890.
- DECONTO, R. M. & POLLARD, D. 2016. Contribution of Antarctica to past and future sea-level rise. *Nature*, 531, 591-597.
- DELLINK, R., CHATEAU, J., LANZI, E. & MAGNÉ, B. 2017. Long-term economic growth projections in the Shared Socioeconomic Pathways. *Global Environmental Change*, 42, 200-214.
- DOBSON, J. E., BRLGHT, E. A., COLEMAN, P. R., DURFEE, R. C. & WORLEY, B. A. 2000. LandScan: A Global Population Database for Estimating Populations at Risk. *Photogrammetric Engineering and Remote Sensing*, 66, 849-857.
- DOXSEY-WHITFIELD, E., MACMANUS, K., ADAMO, S. B., PISTOLESI, L., SQUIRES, J., BORKOVSKA, O. & BAPTISTA, S. R. 2015. Taking Advantage of the Improved Availability of Census Data: A First Look at the Gridded Population of the World, Version 4. *Papers in Applied Geography*, 1, 226-234.
- ERICSON, J. P., VOROSMARTY, C. J., DINGMAN, S. L., WARD, L. G. & MEYBECK, M. 2006. Effective sea-level rise and deltas: Causes of change and human dimension implications. *Global and Planetary Change*, 50, 63-82.
- ESRI 2002. Digital Chart of the World. Redlands, CA.

- EUROPEAN ENVIRONMENT AGENCY 2014. Horizon 2020 mediterranean report.
- EUROPEAN SPACE AGENCY & UNIVERSITÉ CATHOLIQUE DE LOUVAIN 2009. Global Land Cover Map for 2009. [http://due.esrin.esa.int/page\\_globcover.php](http://due.esrin.esa.int/page_globcover.php): GlobCover.
- FARR, T. G., ROSEN, P. A., CARO, E., CRIPPEN, R., DUREN, R., HENSLEY, S., KOBRICK, M., PALLER, M., RODRIGUEZ, E., ROTH, L., SEAL, D., SHAFFER, S., SHIMADA, J., UMLAND, J., WERNER, M., OSKIN, M., BURBANK, D. & ALSDORF, D. 2007. The Shuttle Radar Topography Mission. *Reviews of Geophysics*, 45.
- FEKETE, A., DAMM, M. & BIRKMANN, J. 2010. Scales as a challenge for vulnerability assessment. *Natural Hazards*, 55, 729-747.
- FENG, Y., LIU, Y., TONG, X., LIU, M. & DENG, S. 2011. Modeling dynamic urban growth using cellular automata and particle swarm optimization rules. *Landscape and Urban Planning*, 102, 188-196.
- FERRETTI, A., PRATI, C. & ROCCA, F. 2001. Permanent scatterers in SAR interferometry. *IEEE Transactions on Geoscience and Remote Sensing*, 39, 8–20.
- FETTWEIS, X., FRANCO, B., TEDESCO, M., VAN ANGELEN, J. H., LENAERTS, J. T. M., VAN DEN BROEKE, M. R. & GALLÉE, H. 2013. Estimating the Greenland ice sheet surface mass balance contribution to future sea level rise using the regional atmospheric climate model MAR. *The Cryosphere*, 7, 469–489.
- GAO, J. 2017. Downscaling Global Spatial Population Projections from 1/8-degree to 1-km Grid Cells. Climate and Global Dynamics Laboratory.
- GAO, J. & O'NEILL, B. C. 2020. Mapping global urban land for the 21st century with data-driven simulations and Shared Socioeconomic Pathways. *Nature Communications*, 11, 2302.
- GARSCHAGEN, M. & ROMERO-LANKAO, P. 2013. Exploring the relationships between urbanization trends and climate change vulnerability. *Climatic Change*, 133, 37-52.
- GESCH, D. B. 2009. Analysis of Lidar Elevation Data for Improved Identification and Delineation of Lands Vulnerable to Sea-Level Rise. *Journal of Coastal Research*, 10053, 49–58.
- GESCH, D. B. 2018. Best Practices for Elevation-Based Assessments of Sea-Level Rise and Coastal Flooding Exposure. *Frontiers in Earth Science*, 6.
- GLOBAL ADMINISTRATIVE AREAS (GADM) 2015. Global Administrative Areas. Boundaries without limits. 2.8 ed. <http://www.gadm.org/>.
- GOODWIN, P., HAIGH, I. D., ROHLING, E. J. & SLANGEN, A. 2017. A new approach to projecting 21st century sea-level changes and extremes. *Earth's Future*, 5, 240-253.
- GOROKHOVICH, Y. & VOUSTIANIOUK, A. 2006. Accuracy assessment of the processed SRTM-based elevation data by CGIAR using field data from USA and Thailand and its relation to the terrain characteristics. *Remote Sensing of Environment*, 104, 409–415.
- GRIFFIN, J., LATIEF, H., KONGKO, W., HARIG, S., HORSPOOL, N., HANUNG, R., ROJALI, A., MAHER, N., FUCHS, A., HOSSEN, J., UPI, S., EDI, D., RAKOWSKY, N. & CUMMINS, P. 2015. An evaluation of onshore digital elevation models for modelling tsunami inundation zones. *Frontiers in Earth Science*, 3.

- GÜNERALP, B. & SETO, K. C. 2013. Futures of global urban expansion: uncertainties and implications for biodiversity conservation. *Environmental Research Letters*, 8.
- HAASNOOT, M., BROWN, S., SCUSSOLINI, P., JIMENEZ, J. A., VAFEIDIS, A. T. & NICHOLLS, R. J. 2019. Generic adaptation pathways for coastal archetypes under uncertain sea-level rise. *Environmental Research Communications*, 1, 071006.
- HALLEGATTE, S., GREEN, C., NICHOLLS, R. J. & CORFEE-MORLOT, J. 2013. Future flood losses in major coastal cities. *Nature Clim. Change*, 3, 802-806.
- HAMLINGTON, B. D., GARDNER, A. S., IVINS, E., LENAERTS, J. T. M., REAGER, J. T., TROSSMAN, D. S., ZARON, E. D., ADHIKARI, S., ARENDT, A., ASCHWANDEN, A., BECKLEY, B. D., BEKAERT, D. P. S., BLEWITT, G., CARON, L., CHAMBERS, D. P., CHANDANPURKAR, H. A., CHRISTIANSON, K., CSATHO, B., CULLATHER, R. I., DECONTO, R. M., FASULLO, J. T., FREDERIKSE, T., FREYMUELLER, J. T., GILFORD, D. M., GIROTTO, M., HAMMOND, W. C., HOCK, R., HOLSCHUH, N., KOPP, R. E., LANDERER, F., LAROUB, E., MENEMENLIS, D., MERRIFIELD, M., MITROVICA, J. X., NEREM, R. S., NIAS, I. J., NIEVES, V., NOWICKI, S., PANGALURU, K., PIECUCH, C. G., RAY, R. D., ROUNCE, D. R., SCHLEGEL, N. J., SEROUSSI, H., SHIRZAEI, M., SWEET, W. V., VELICOGNA, I., VINOGRADOVA, N., WAHL, T., WIESE, D. N. & WILLIS, M. J. 2020. Understanding of Contemporary Regional Sea-Level Change and the Implications for the Future. *Rev Geophys*, 58, e2019RG000672.
- HASSELMANN, S., HASSELMANN, K., BAUER, E., JANSSEN, P., KOMEN, G., BERTOTTI, L., LIONELLO, P., GUILLAUME, A., CARDONE, V. & GREENWOOD, J. 1988. WAMDI group. *The WAM model—a third generation ocean wave prediction model*, *J. Phys. Oceanogr*, 18, 1775-1810.
- HASTINGS, D. A. & DUNBAR, P. K. 1999. Global Land One-kilometer Base Elevation (GLOBE) Digital Elevation Model, Documentation, Volume 1.0. *Key to Geophysical Records Documentation (KGRD) 34*. 325 Broadway, Boulder, Colorado 80303, U.S.A.: National Oceanic and Atmospheric Administration, National Geophysical Data Center.
- HAUER, M. E. 2019. Population projections for U.S. counties by age, sex, and race controlled to shared socioeconomic pathway. *Scientific Data*, 6, 190005.
- HAWKER, L., BATES, P., NEAL, J. & ROUGIER, J. 2018. Perspectives on Digital Elevation Model (DEM) Simulation for Flood Modeling in the Absence of a High-Accuracy Open Access Global DEM. *Frontiers in Earth Science*, 6.
- HAWKER, L., NEAL, J. & BATES, P. 2019. Accuracy assessment of the TanDEM-X 90 Digital Elevation Model for selected floodplain sites. *Remote Sensing of Environment*, 232.
- HINKEL, J., CHURCH, J. A., GREGORY, J. M., LAMBERT, E., LE COZANNET, G., LOWE, J., MCINNES, K. L., NICHOLLS, R. J., POL, T. D. & WAL, R. 2019. Meeting User Needs for Sea Level Rise Information: A Decision Analysis Perspective. *Earth's Future*, 7, 320-337.
- HINKEL, J., JAEGER, C., NICHOLLS, R. J., LOWE, J., RENN, O. & PEIJUN, S. 2015. Sea-level rise scenarios and coastal risk management. *Nature Climate Change*, 5, 188–190.
- HINKEL, J., LINCKE, D., VAFEIDIS, A. T., PERRETTE, M., NICHOLLS, R. J., TOL, R. S. J., MARZEION, B., FETTWEIS, X., IONESCU, C. & LEVERMANN, A. 2014. Coastal flood damage and adaptation costs under 21st century sea-level rise. *Proceedings of the National Academy of Sciences of the United States of America*, 111, 3292–3297.

- HINKEL, J., NICHOLLS, R. J., TOL, R. S. J., WANG, Z. B., HAMILTON, J. M., BOOT, G., VAFEIDIS, A. T., MCFADDEN, L., GANOPOLSKI, A. & KLEIN, R. J. T. 2013. A global analysis of erosion of sandy beaches and sea-level rise: An application of DIVA. *Global and Planetary Change*, 111, 150-158.
- HOFTON, M., DUBAYAH, R., BLAIR, B. & RABINE, D. 2006. Validation of SRTM Elevations Over Vegetated and Non-vegetated Terrain Using Medium Footprint Lidar. *Photogrammetric Engineering & Remote Sensing*, 279-285.
- HOOZEMANS, F., MARCHAND, M. & PENNEKAMP, H. 1993. Sea level rise: a global vulnerability assessment vulnerability assessments for population, coastal wetlands and rice production on a global scale. *Deltares (WL)*.
- HORTON, B. P., KOPP, R. E., GARNER, A. J., HAY, C. C., KHAN, N. S., ROY, K. & SHAW, T. A. 2018. Mapping Sea-Level Change in Time, Space, and Probability. *Annual Review of Environment and Resources*, 43, 481-521.
- HOUTENBOS, A. P. E. M., HOUNJET, M. W. A. & BARENDIS, B. J. Subsidence from geodetic measurements in the Ravenna area. . Proceedings of the 7th International Symposium on Land Subsidence, 2005 Shanghai, China 79-99.
- HUIZINGA, J., DE MOEL, H. & SZEWCZYK, W. 2017. Global flood depth-damage functions. Methodology and the database with guidelines. *JRC Technical Reports. EUR 28552 EN*.
- HUNTER, J. R., WOODWORTH, P. L., WAHL, T. & NICHOLLS, R. J. 2017. Using global tide gauge data to validate and improve the representation of extreme sea levels in flood impact studies. *Global and Planetary Change*, 156, 34-45.
- IIZUKA, K., JOHNSON, B. A., ONISHI, A., MAGCALE-MACANDOG, D. B., ENDO, I. & BRAGAIS, M. 2017. Modeling Future Urban Sprawl and Landscape Change in the Laguna de Bay Area, Philippines. *Land*, 6.
- INTERNATIONAL INSTITUTE FOR APPLIED SYSTEMS ANALYSIS. 2015. *SSP Database* [Online]. Available: <https://tntcat.iiasa.ac.at/SspDb> [Accessed 2016-04-26].
- INTERNATIONAL STANDARD ISO 3166-1. 2006. *Codes for the representation of names of countries and their subdivisions--Part 1: Country codes, ISO 3166-1: 2006 (E/F)* [Online]. Geneva: International Organization on Standardization. [Accessed 2016].
- IPCC 2019. IPCC Special Report on the Ocean and Cryosphere in a Changing Climate. In: PÖRTNER, H.-O., ROBERTS, D. C., MASSON-DELMOTTE, V., ZHAI, P., TIGNOR, M., POLOCZANSKA, E., MINTENBECK, K., ALEGRÍA, A., NICOLAI, M., OKEM, A., PETZOLD, J., RAMA, B. & WEYER, N. M. (eds.).
- ISTAT 2009. Pil pro capite per regione.
- JARVIS, A., REUTER, H. I., NELSON, A. & GUEVARA, E. 2008. *Hole-filled SRTM for the globe Version 4: Available from the CGIAR-CSI SRTM 90m Database*. Available: <http://srtm.csi.cgiar.org>.
- JENI, L. A., COHN, J. F. & DE LA TORRE, F. 2013. Facing Imbalanced Data Recommendations for the Use of Performance Metrics. *International Conference on Affective Computing and Intelligent Interaction and workshops : [proceedings]. ACII (Conference)*, 2013, 245-251.

- JEVREJEVA, S., FREDERIKSE, T., KOPP, R. E., LE COZANNET, G., JACKSON, L. P. & VAN DE WAL, R. S. W. 2019. Probabilistic Sea Level Projections at the Coast by 2100. *Surveys in Geophysics*, 40, 1673-1696.
- JEVREJEVA, S., GRINSTED, A. & MOORE, J. C. 2014. Upper limit for sea level projections by 2100. *Environmental Research Letters*, 9, 104008.
- JIANG, L. & O'NEILL, B. C. 2017. Global urbanization projections for the Shared Socioeconomic Pathways. *Global Environmental Change*, 42, 193-199.
- JIMENEZ, J. A., VALDEMORO, H. I., BOSOM, E., SANCHEZ-ARCILLA, A. & NICHOLLS, R. J. 2017. Impacts of sea-level rise-induced erosion on the Catalan coast. *Regional Environmental Change*, 17, 593-603.
- JONES, B. & O'NEILL, B. C. 2016. Spatially explicit global population scenarios consistent with the Shared Socioeconomic Pathways. *Environmental Research Letters*, 11.
- JONES, N., KOUKOULAS, S., CLARK, J. R. A., EVANGELINOS, K. I., DIMITRAKOPOULOS, P. G., EFTIHIDOU, M. O., KOLIOU, A., MPALASKA, M., PAPANIKOLAOU, S., STATHI, G. & TSALIKI, P. 2014. Social capital and citizen perceptions of coastal management for tackling climate change impacts in Greece. *Regional Environmental Change*, 14, 1083-1093.
- JONGMAN, B., KREIBICH, H., APEL, H., BARREDO, J. I., BATES, P. D., FEYEN, L., GERICKE, A., NEAL, J., AERTS, J. C. J. H. & WARD, P. J. 2012. Comparative flood damage model assessment: towards a European approach. *Nat. Hazards Earth Syst. Sci.*, 12, 3733-3752.
- KAISER, G., SCHEELE, L., KORTENHAUS, A., LØVHOLT, F., RÖMER, H. & LESCHKA, S. 2011. The influence of land cover roughness on the results of high resolution tsunami inundation modeling. *Nat. Hazards Earth Syst. Sci.*, 11, 2521-2540.
- KASANKO, M., BARREDO, J. I., LAVALLE, C., MCCORMICK, N., DEMICHELI, L., SAGRIS, V. & BREZGER, A. 2006. Are European cities becoming dispersed? *Landscape and Urban Planning*, 77, 111-130.
- KC, S. & LUTZ, W. 2017. The human core of the shared socioeconomic pathways: Population scenarios by age, sex and level of education for all countries to 2100. *Global Environmental Change*.
- KELLNDORFER, J., WALKER, W., PIERCE, L., DOBSON, C., FITES, J. A., HUNSAKER, C., VONA, J. & CLUTTER, M. 2004. Vegetation height estimation from Shuttle Radar Topography Mission and National Elevation Datasets. *Remote Sensing of Environment*, 93, 339-358.
- KOPP, R. E., DECONTO, R. M., BADER, D. A., HAY, C. C., HORTON, R. M., KULP, S., OPPENHEIMER, M., POLLARD, D. & STRAUSS, B. H. 2017. Evolving Understanding of Antarctic Ice-Sheet Physics and Ambiguity in Probabilistic Sea-Level Projections. *Earth's Future*, 5, 1217-1233.
- KOPP, R. E., HORTON, R. M., LITTLE, C. M., MITROVICA, J. X., OPPENHEIMER, M., RASMUSSEN, D. J., STRAUSS, B. H. & TEBALDI, C. 2014. Probabilistic 21st and 22nd century sea-level projections at a global network of tide-gauge sites. *Earths Future*, 2, 383-406.

- KULP, S. A. & STRAUSS, B. H. 2018. CoastalDEM: A global coastal digital elevation model improved from SRTM using a neural network. *Remote Sensing of Environment*, 206, 231-239.
- KULP, S. A. & STRAUSS, B. H. 2019. New elevation data triple estimates of global vulnerability to sea-level rise and coastal flooding. *Nature Communications*, 10, 4844.
- KUMMU, M., DE MOEL, H., SALVUCCI, G., VIVIROLI, D., WARD, P. J. & VARIS, O. 2016. Over the hills and further away from coast: global geospatial patterns of human and environment over the 20th–21st centuries. *Environmental Research Letters*, 11.
- LE COZANNET, G., ROHMER, J., CAZENAVE, A., IDIER, D., VAN DE WAL, R., DE WINTER, R., PEDREROS, R., BALOUIN, Y., VINCHON, C. & OLIVEROS, C. 2015. Evaluating uncertainties of future marine flooding occurrence as sea-level rises. *Environmental Modelling & Software*, 73, 44-56.
- LEVERMANN, A., ALBRECHT, T., WINKELMANN, R., MARTIN, M. A., HASELOFF, M. & JOUGHIN, I. 2012. Kinematic first-order calving law implies potential for abrupt ice-shelf retreat. *The Cryosphere*, 6, 273–286.
- LEWIS, M., BATES, P., HORSBURGH, K., NEAL, J. & SCHUMANN, G. 2013. A storm surge inundation model of the northern Bay of Bengal using publicly available data. *Quarterly Journal of the Royal Meteorological Society*, 139, 358-369.
- LEYK, S., GAUGHAN, A. E., ADAMO, S. B., DE SHERBININ, A., BALK, D., FREIRE, S., ROSE, A., STEVENS, F. R., BLANKESPOOR, B., FRYE, C., COMENETZ, J., SORICHTTA, A., MACMANUS, K., PISTOLESI, L., LEVY, M., TATEM, A. J. & PESARESI, M. 2019. The spatial allocation of population: a review of large-scale gridded population data products and their fitness for use. *Earth System Science Data*, 11, 1385-1409.
- LEYK, S., UHL, J. H., CONNOR, D. S., BRASWELL, A. E., MIETKIEWICZ, N., BALCH, J. K. & GUTMANN, M. 2020. Two centuries of settlement and urban development in the United States. *Science Advances*, 6, eaba2937.
- LI, X., ZHOU, Y., EOM, J., YU, S. & ASRAR, G. R. 2019. Projecting Global Urban Area Growth Through 2100 Based on Historical Time Series Data and Future Shared Socioeconomic Pathways. *Earth's Future*, 7, 351-362.
- LICHTER, M., VAFEIDIS, A. T., NICHOLLS, R. J. & KAISER, G. 2011. Exploring Data-Related Uncertainties in Analyses of Land Area and Population in the "Low-Elevation Coastal Zone" (LECZ). *Journal of Coastal Research*, 274, 757–768.
- LINCKE, D. & HINKEL, J. 2018. Economically robust protection against 21st century sea-level rise. *Global Environmental Change*, 51, 67-73.
- LINCKE, D., WOLFF, C., HINKEL, J., VAFEIDIS, A., BLICKENS DÖRFER, L. & POVH SKUGOR, D. 2020. The effectiveness of setback zones for adapting to sea-level rise in Croatia. *Regional Environmental Change*, 20, 46.
- LIONELLO, P., COGO, S., GALATI, M. B. & SANNA, A. 2008. The Mediterranean surface wave climate inferred from future scenario simulations. *Global and Planetary Change*, 63, 152-162.
- LIONELLO, P. & SANNA, A. 2005. Mediterranean wave climate variability and its links with NAO and Indian Monsoon. *Climate Dynamics*, 25, 611-623.



- LUPINO, P., BELLACICCO, S., DI COSIMO, M., SCALONI, P., PEDETTA PECCIA, S., MONTANARI, R., BONAZZI, A. & MARASMI, C. 2014. Practical Guide to COASTGAP MED Capitalisation Initiative Lazio Region/Emilia-Romagna Region.
- MALVAREZ, G. C., PINTADO, E. G., NAVAS, F. & GIORDANO, A. 2015. Spatial data and its importance for the implementation of UNEP MAP ICZM Protocol for the Mediterranean. *Journal of Coastal Conservation*, 19, 633-641.
- MARZEION, B., JAROSCH, A. H. & HOFER, M. 2012. Past and future sea-level change from the surface mass balance of glaciers. *The Cryosphere*, 6, 1295–1322.
- MAS, J. F. & FLORES, J. J. 2008. The application of artificial neural networks to the analysis of remotely sensed data. *International Journal of Remote Sensing*, 29, 617-663.
- MCFADDEN, L., NICHOLLS, R. J., VAFEIDIS, A. & TOL, R. S. J. 2007. A Methodology for Modeling Coastal Space for Global Assessment. *Journal of Coastal Research*, 234, 911–920.
- MCGILL, J. T. 1958. MAP OF COASTAL LANDFORMS OF THE WORLD. *Geographical Review*, 48, 402-405.
- MCGRANAHAN, G., BALK, D. & ANDERSON, B. 2007. The rising tide: assessing the risks of climate change and human settlements in low elevation coastal zones. *Environment and Urbanization*, 19, 17–37.
- MCLEOD, E., POULTER, B., HINKEL, J., REYES, E. & SALM, R. 2010. Sea-level rise impact models and environmental conservation: A review of models and their applications. *Ocean & Coastal Management*, 53, 507-517.
- MCOWEN, C., WEATHERDON, L., BOCHOVE, J.-W., SULLIVAN, E., BLYTH, S., ZOCKLER, C., STANWELL-SMITH, D., KINGSTON, N., MARTIN, C., SPALDING, M. & FLETCHER, S. 2017. A global map of saltmarshes. *Biodiversity Data Journal*, 5, e11764.
- MELCHIORRI, M., PESARESI, M., FLORCZYK, A., CORBANE, C. & KEMPER, T. 2019. Principles and Applications of the Global Human Settlement Layer as Baseline for the Land Use Efficiency Indicator—SDG 11.3.1. *ISPRS International Journal of Geo-Information*, 8.
- MELET, A., MEYSSIGNAC, B., ALMAR, R. & LE COZANNET, G. 2018. Under-estimated wave contribution to coastal sea-level rise. *Nature Climate Change*, 8, 234-239.
- MERKENS, J.-L., LINCKE, D., HINKEL, J., BROWN, S. & VAFEIDIS, A. T. 2018. Regionalisation of population growth projections in coastal exposure analysis. *Climatic Change*, 151, 413-426.
- MERKENS, J.-L., REIMANN, L., HINKEL, J. & VAFEIDIS, A. T. 2016. Gridded population projections for the coastal zone under the Shared Socioeconomic Pathways. *Global and Planetary Change*, 145, 57–66.
- MONDAL, P. & TATEM, A. J. 2012. Uncertainties in measuring populations potentially impacted by sea level rise and coastal flooding. *PLoS One*, 7, e48191.
- MONTANARI, R. & MARASMI, C. 2014. Il sistema gestionale delle celle litoranee SICELL *aggiornamento 2006-2012*. Regione Emilia-Romagna. Servizio Difesa del Suolo, della Costa e Bonifica.

- MUIS, S., GUNERALP, B., JONGMAN, B., AERTS, J. C. & WARD, P. J. 2015. Flood risk and adaptation strategies under climate change and urban expansion: A probabilistic analysis using global data. *Sci Total Environ*, 538, 445-57.
- MUIS, S., VERLAAN, M., NICHOLLS, R. J., BROWN, S., HINKEL, J., LINCKE, D., VAFEIDIS, A. T., SCUSSOLINI, P., WINSEMIUS, H. C. & WARD, P. J. 2017. A comparison of two global datasets of extreme sea levels and resulting flood exposure. *Earths Future*, 5, 379-392.
- MUIS, S., VERLAAN, M., WINSEMIUS, H. C., AERTS, J. C. J. H. & WARD, P. J. 2016. A global reanalysis of storm surges and extreme sea levels. *Nature Communications*, 7.
- MULLER, C. L., CHAPMAN, L., JOHNSTON, S., KIDD, C., ILLINGWORTH, S., FOODY, G., OVEREEM, A. & LEIGH, R. R. 2015. Crowdsourcing for climate and atmospheric sciences: current status and future potential. *International Journal of Climatology*, 35, 3185-3203.
- NEUMANN, B., VAFEIDIS, A. T., ZIMMERMANN, J. & NICHOLLS, R. J. 2015. Future coastal population growth and exposure to sea-level rise and coastal flooding--a global assessment. *PLoS One*, 10.
- NICHOLLS, R. J. 1995. Coastal megacities and climate change. *GeoJournal*, 37, 369-379.
- NICHOLLS, R. J., BROWN, S., GOODWIN, P., WAHL, T., LOWE, J., SOLAN, M., GODBOLD, J. A., HAIGH, I. D., LINCKE, D., HINKEL, J., WOLFF, C. & MERKENS, J. L. 2018. Stabilization of global temperature at 1.5 degrees C and 2.0 degrees C: implications for coastal areas. *Philosophical Transactions of the Royal Society a-Mathematical Physical and Engineering Sciences*, 376, 20.
- NICHOLLS, R. J., HANSON, S. E., LOWE, J. A., WARRICK, R. A., LU, X. & LONG, A. J. 2014. Sea-level scenarios for evaluating coastal impacts. *Wiley Interdisciplinary Reviews: Climate Change*, 5, 129-150.
- NORDSTROM, K. F., ARMAROLI, C., JACKSON, N. L. & CIAVOLA, P. 2015. Opportunities and constraints for managed retreat on exposed sandy shores: Examples from Emilia-Romagna, Italy. *Ocean & Coastal Management*, 104, 11-21.
- O'LOUGHLIN, F. E., PAIVA, R. C. D., DURAND, M., ALSDORF, D. E. & BATES, P. D. 2016. A multi-sensor approach towards a global vegetation corrected SRTM DEM product. *Remote Sensing of Environment*, 182, 49-59.
- O'NEILL, B., KRIEGLER, E., RIAHI, K., EBI, K., HALLEGATTE, S., CARTER, T., MATHUR, R. & VAN VUUREN, D. 2014. A new scenario framework for climate change research: the concept of shared socioeconomic pathways. *Climatic Change*, 122, 387-400.
- O'NEILL, B. C., KRIEGLER, E., EBI, K. L., KEMP-BENEDICT, E., RIAHI, K., ROTHMAN, D. S., VAN RUIJVEN, B. J., VAN VUUREN, D. P., BIRKMANN, J., KOK, K., LEVY, M. & SOLECKI, W. 2017. The roads ahead: Narratives for shared socioeconomic pathways describing world futures in the 21st century. *Global Environmental Change*, 42, 169-180.
- OPPENHEIMER, M., CAMPOS, M., WARREN, R., BIRKMANN, J., LUBER, G., O'NEILL, B. & TAKAHASHI, K. 2014. Emergent risks and key vulnerabilities. In: FIELD, C. B., BARROS, V. R., DOKKEN, D. J., MACH, K. J., MASTRANDREA, M. D., BILIR, T. E., CHATTERJEE, M., EBI, K. L., ESTRADA, Y. O., GENOVA, R. C., GIRMA, B., KISSEL, E. S., LEVY, A. N., MACCRACKEN, S., MASTRANDREA, P. R. & WHITE, L. L. (eds.)

*Climate Change 2014: Impacts, Adaptation, and Vulnerability. Part A: Global and Sectoral Aspects. Contribution of Working Group II to the Fifth Assessment Report of the Intergovernmental Panel of Climate Change.* Cambridge, United Kingdom and New York, NY, USA: Cambridge University Press.

- OPPENHEIMER, M., GLAVOVIC, B. C., HINKEL, J., VAN DE WAL, R., MAGNAN, A. K., ABD-ELGAWAD, A., CAI, R., CIFUENTESJARA, M., DECONTO, R. M., GHOSH, T., HAY, J., ISLA, F., MARZEION, B., MEYSSIGNAC, B. & SEBESVARI, Z. 2019. Sea Level Rise and Implications for Low-Lying Islands, Coasts and Communities. In: IPCC Special Report on the Ocean and Cryosphere in a Changing Climate. In: PÖRTNER, H.-O., ROBERTS, D. C., MASSON-DELMOTTE, V., ZHAI, P., TIGNOR, M., POLOCZANSKA, E., MINTENBECK, K., ALEGRÍA, A., NICOLAI, M., OKEM, A., PETZOLD, J., RAMA, B. & WEYER, N. M. (eds.).
- PAPROTNY, D., MORALES-NÁPOLES, O. & JONKMAN, S. N. 2018. HANZE: a pan-European database of exposure to natural hazards and damaging historical floods since 1870. *Earth System Science Data*, 10, 565-581.
- PAPROTNY, D., MORALES-NÁPOLES, O., VOUSDOUKAS, M. I., JONKMAN, S. N. & NIKULIN, G. 2019. Accuracy of pan-European coastal flood mapping. *Journal of Flood Risk Management*, 12.
- PELTIER, W. 2000. ICE4g (VM2) Glacial isostatic adjustment correction on Sea Level rise, History and Consequences. *Academic Press, San Diego, International Geophysics Series*, 75.
- PELTIER, W. R. 2004. Global glacial isostasy and the surface of the ice-age earth: The ice-5G (VM2) model and grace. *Annual Review of Earth and Planetary Sciences*, 32, 111-149.
- PELTIER, W. R., ARGUS, D. F. & DRUMMOND, R. 2015. Space geodesy constrains ice age terminal deglaciation: The global ICE-6G\_C (VM5a) model. *Journal of Geophysical Research-Solid Earth*, 120, 450-487.
- PICKERING, M. D. 2014. *The impact of future sea-level rise on the tides*. Phd, University of Southampton.
- PICKERING, M. D., HORSBURGH, K. J., BLUNDELL, J. R., HIRSCHI, J. J. M., NICHOLLS, R. J., VERLAAN, M. & WELLS, N. C. 2017. The impact of future sea-level rise on the global tides. *Continental Shelf Research*, 142, 50-68.
- PIJANOWSKI, B. C., BROWN, D. G., SHELLITO, B. A. & MANIK, G. A. 2002a. Using neural networks and GIS to forecast land use changes: a Land Transformation Model. *Computers, Environment and Urban Systems*, 26, 553-575.
- PIJANOWSKI, B. C., SHELLITO, B., PITHADIA, S. & ALEXANDRIDIS, K. 2002b. Forecasting and assessing the impact of urban sprawl in coastal watersheds along eastern Lake Michigan. *Lakes and Reservoirs: Research and Management*, 7, 271-285.
- PIJANOWSKI, B. C., TAYYEBI, A., DELAVAR, M. R. & YAZDANPANA, M. J. 2009. Urban Expansion Simulation Using Geospatial Information System and Artificial Neural Networks. *International Journal of Environmental Research*, 3, 493-502.
- PIJANOWSKI, B. C., TAYYEBI, A., DOUCETTE, J., PEKIN, B. K., BRAUN, D. & PLOURDE, J. 2014. A big data urban growth simulation at a national scale: Configuring the GIS

- and neural network based Land Transformation Model to run in a High Performance Computing (HPC) environment. *Environmental Modelling & Software*, 51, 250-268.
- PONTIUS, G. R. & MALANSON, J. 2005. Comparison of the structure and accuracy of two land change models. *International Journal of Geographical Information Science*, 19, 243-265.
- POULTER, B. & HALPIN, P. N. 2008. Raster modelling of coastal flooding from sea-level rise. *International Journal of Geographical Information Science*, 22, 167–182.
- PRETI, M., DE NIGRIS, N., MORELLI, M., MONTI, M., BONSIGNORE, F. & AGUZZI, M. 2009. Stato del litorale emiliano-romagnolo all'anno 2007 e piano decennale di gestione. *Quaderni ARPA-Regione Emilia Romagna*.
- QUINN, N., LEWIS, M., WADEY, M. P. & HAIGH, I. D. 2014. Assessing the temporal variability in extreme storm-tide time series for coastal flood risk assessment. *Journal of Geophysical Research-Oceans*, 119, 4983-4998.
- RAHMSTORF, S. 2017. Rising hazard of storm-surge flooding. *Proceedings of the National Academy of Sciences*.
- RAMIREZ, J. A., LICHTER, M., COULTHARD, T. J. & SKINNER, C. 2016. Hyper-resolution mapping of regional storm surge and tide flooding: comparison of static and dynamic models. *Natural Hazards*, 82, 571-590.
- REIMANN, L., MERKENS, J.-L. & VAFEIDIS, A. T. 2017. Regionalized Shared Socioeconomic Pathways: narratives and spatial population projections for the Mediterranean coastal zone. *Regional Environmental Change*.
- REIMANN, L., VAFEIDIS, A. T., BROWN, S., HINKEL, J. & TOL, R. S. J. 2018. Mediterranean UNESCO World Heritage at risk from coastal flooding and erosion due to sea-level rise. *Nature Communications*, 9, 4161.
- RIO, M. H., MULET, S. & PICOT, N. 2014. Beyond GOCE for the ocean circulation estimate: Synergetic use of altimetry, gravimetry, and in situ data provides new insight into geostrophic and Ekman currents. *Geophysical Research Letters*, 41, 8918-8925.
- ROCHETTE, J., DU PUY-MONTBRUN, G., WEMAËRE, M. & BILLÉ, R. 2010. Coastal setback zones in the Mediterranean: A study on Article 8-2 of the Mediterranean ICZM Protocol. IDDRI.
- RODRIGUEZ, E., MORRIS, C. S. & BELZ, J. E. 2006. A global assessment of the SRTM performance. *Photogrammetric Engineering and Remote Sensing*, 72, 249-260.
- ROY, D. C. & BLASCHKE, T. 2015. Spatial vulnerability assessment of floods in the coastal regions of Bangladesh. *Geomatics, Natural Hazards and Risk*, 6, 21-44.
- SALTELLI, A. & ANNONI, P. 2010. How to avoid a perfunctory sensitivity analysis. *Environmental Modelling & Software*, 25, 1508-1517.
- SALTELLI, A., TARANTOLA, S. & CAMPOLONGO, F. 2000. Sensitivity analysis as an ingredient of modeling. *Statistical Science*, 15, 377-395.
- SÁNCHEZ-ARCILLA, A., MÖSSO, C., SIERRA, J. P., MESTRES, M., HARZALLAH, A., SENOUCI, M. & EL RAEY, M. 2010. Climatic drivers of potential hazards in Mediterranean coasts. *Regional Environmental Change*, 11, 617-636.

- SANTINI, M., TARAMELLI, A. & SORICHETTA, A. 2010. ASPHAA: A GIS-Based Algorithm to Calculate Cell Area on a Latitude-Longitude (Geographic) Regular Grid. *Transactions in GIS*, 14, 351-377.
- SANTORO, F., LESCRAUWAET, A. K., TAYLOR, J. & BRETON, F. 2014. Integrated Regional Assessments in support of ICZM in the Mediterranean and Black Sea Basins. Paris: Intergovernmental Oceanographic Commission of UNESCO.
- SCHAEFFER, P., FAUGÉRE, Y., LEGEAIS, J. F., OLLIVIER, A., GUINLE, T. & PICOT, N. 2012. The CNES\_CLS11 Global Mean Sea Surface Computed from 16 Years of Satellite Altimeter Data. *Marine Geodesy*, 35, 3-19.
- SCHEFFERS, A. M., SCHEFFERS, S. R. & KELLETAT, D. H. 2012. *The Coastlines of the World with Google Earth*, Dordrecht, Springer Netherlands.
- SCHNEIDER, A., FRIEDL, M. A. & POTERE, D. 2009. A new map of global urban extent from MODIS satellite data. *Environmental Research Letters*, 4.
- SCHNEIDER, A., MERTES, C. M., TATEM, A. J., TAN, B., SULLA-MENASHE, D., GRAVES, S. J., PATEL, N. N., HORTON, J. A., GAUGHAN, A. E., ROLLO, J. T., SCHELLY, I. H., STEVENS, F. R. & DASTUR, A. 2015. A new urban landscape in East–Southeast Asia, 2000–2010. *Environmental Research Letters*, 10.
- SERAFIN, K. A., RUGGIERO, P. & STOCKDON, H. F. 2017. The relative contribution of waves, tides, and non-tidal residuals to extreme total water levels on US West Coast sandy beaches. *Geophysical Research Letters*.
- SETO, K. C., FRAGKIAS, M., GUNERALP, B. & REILLY, M. K. 2011. A meta-analysis of global urban land expansion. *PLoS One*, 6, e23777.
- SETO, K. C., GUNERALP, B. & HUTYRA, L. R. 2012. Global forecasts of urban expansion to 2030 and direct impacts on biodiversity and carbon pools. *Proc Natl Acad Sci U S A*, 109, 16083-8.
- SMALL, C. & NICHOLLS, R. J. 2003. A global analysis of human settlement in coastal zones. *Journal of Coastal Research*.
- SONG, J., FU, X., WANG, R., PENG, Z.-R. & GU, Z. 2017. Does planned retreat matter? Investigating land use change under the impacts of flooding induced by sea level rise. *Mitigation and Adaptation Strategies for Global Change*, 23, 703-733.
- SPENCER, T., SCHUERCH, M., NICHOLLS, R. J., HINKEL, J., LINCKE, D., VAFEIDIS, A. T., REEF, R., MCFADDEN, L. & BROWN, S. 2016. Global coastal wetland change under sea-level rise and related stresses: The DIVA Wetland Change Model. *Global and Planetary Change*, 139, 15-30.
- STERR, H. 2008. Assessment of Vulnerability and Adaptation to Sea-Level Rise for the Coastal Zone of Germany. *Journal of Coastal Research*, 242, 380–393.
- SYVITSKI, J. P. M., KETTNER, A. J., OVEREEM, I., HUTTON, E. W. H., HANNON, M. T., BRAKENRIDGE, G. R., DAY, J., VÖRÖSMARTY, C., SAITO, Y., GIOSAN, L. & NICHOLLS, R. J. 2009. Sinking deltas due to human activities. *Nature Geoscience*, 2, 681–686.
- TAHERKHANI, M., VITOUSEK, S., BARNARD, P. L., FRAZER, N., ANDERSON, T. R. & FLETCHER, C. H. 2020. Sea-level rise exponentially increases coastal flood frequency. *Scientific Reports*, 10, 6466.

- TARAMELLI, A., DI MATTEO, L., CIAVOLA, P., GUADAGNANO, F. & TOLOMEI, C. 2014. Temporal evolution of patterns and processes related to subsidence of the coastal area surrounding the Bevano River mouth (Northern Adriatic) – Italy. *Ocean & Coastal Management*.
- TAYYEBI, A., PIJANOWSKI, B. C. & TAYYEBI, A. H. 2011. An urban growth boundary model using neural networks, GIS and radial parameterization: An application to Tehran, Iran. *Landscape and Urban Planning*, 100, 35-44.
- THEODORIDIS, S. 2015. *Machine Learning: A Bayesian and Optimization Perspective*, Academic Press, Inc.
- TIGGELOVEN, T., DE MOEL, H., WINSEMIUS, H. C., EILANDER, D., ERKENS, G., GEBREMEDHIN, E., DIAZ LOAIZA, A., KUZMA, S., LUO, T., ICELAND, C., BOUWMAN, A., VAN HUIJSTEE, J., LIGTVOET, W. & WARD, P. J. 2020. Global-scale benefit–cost analysis of coastal flood adaptation to different flood risk drivers using structural measures. *Natural Hazards and Earth System Sciences*, 20, 1025-1044.
- TOIMIL, A., LOSADA, I. J., NICHOLLS, R. J., DALRYMPLE, R. A. & STIVE, M. J. F. 2020. Addressing the challenges of climate change risks and adaptation in coastal areas: A review. *Coastal Engineering*, 156, 103611.
- UNEP/MAP 2016. Mediterranean Strategy for Sustainable Development 2016-2025. Valbonne: Plan Bleu, Regional Activity Centre.
- UNEP/MAP/PAP 2008. Protocol on Integrated Coastal Zone Management in The Mediterranean. Split: Priority Actions Programme Regional Activity Centre.
- UNITED NATIONS ENVIRONMENT PROGRAMME/MEDITERRANEAN ACTION PLAN (UNEP/MAP)-PLAN BLEU 2009. State of the environment and development in the Mediterranean Athens: UNEP/MAP-Plan Bleu.
- VAFEIDIS, A. T., NICHOLLS, R. J., MCFADDEN, L., TOL, R. S. J., HINKEL, J., SPENCER, T., GRASHOFF, P. S., BOOT, G. & KLEIN, R. J. T. 2008. A New Global Coastal Database for Impact and Vulnerability Analysis to Sea-Level Rise. *J COASTAL RES*, 244, 917–924.
- VAFEIDIS, A. T., SCHUERCH, M., WOLFF, C., SPENCER, T., MERKENS, J. L., HINKEL, J., LINCKE, D., BROWN, S. & NICHOLLS, R. J. 2019. Water-level attenuation in global-scale assessments of exposure to coastal flooding: a sensitivity analysis. *Natural Hazards and Earth System Sciences*, 19, 973-984.
- VAN DE SANDE, B., LANSEN, J. & HOYNG, C. 2012. Sensitivity of Coastal Flood Risk Assessments to Digital Elevation Models. *Water*, 4, 568-579.
- VAN DE WAL, R. S. W., ZHANG, X., MINOBE, S., JEVREJEVA, S., RIVA, R. E. M., LITTLE, C., RICHTER, K. & PALMER, M. D. 2019. Uncertainties in Long-Term Twenty-First Century Process-Based Coastal Sea-Level Projections. *Surveys in Geophysics*, 40, 1655-1671.
- VERBURG, P. H. & OVERMARS, K. P. 2007. Dynamic Simulation of Land-Use Change Trajectories with the Clue-S Model. In: KOOMEN, E., STILLWELL, J., BAKEMA, A. & SCHOLTEN, H. J. (eds.) *Modelling Land-Use Change: Progress and Applications*. Dordrecht: Springer Netherlands.
- VOUSDOKAS, M., MENTASCHI, L., CISCAR, J. C., HINKEL, J., WARD, P. J. & FEYEN, L. 2020a. Economic incentives for raising coastal flood defenses in Europe. *EarthArXiv*.

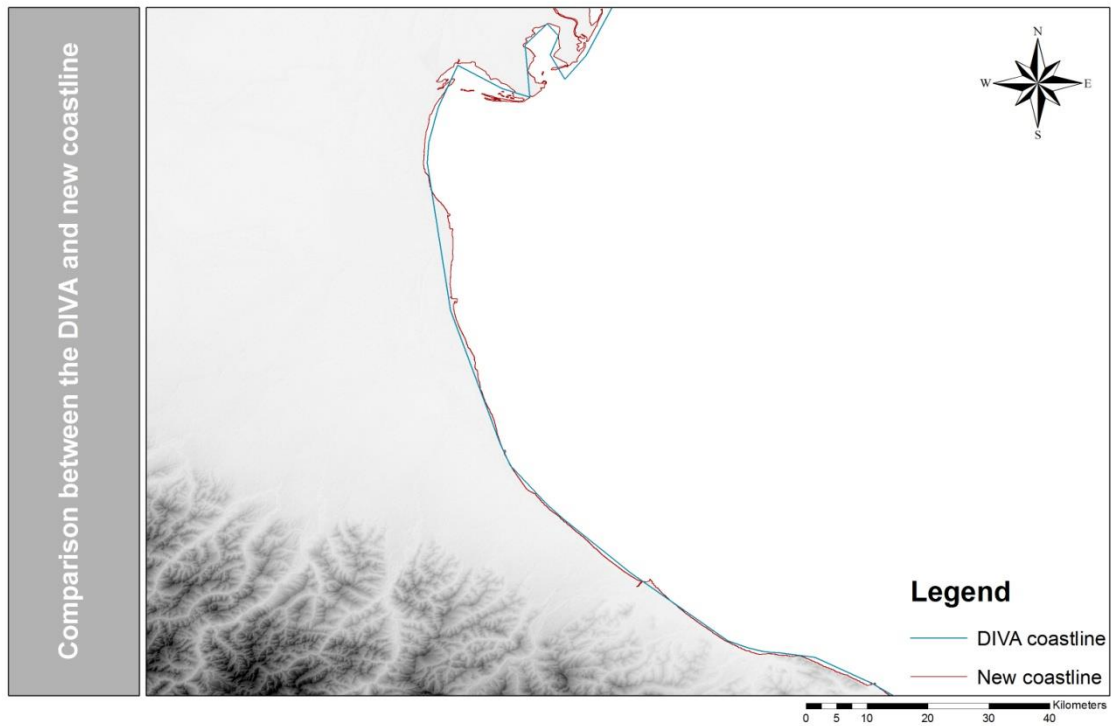
- VOUSDOUKAS, M. I., BOUZIOTAS, D., GIARDINO, A., BOUWER, L. M., MENTASCHI, L., VOUKOUVALAS, E. & FEYEN, L. 2018a. Understanding epistemic uncertainty in large-scale coastal flood risk assessment for present and future climates. *Natural Hazards and Earth System Sciences*, 18, 2127-2142.
- VOUSDOUKAS, M. I., MENTASCHI, L., HINKEL, J., WARD, P. J., MONGELLI, I., CISCAR, J.-C. & FEYEN, L. 2020b. Economic motivation for raising coastal flood defenses in Europe. *Nature Communications*, 11, 2119.
- VOUSDOUKAS, M. I., MENTASCHI, L., VOUKOUVALAS, E., BIANCHI, A., DOTTORI, F. & FEYEN, L. 2018b. Climatic and socioeconomic controls of future coastal flood risk in Europe. *Nature Climate Change*, 8, 776-780.
- VOUSDOUKAS, M. I., MENTASCHI, L., VOUKOUVALAS, E., VERLAAN, M. & FEYEN, L. 2017. Extreme sea levels on the rise along Europe's coasts. *Earths Future*, 5, 304-323.
- VOUSDOUKAS, M. I., MENTASCHI, L., VOUKOUVALAS, E., VERLAAN, M., JEVREJEVA, S., JACKSON, L. P. & FEYEN, L. 2018c. Global probabilistic projections of extreme sea levels show intensification of coastal flood hazard. *Nat Commun*, 9, 2360.
- VOUSDOUKAS, M. I., VOUKOUVALAS, E., ANNUNZIATO, A., GIARDINO, A. & FEYEN, L. 2016. Projections of extreme storm surge levels along Europe. *Climate Dynamics*, 47, 3171-3190.
- WAHL, T., HAIGH, I. D., NICHOLLS, R. J., ARNS, A., DANGENDORF, S., HINKEL, J. & SLANGEN, A. B. A. 2017. Understanding extreme sea levels for broad-scale coastal impact and adaptation analysis. *Nature Communications*, 8.
- WAKELIN, S. L. & PROCTOR, R. 2002. The impact of meteorology on modelling storm surges in the Adriatic Sea. *Global and Planetary Change*, 34, 97-119.
- WARD, P. J., JONGMAN, B., WEILAND, F. S., BOUWMAN, A., VAN BEEK, R., BIERKENS, M. F. P., LIGTVOET, W. & WINSEMIUS, H. C. 2013. Assessing flood risk at the global scale: model setup, results, and sensitivity. *Environmental Research Letters*, 8, 044019.
- WARD, P. J., BLAUHUT, V., BLOEMENDAAL, N., DANIELL, J. E., DE RUITER, M. C., DUNCAN, M. J., EMBERSON, R., JENKINS, S. F., KIRSCHBAUM, D., KUNZ, M., MOHR, S., MUIS, S., RIDDELL, G. A., SCHÄFER, A., STANLEY, T., VELDKAMP, T. I. E. & WINSEMIUS, H. C. 2020. Review article: Natural hazard risk assessments at the global scale. *Natural Hazards and Earth System Sciences*, 20, 1069-1096.
- WARDROP, N. A., JOCHEM, W. C., BIRD, T. J., CHAMBERLAIN, H. R., CLARKE, D., KERR, D., BENGTTSSON, L., JURAN, S., SEAMAN, V. & TATEM, A. J. 2018. Spatially disaggregated population estimates in the absence of national population and housing census data. *Proc Natl Acad Sci U S A*, 115, 3529-3537.
- WEATHERALL, P., MARKS, K. M., JAKOBSSON, M., SCHMITT, T., TANI, S., ARNDT, J. E., ROVERE, M., CHAYES, D., FERRINI, V. & WIGLEY, R. 2015. A new digital bathymetric model of the world's oceans. *Earth and Space Science*, 2, 331-345.
- WOLFF, C., VAPEIDIS, A. T., LINCKE, D., MARASMI, C. & HINKEL, J. 2016. Effects of Scale and Input Data on Assessing the Future Impacts of Coastal Flooding: An Application of DIVA for the Emilia-Romagna Coast. *Frontiers in Marine Science*, 3, 41.

- WOLFF, C., VAFEIDIS, A. T., MUIS, S., LINCKE, D., SATTA, A., LIONELLO, P., JIMENEZ, J. A., CONTE, D. & HINKEL, J. 2018. A Mediterranean coastal database for assessing the impacts of sea-level rise and associated hazards. *Scientific Data*, 5, 11.
- WONG, P. P., LOSADA, I. J., GATTUSO, J. P., HINKEL, J., KHATTABI, A., MCINNES, K. L., SAITO, Y. & SALLENGER, A. 2014. Coastal systems and low-lying areas. *In: FIELD, C. B., BARROS, V. R., DOKKEN, D. J., MACH, K. J., MASTRANDREA, M. D., BILIR, T. E., CHATTERJEE, M., EBI, K. L., ESTRADA, Y. O., GENOVA, R. C., GIRMA, B., KISSEL, E. S., LEVY, A. N., MACCRACKEN, S., MASTRANDREA, P. R. & WHITE, L. L. (eds.) Climate Change 2014: Impacts, Adaptation, and Vulnerability. Part A: Global and Sectoral Aspects. Contribution of Working Group II to the Fifth Assessment Report of the Intergovernmental Panel of Climate Change.* Cambridge, United Kingdom and New York, NY, USA: Cambridge University Press.
- WOODWORTH, P. L., HUNTER, J. R., MARCOS, M., CALDWELL, P., MENENDEZ, M. & HAIGH, I. 2016. Towards a global higher-frequency sea level dataset. *Geoscience Data Journal*, 3, 50-59.
- WORLD BANK. 2016. *GDP per capita, PPP (current international \$)* [Online]. <http://data.worldbank.org/indicator/NY.GDP.PCAP.PP.CD>. Available: <http://data.worldbank.org/indicator/NY.GDP.PCAP.PP.CD> [Accessed 08.03.2017].
- WORLD TOURISM ORGANIZATION, YEARBOOK OF TOURISM STATISTICS & COMPENDIUM OF TOURISM STATISTICS AND DATA FILES. 2014. *International tourism, number of arrivals* [Online]. World Bank. Available: <http://data.worldbank.org/indicator/ST.INT.ARVL> [Accessed 2017].
- YAMAZAKI, D., IKESHIMA, D., TAWATARI, R., YAMAGUCHI, T., O'LOUGHLIN, F., NEAL, J. C., SAMPSON, C. C., KANAE, S. & BATES, P. D. 2017. A high-accuracy map of global terrain elevations. *Geophysical Research Letters*, 44, 5844-5853.
- YANG, X., YAO, C., CHEN, Q., YE, T. & JIN, C. 2019. Improved Estimates of Population Exposure in Low-Elevation Coastal Zones of China. *Int J Environ Res Public Health*, 16.
- ZHOU, Y., VARQUEZ, A. C. G. & KANDA, M. 2019. High-resolution global urban growth projection based on multiple applications of the SLEUTH urban growth model. *Sci Data*, 6, 34.

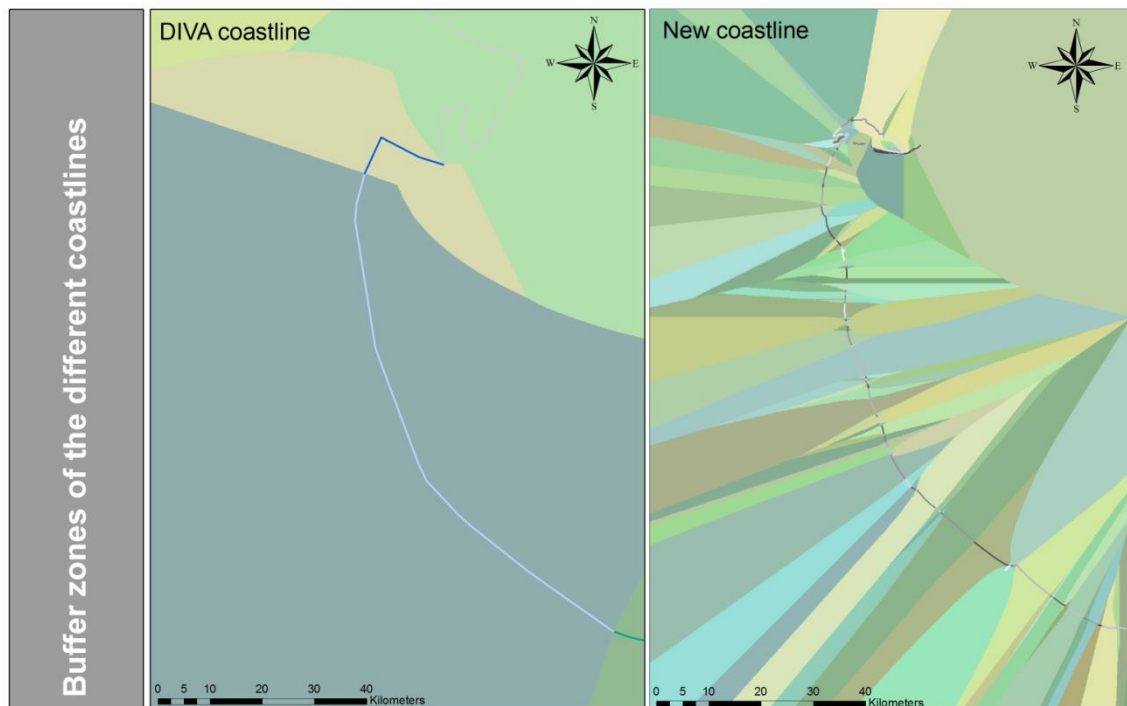


## APPENDIX A

**Supplementary Figure 2-1:** Comparison of the global DIVA and detailed coastline



**Supplementary Figure 2-2:** Buffer zones of the global and high-resolution segmentation



**Supplementary Table 2-1:** Expected number of people flooded annually in Emilia-Romagna using different datasets and assessment scales in 2015 and 2100

People flooded annually [year]		2015	2100								
			Low SLR			Medium SLR			High SLR		
			SSP2	SSP3	SSP5	SSP2	SSP3	SSP5	SSP2	SSP3	SSP5
Coastline segmentation	Datasets										
High-resolution	LiDAR + LandScan	149,716	137,864	68,198	225,717	157,917	78,118	258,550	220,184	108,920	360,496
	LiDAR + GRUMP	155,522	143,043	70,759	234,194	163,290	80,775	267,344	204,014	100,921	334,019
	SRTM+ LandScan	245,986	223,078	110,352	365,233	249,931	123,635	409,197	293,381	145,129	480,335
	SRTM + GRUMP	269,601	244,126	120,765	399,691	272,898	134,998	446,798	312,233	154,456	511,198
	LiDAR + LandScan +	158,866	174,030	86,089	284,931	197,267	97,584	322,975	259,874	128,544	425,478
Global	SRTM + GRUMP	198,752	183,722	90,909	300,878	210,258	104,011	344,240	243,001	120,209	397,849

**Supplementary Table 2-2:** Expected seafood cost in Emilia-Romagna using different datasets and assessment scales in 2015 and 2100.

Seafoodcost [million US\$]		2015	2100								
			Low SLR			Medium SLR			High SLR		
			SSP2	SSP3	SSP5	SSP2	SSP3	SSP5	SSP2	SSP3	SSP5
Coastline segmentation	Datasets										
High-resolution	LiDAR + LandScan	3,657	11,477	3,866	36,360	14,429	4,860	45,711	23,676	7,976	75,009
	LiDAR + GRUMP	3,810	11,939	4,022	37,822	14,986	5,048	47,478	23,495	7,915	74,432
	SRTM+ LandScan	6,224	19,154	6,452	60,680	23,702	7,985	75,089	38,472	11,950	112,377
	SRTM + GRUMP	6,843	21,022	7,082	66,599	25,975	8,750	82,290	38,417	12,942	121,707
	LiDAR + LandScan + PInSAR	4,026	16,473	5,549	52,189	19,757	6,655	62,291	29,935	10,083	94,835
Global	SRTM + GRUMP	6,252	19,784	6,665	62,677	24,979	8,415	79,136	38,329	12,912	121,428

**Supplementary Table 2-3:** Potentially flooded area below H100 in Emilia-Romagna using different datasets and assessment scales in 2015 and 2100.

Potential flood area [km <sup>2</sup> ]		2015	2100		
Coastline segmentation	Datasets		Low SLR	Medium SLR	High SLR
High-resolution	LiDAR	1783	1958	2033	2260
	SRTM	2819	3060	3126	3309
	LiDAR + PSInSAR	1820	2059	2138	2353
Global	SRTM	2112	2340	2387	2520




## APPENDIX B

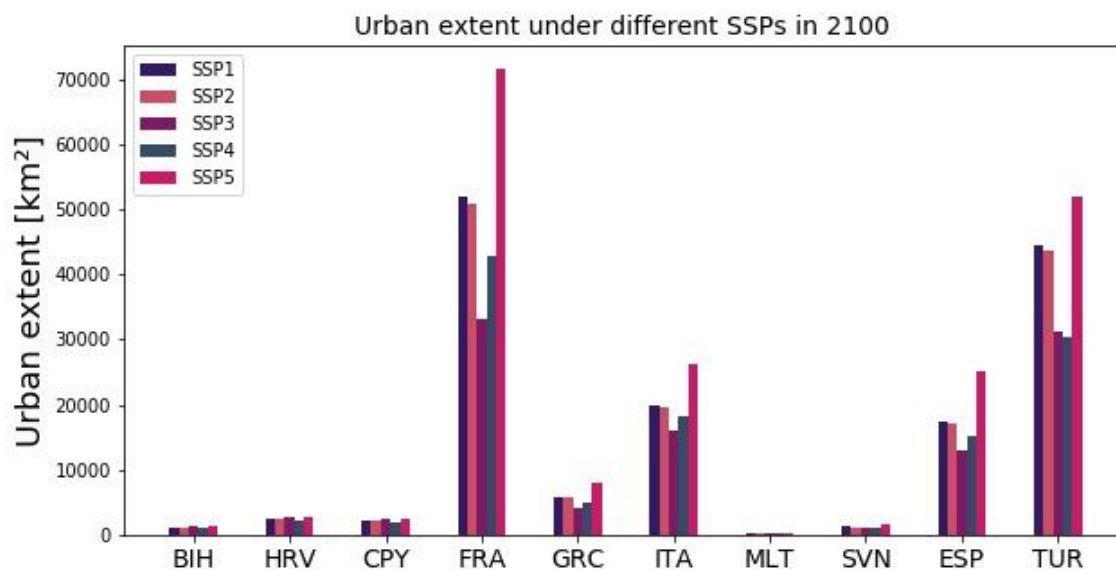
**Supplementary Table 4-1:** Country specific absolute urban extent in 2100 per SSP [in km<sup>2</sup>]

ISO	SSP1	SSP2	SSP3	SSP4	SSP5
<b>BIH</b>	1179	1235	1354	1062	1269
<b>HRV</b>	2416	2599	2828	2248	2634
<b>CYP</b>	2077	2338	2369	1900	2399
<b>FRA</b>	52005	50781	33269	42732	71523
<b>GRC</b>	5917	5723	4068	4957	7922
<b>ITA</b>	19970	19549	16146	18128	26190
<b>MLT</b>	177	197	180	154	191
<b>SVN</b>	1293	1210	1011	1156	1783
<b>ESP</b>	17375	17191	12956	15216	25028
<b>TUR</b>	44471	43701	31252	30366	51827

**Supplementary Table 4-2:** SSP ranging from lowest (left) to the highest (right) urban extent for all countries in 2100

ISO	Lowest urban extent				Highest urban extent
<b>BIH</b>	SSP4	SSP1	SSP2	SSP5	SSP3
<b>HRV</b>	SSP4	SSP1	SSP2	SSP5	SSP3
<b>CYP</b>	SSP4	SSP1	SSP2	SSP5	SSP3
<b>FRA</b>	SSP3	SSP4	SSP2	SSP1	SSP5
<b>GRC</b>	SSP3	SSP4	SSP2	SSP1	SSP5
<b>SVN</b>	SSP3	SSP4	SSP2	SSP1	SSP5
<b>ESP</b>	SSP3	SSP4	SSP2	SSP1	SSP5
<b>ITA</b>	SSP3	SSP4	SSP2	SSP1	SSP5
<b>TUR</b>	SSP4	SSP3	SSP2	SSP1	SSP5
<b>MLT</b>	SSP4	SSP1	SSP3	SSP5	SSP2

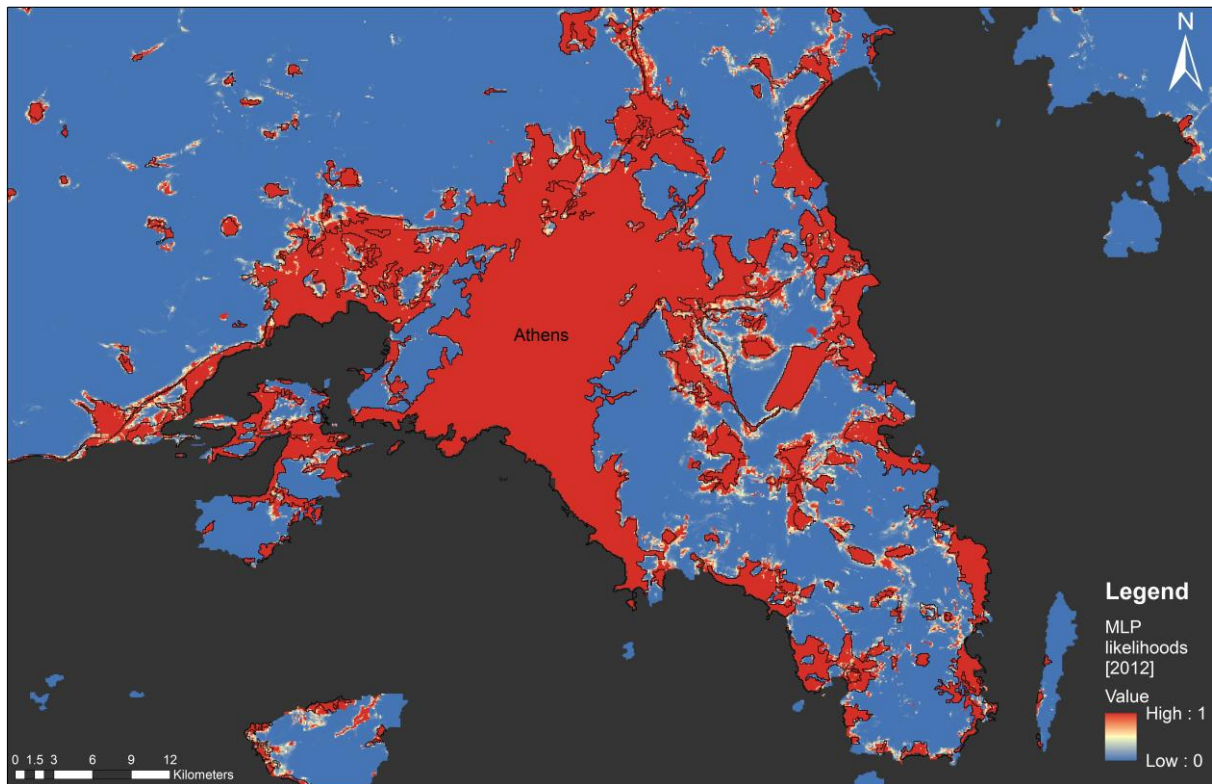
**Supplementary Figure 4-1:** Country-specific absolute urban extent [in km<sup>2</sup>] for the five SSPs in 2100.



**Supplementary Table 4-3:** Country-specific absolute urban extent in the Mediterranean E-LECZ in 2012 and 2100 per SSP [in km<sup>2</sup>]

ISO	Base year 2012	SSP1 2100	SSP2 2100	SSP3 2100	SSP4 2100	SSP5 2100
<b>BIH</b>	4.3	7.3	7.6	8.1	6.6	7.8
<b>HRV</b>	224.6	263.6	276.0	290.0	250.7	278.2
<b>CYP</b>	129.1	250.3	269.0	271.3	236.8	273.9
<b>FRA</b>	2246.9	3780.3	3711.3	2439.8	3192.9	4770.2
<b>GRC</b>	799.1	1219.3	1183.4	836.2	1028.9	1528.1
<b>ITA</b>	3092.8	3968.7	3887.9	3124.1	3615.6	5199.5
<b>MLT</b>	11.7	16.3	19.0	16.4	14.8	17.5
<b>SVN</b>	11.0	12.7	12.5	12.0	12.3	14.1
<b>ESP</b>	1494.7	1990.0	1974.7	1561.3	1796.1	2530.8
<b>TUR</b>	1169.1	2746.9	2722.0	2240.0	2200.5	2968.8

**Supplementary Figure 4-2:** Spatial map of Athens showing the CORINE urban 2012 Land Cover data by the black outline. Colors show the likelihood of the MLP model.



**Supplementary Table 4-4:** Best MLP model architecture per country

Country	Hidden layer 1 [Nr of neurons]	Hidden layer 2 [Nr of neurons]	Hidden layer 3 [Nr of neurons]	Hidden layer 4 [Nr of neurons]	Activation function for the hidden layer	Under sampling factor	Activation function output layer	Optimization algorithm
BIH	400	400	400	200	Relu	10	Sigmoid	Adam
CYP	400	400	200	-	Relu	10	Sigmoid	Adam
ESP	400	400	200	-	Relu	8	Sigmoid	Adam
FRA	400	400	400	200	Relu	10	Sigmoid	Adam
GRC	400	400	200	-	Relu	10	Sigmoid	Adam
HRV	400	400	400	200	Relu	8	Sigmoid	Adam
ITA	400	400	200	-	Relu	12	Sigmoid	Adam
MLT	200	200	200	100	Relu	False	Sigmoid	Adam
SVN	400	400	200	-	Relu	10	Sigmoid	Adam
TUR	400	400	400	200	Relu	10	sigmoid	Adam

## Mutual Information and Entropy

The entropy can be calculated for a random variable  $Y$  by the following formula:

$$H(Y) = - \sum_y \mathbb{P}(y) \log_2(\mathbb{P}(y))$$

where  $\mathbb{P}(y)$  is the probability function of the random variable  $Y$ , and  $\log_2$  is the logarithm with base 2. Entropy is a measure of the uncertainty related to observing, or measuring the value of  $Y$ , which is only known prior to the observation with a certain probability. E.g. in a coin tossing experiment, we do not know beforehand the outcome (heads or tails), only the probability (50% if the coin is 'fair') that one of the will occur. The binary variable of a pixel in our study had the values urban or rural. The probability of a pixel being urban ( $p$ ) (this can be calculated by counting the urban pixels and dividing by the total number of pixels), then the probability of a pixel being rural will be  $1 - p$ . The entropy, in this case, is given (as a function of  $p$ ) by:

$$H(p) = -p \log_2(p) - (1 - p) \log_2(1 - p)$$

This function has the following properties: It takes values in the interval  $[0, 1]$ . It attains its maximum  $H = 1$  when the two events are equiprobable i.e. when  $p = 1/2$ . This is in agreement with the intuition that the uncertainty related to a binary random experiment is maximum when the two events have equal probability. On the other hand, if one of the two possible outcomes is known to occur with certainty (so actually we are not dealing with a random experiment), which in probabilistic terms would mean that  $p = 0$  or  $p = 1$ , then the entropy is zero i.e.  $H = 0$ , reflecting the fact that there is no uncertainty about the outcome. The conclusion is that the more random an experiment is, the larger the uncertainty about the outcome as given by the entropy formula. The mutual information of two random variables  $X, Y$  is given by a similar formula,

$$I(X, Y) = \sum_{x,y} \mathbb{P}(x, y) \log_2 \left( \frac{\mathbb{P}(y|x)}{\mathbb{P}(y)} \right)$$

where  $\mathbb{P}(x, y)$  is the joint probability function of the input-output pair  $X, Y$ ,  $\mathbb{P}(y|x)$  is the conditional probability of observing an output  $y$  given a particular value  $X = x$  of the input and  $\mathbb{P}(y)$  is the probability function of the output. To understand what this formula says consider the two extremes: The output is independent of the input, i.e. the input does not have any effect on the output. This is expressed in probabilistic terms by  $\mathbb{P}(y|x) = \mathbb{P}(y)$ . Then the argument of the log equals one, and the log equals zero resulting in zero mutual information. On the contrary, if by observing  $x$  it is certain that  $y$  will occur,  $\mathbb{P}(y|x) = 1$ , and the mutual information equals the entropy of  $Y$ .



**Supplementary Table 4-5:** Mutual information and entropy per input variable and country

	ALB	BIH	CYP	ESP	FRA	GRC	HRV	ITA	MLT	SVN	TUR
<b>arable00</b>	0.014277	0.012878	0.036403	0.037891	0.077408	0.013689	0.02264	0.054726	0.296187	0.015908	0.043129
<b>coast_dis</b>	0.01404	0.00627	0.016264	0.010478	0.005822	0.004376	0.0109	0.01135	0.002558	0.015318	0.003487
<b>forest00</b>	0.020969	0.017984	0.020705	0.013125	0.059657	0.009047	0.018050	0.023984	0.069373	0.032313	0.004352
<b>gpw2000</b>	0.064269	0.03221	0.131660	0.061214	0.113133	0.074354	0.062447	0.099742	0.26709	0.07474	0.03570
<b>grass00</b>	0.020979	0.004473	0.016082	0.02859	0.007633	0.017125	0.008980	0.017829	0.105417	0.003096	0.027074
<b>road_dis</b>	0.022924	0.014402	0.04032	0.023461	0.060569	0.020194	0.032097	0.040120	0.035114	0.02189	0.016398
<b>slope</b>	0.021069	0.008303	0.024429	0.004	0.007552	0.012931	0.00543	0.02332	0.027745	0.018113	0.006148
<b>srtm</b>	0.024697	0.009738	0.021264	0.013164	0.013184	0.012987	0.013068	0.020618	0.020331	0.017115	0.008565
<b>urban00</b>	0.064790	0.06084	0.216974	0.063181	0.198527	0.084661	0.116700	0.178651	0.59792	0.11344	0.057876
<b>Entropy</b>	0.178141	0.116991	0.425583	0.163098	0.308511	0.188608	0.210101	0.298806	0.873874	0.191646	0.128381

**Supplementary Table 6:** Mutual Information ranging (classification of the same order of magnitude) to show that all variables seem to be important input variables in modelling future urban extent

Country	10 <sup>-1</sup>	10 <sup>-2</sup>	10 <sup>-3</sup>
ALB		urban00, arable00, forest00, road_dis, coast_dis, srtm, gpw2000, grass00, slope	
BIH		arable00, forest00, gpw2000, road_dis, urban00	coast_dis, grass00, slope, srtm
CYP	urban00, gpw2000	arable00, forest00, road_dis, coast_dis, grass00, slope, srtm	
ESP		arable00, forest00, road_dis, coast_dis, grass00, srtm, urban00, gpw2000	slope
FRA	urban00, gpw2000	arable00, forest00, road_dis, srtm,	coast_dis, grass00, slope
GRC		arable00, road_dis, grass00, srtm, urban00, gpw2000, slope	coast_dis, forest00
HRV	urban00	arable00, forest00, road_dis, coast_dis, srtm, gpw2000	grass00, slope
ITA	urban00	arable00, forest00, road_dis, coast_dis, srtm, gpw2000, grass00, slope	
MLT	urban00, arable00, gpw2000, grass00	forest00, road_dis, srtm, slope	coast_dis
SVN	urban00	arable00, forest00, road_dis, coast_dis, srtm, gpw2000, slope	grass00
TUR		urban00, arable00, road_dis, gpw2000, grass00	coast_dis, forest00, srtm, slope



## ACKNOWLEDGEMENTS

Now, at the end of my thesis, there is a long list of people who all, in their ways, have supported me along the way. I want to thank all those colleagues, friends and family who helped me succeeding on this journey:

Of course, first of all **Nassos Vafeidis** – you really earn the attribute ‘Doktorvater’. Thanks for everything, from making this thesis possible in the first place, to the constant support, constructive feedback and discussions. I look up to you in many ways: you are a good person with high moral standards, which is truly inspiring not only for science but also on a personal level; you are a great scientist with an open mind and an excellent coffee drinker. The only thing I regret is not starting to play tennis against you earlier.

**Jochen Hinkel**, although rather remote I want to thank you for your valuable scientific advice and commitment in pushing my science forward, our productive discussions, and the possibility to do my Internship during my studies at your place and dive into the DIVA modelling framework which was a milestone for this thesis.

Special appreciations go to my co-authors: **Theodore Nikolettopoulos, Daniel Lincke, Sanne Muis, Jose Jimenez, Christian Marasmi, Alessio Satta, Piero Lionello**, and **Dario Conte** for their valuable inputs, smart comments and constantly pleasant collaborations which helped me shape this thesis.

All the mates of the Coastal Risks and Sea-Level Rise working group that have provided much needed input for the success of this thesis in the form of excellent coffee and lunch breaks with excellent company. I am really glad I could spend so much of my PhD life surrounded by you: **Joshua Kiesel** – you are the best office mate one could ask for. Thanks for being such a good friend and human being. **Sara Santamaria-Aguilar** – you are the best travel companion I can imagine. Thanks for spending so much time together on different beaches around the globe. **Lena Reimann** – it was great to go on this journey with you from day 1. Thanks for your support and our random conversations. **Jan Merkens** – our trip to the Arches National Park will be one of the best memories of the PhD time. Thanks for driving us safely through the Rocky Mountains directly after the blizzard (snow chaos). **Leigh MacPherson** – you’re are the best and funniest bread baker in town. I really enjoy going for a drink with you (beer for you and apple juice for me). **Bente Vollstedt** – thank you for sharing a lot of interests outside academy. I really enjoy our pleasant conversations and big smiles. **Jana Koerth** – thank you for getting me into pottery. You are the person that gave me a new hobby. **Maureen Tsakiris** – you are so creative and talented. Many thanks for polishing some of my graphs and posters. **Mark Schürch** – you are an excellent scientist, sailor and drinking companion. The excursion to Greece is just one memory that I gladly look back on.

**Tobias Dolch, Barbara Neumann, Lars Michelsen, Sunna Kupfer, Philipp Saggau und Marcel König** – it is always a pleasure to have you around for lunch, coffee, long conversations and loud laughs.

To all the friends who reminded me that there might also be important and interesting aspects of life besides work: **Janina Löwe, Isabelle Kaufmann, Lena Voß, Tobias Laufenberg, Svenja Aschenbach, Malte Janssen, Lisa Paglialonga, Fabian Aschenbach, Patricia Wiff, Jasper Schwampe, Sinja Dittmann, Marie Borchardt, Julia Reschke, Josephine Wilhelm-Hillert** and many more – all of you have made my life more balanced and richer, everyone in their own way.

To my Family: **Mutti, Marko, Nicky** (you three are the main persons behind that achievement), **Josie, Max, Hartmut, Kerstin** (thanks for believing in me) and all the members of the **Wolff/Stadie/Beyer-Clan**, thanks for all the support, love, and for keeping me grounded.

Finally, **Constantin** – I am grateful for many things in my life but you stand at the top of the list.





## ERKLÄRUNG

Hiermit erkläre ich, dass ich die vorliegende Dissertation, abgesehen von der Beratung durch meine Betreuer, nach Inhalt und Form selbständig verfasst habe und keine weiteren Quellen und Hilfsmittel als die hier angegebenen verwendet habe. Diese Arbeit hat weder ganz noch in Teilen bereits an anderer Stelle im Rahmen eines Dissertationsprüfungsverfahrens vorgelegen. Als kumulative Dissertation sind Kapitel 2 bis 4 wie zu Beginn der Kapitel vermerkt in den genannten Zeitschriften veröffentlicht. Ich erkläre, dass die vorliegende Arbeit unter Einhaltung der Regeln guter wissenschaftlicher Praxis der Deutschen Forschungsgemeinschaft entstanden ist. Weiterhin versichere ich hiermit, dass mir bisher kein akademischer Grad entzogen wurde.

Kiel, 2020